rijksuniversiteit groningen / faculteit wiskunde en natuurwetenschappen / kapteyn instituut

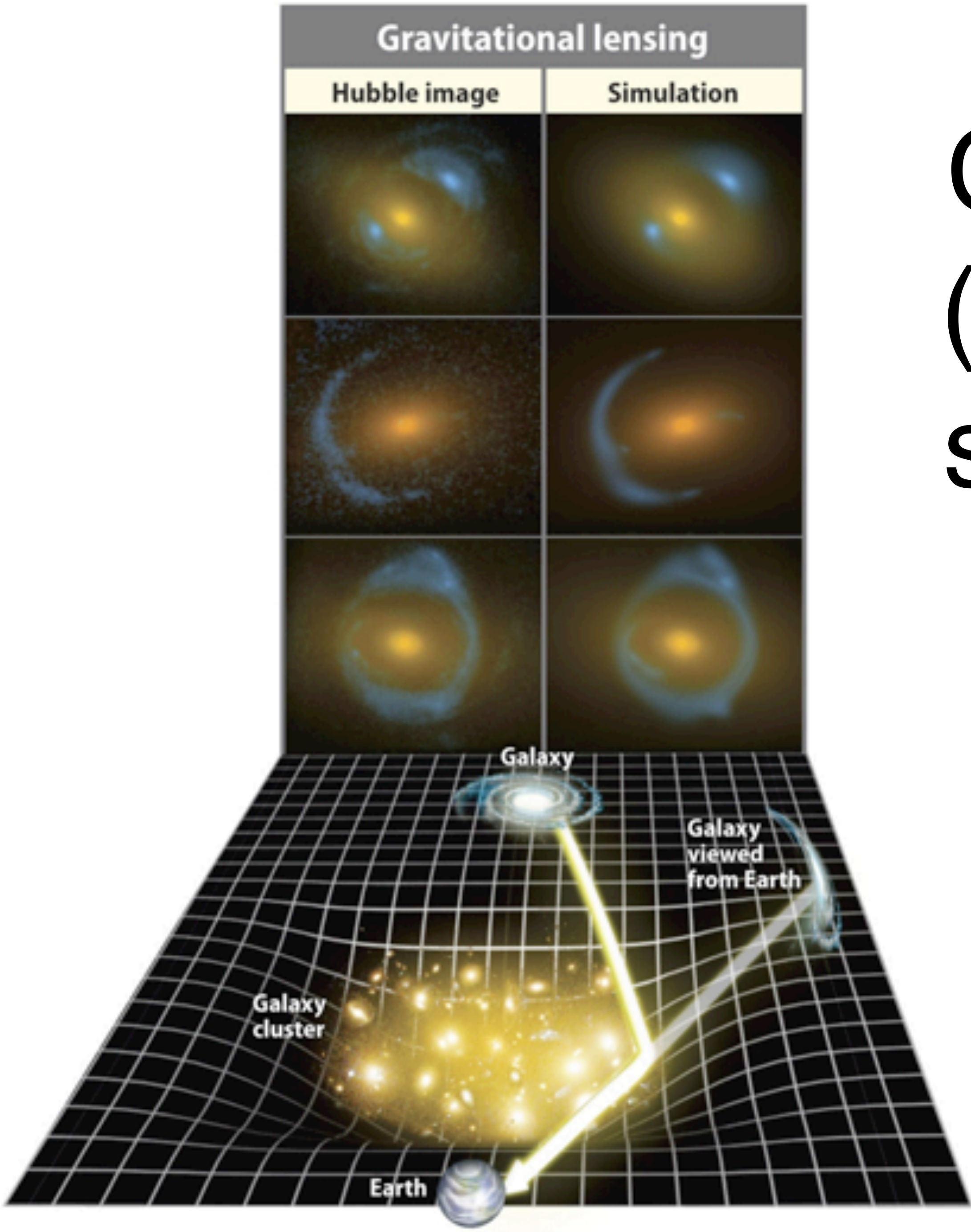

Constraints on dark-matter (and galaxy structure) from strong gravitational lensing

Léon Koopmans
(Kapteyn Astronomical Institute)

19 November 2014, IPMU Tokyo, Japan

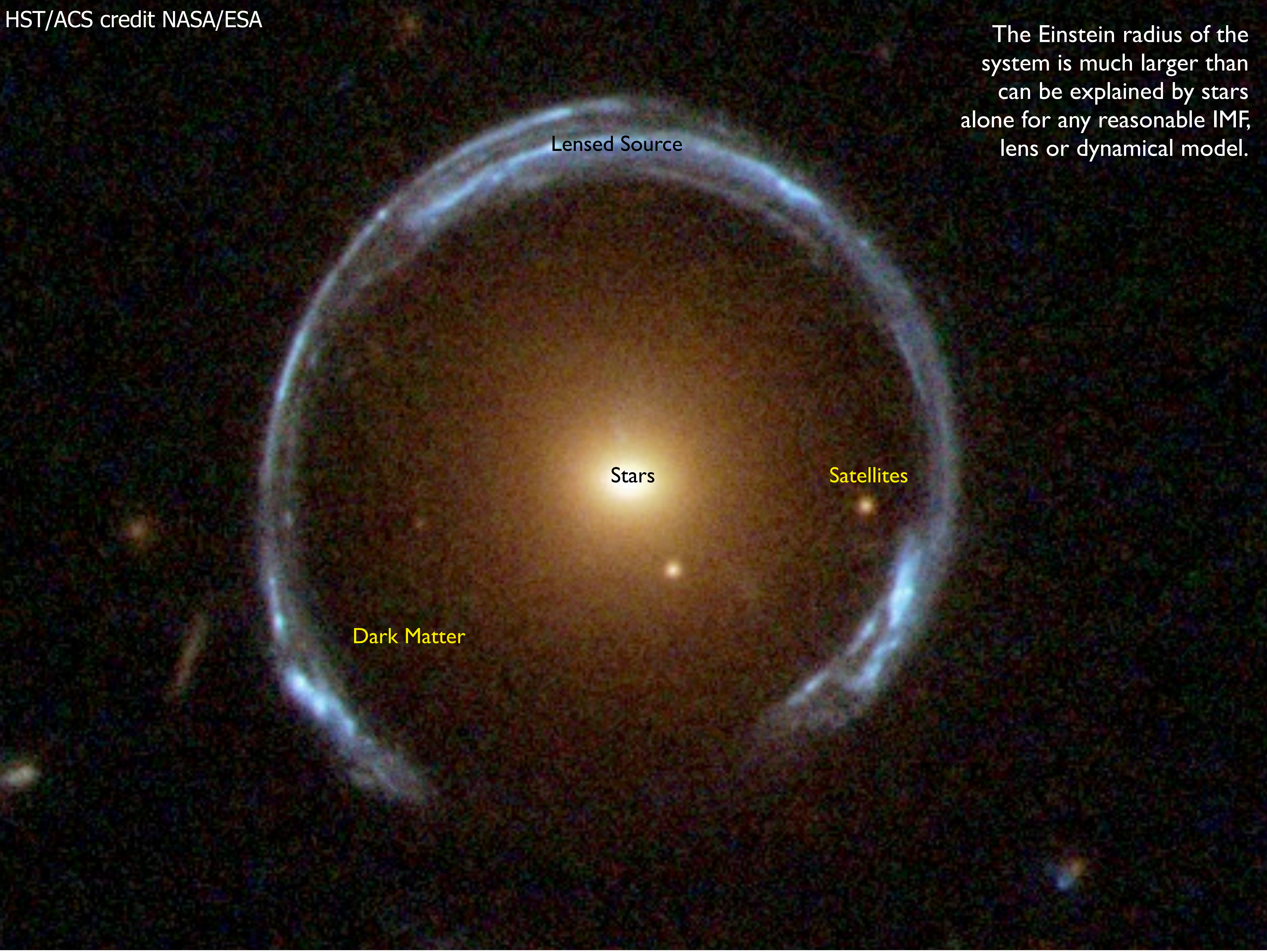
HST/ACS credit NASA/ESA
The Einstein radius of the system is much larger than can be explained by stars alone for any reasonable IMF, lens or dynamical model.
Lensed Source
Stars
Satellites
Dark Matter

Strong Lens Galaxies: Integrated Approach

Galaxy Structure/ Dark Matter

Stellar Dynamics

Stellar + Dark Matter
around the effective radius
Phase-space density
Grid-based methods

Strong Lensing

Stellar + Dark Matter
around the Einstein Radius
CDM Substructure
Grid-based methods

Stellar Population Synthesis

Stellar masses/ IMF shape
SPS modeling: color/spectra

Weak Lensing

Environment &
Outer DM halo
Grid-based methods

Micro Lensing

Stellar + Dark Matter
at the Einstein Radius

Galaxy Structure & Evolution

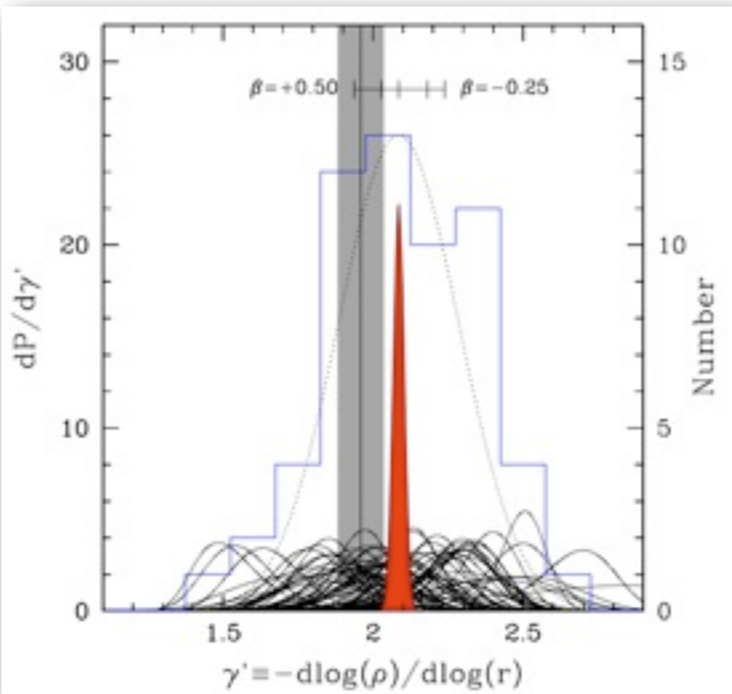

Total Density Profile

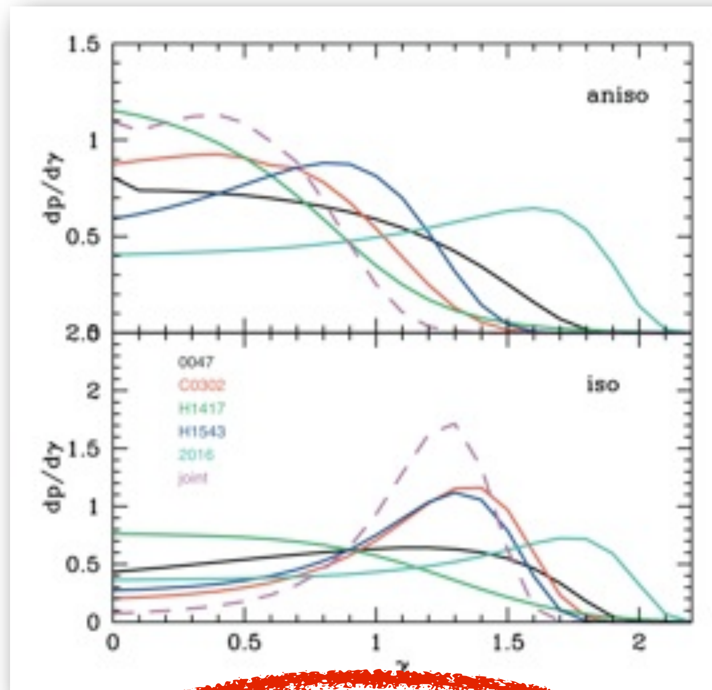

DM Density Profile

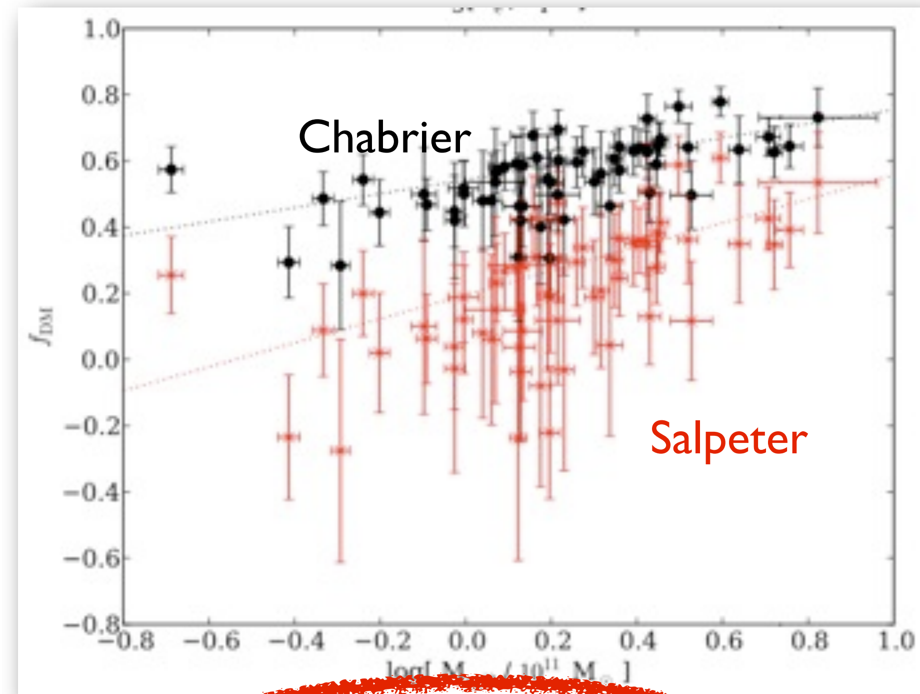

Stellar/DM Mass Fractions

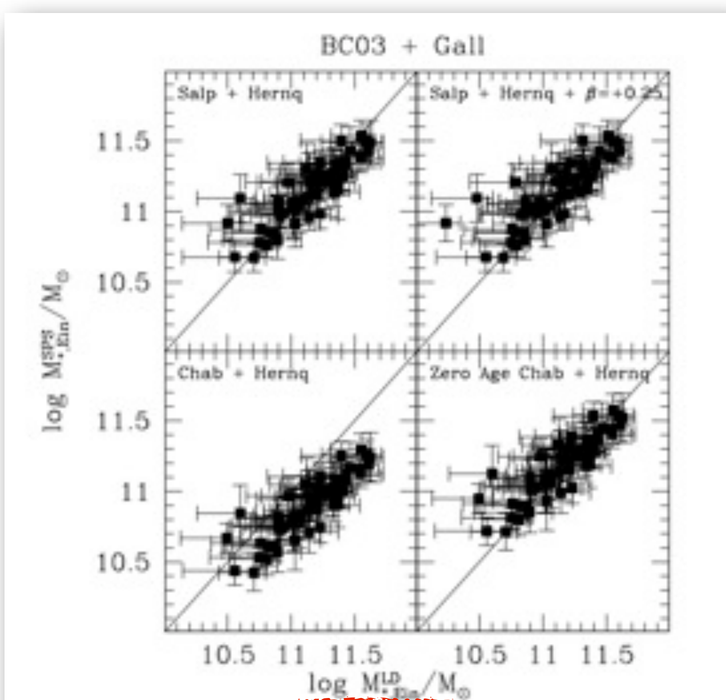

Stellar IMF

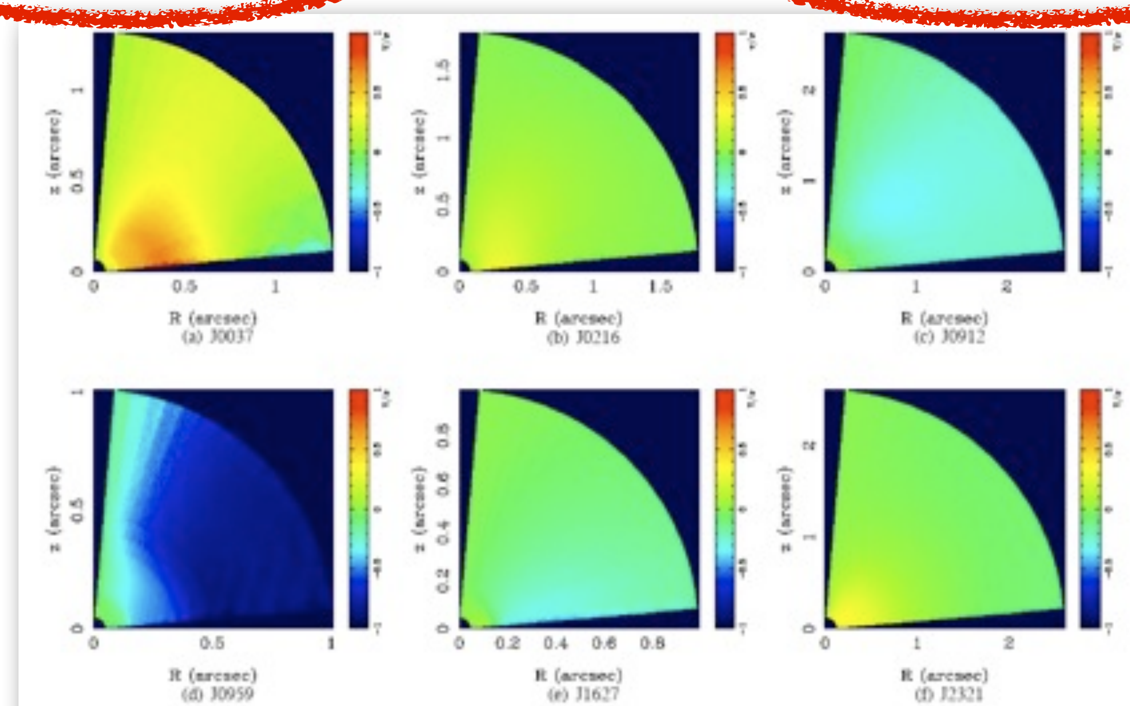

Kinematic Structure

Early-type Galaxies:

Evidence Against Constant M/L Mass Models from Strong Lensing (+ Dynamics)

Some Early Evidence for DM in Galaxies from Strong Lensing

Observed lenses sometimes have image separations >2”, which should not happen in case of constant stellar M/L models (e.g. deV).

When a massive DM halo is added and $\rho \sim r^{-2}$, then lensing statistics matches observations (this is confirmed in many studies).

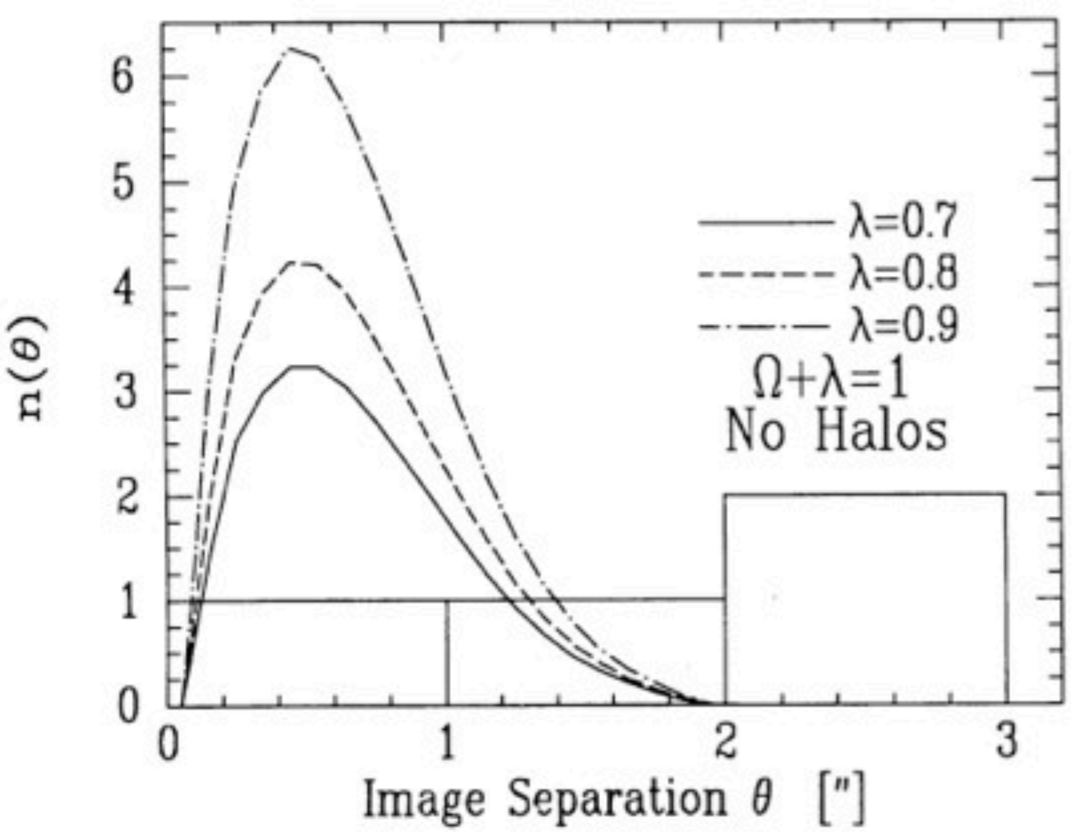

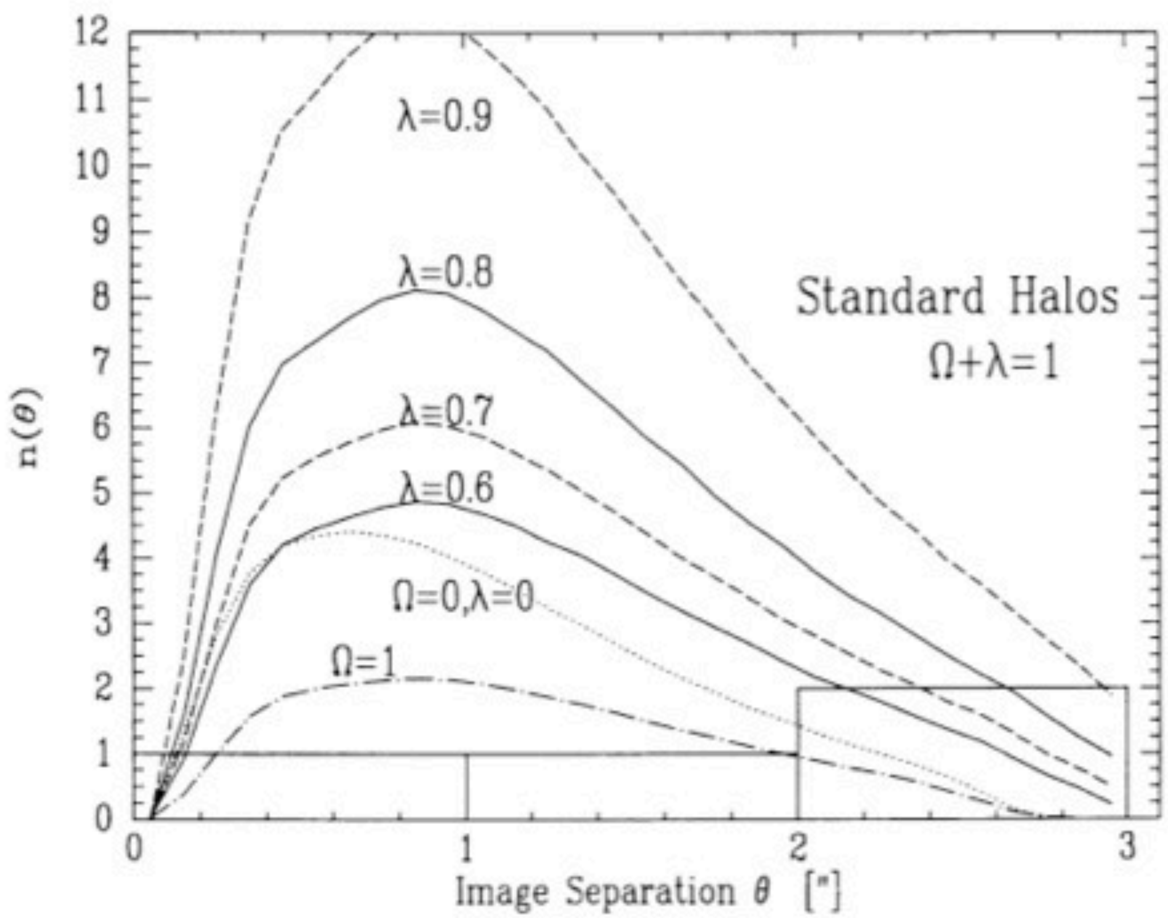

Maoz et al. 1993

Some Early Evidence for DM in Galaxies from Strong Lensing

Data: Radio Einstein ring MG1654+134

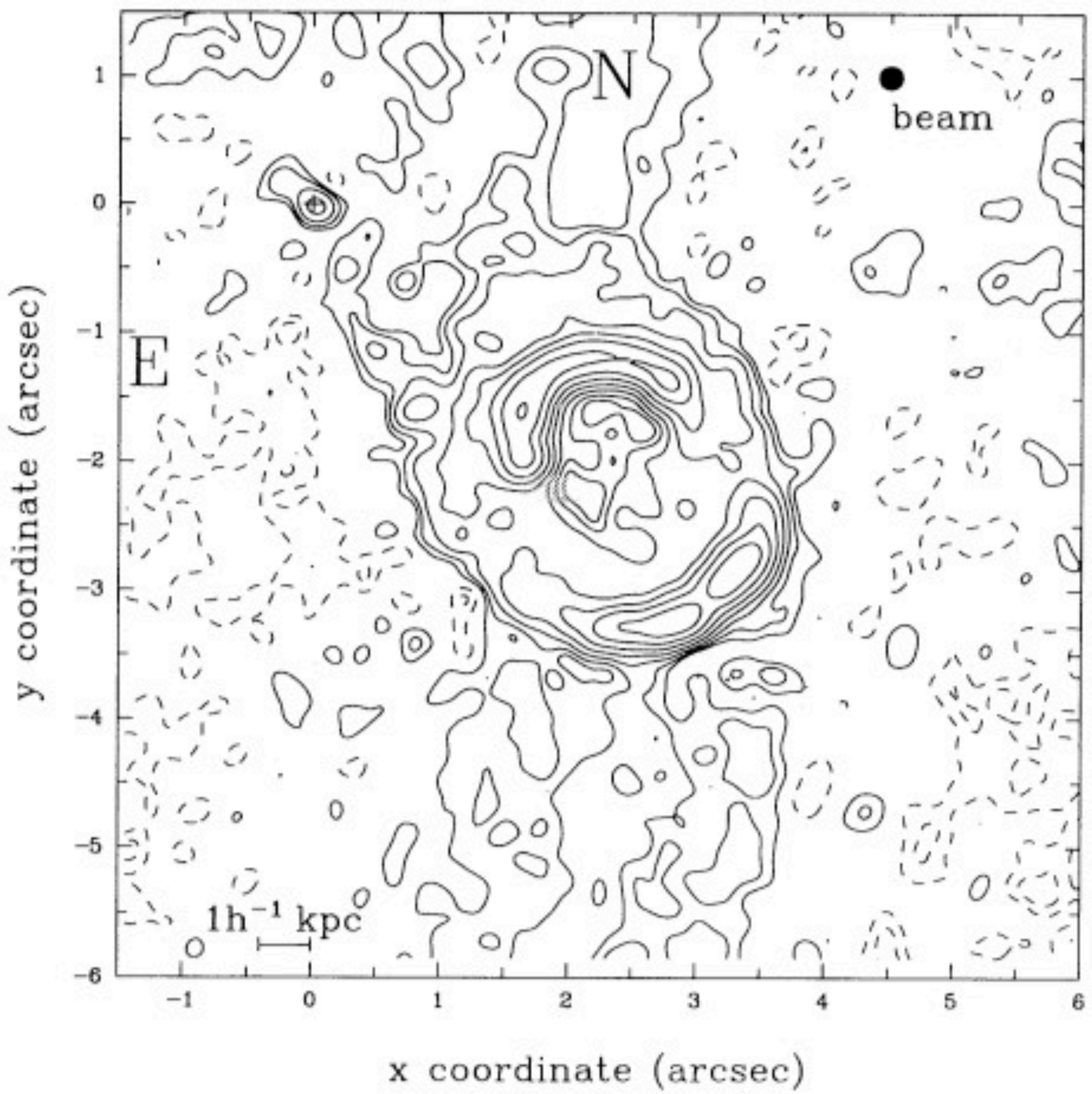

Using LENSCLEAN one can determine a fit to the extended Einstein ring and obtain a model of the source and mass distribution

Best model with residuals

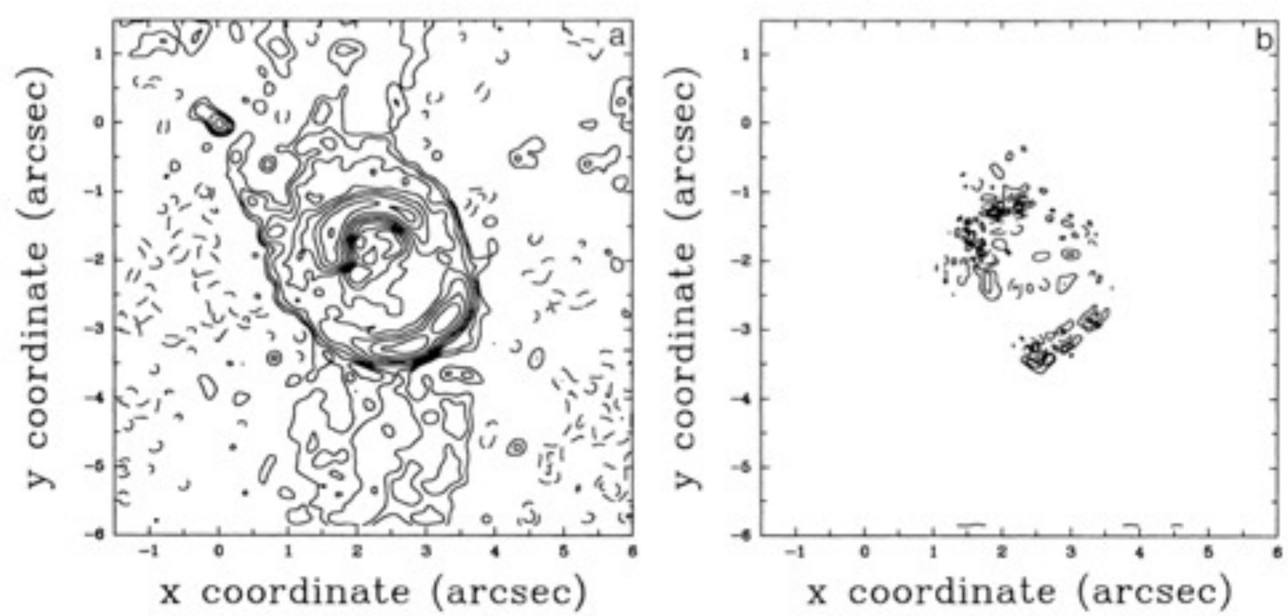

Kochanek 1995

Some Early Evidence for DM in Galaxies from Strong Lensing

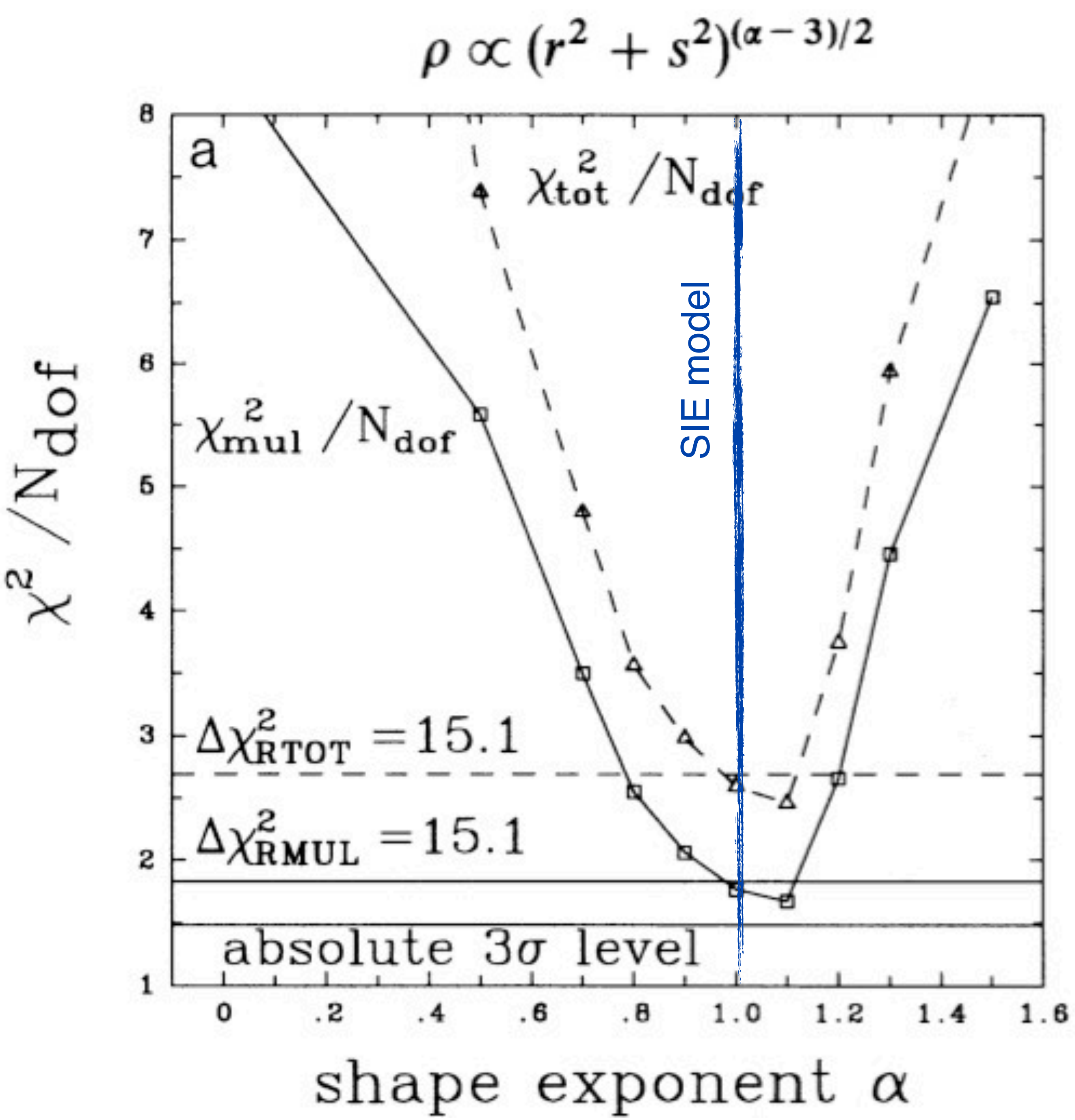

Constant M/L models (deVaucouleurs) are only marginally consistent with data:

- (i) very large M/L_B~20, taking passive evolution in to account.
- (ii) R_{eff} exceeding observations

The M/L is ~3x larger than locally observed and expected from SPS models

SIE model fits the data very well and predicted stellar dispersion matches FP.

Conclusion: Constant M/L models fail to fit the data and DM is needed in this galaxy.

Two-Component Models: Stars + DM

Grid-based inversion of the lensed images makes use of all information: tight constraints on density profile

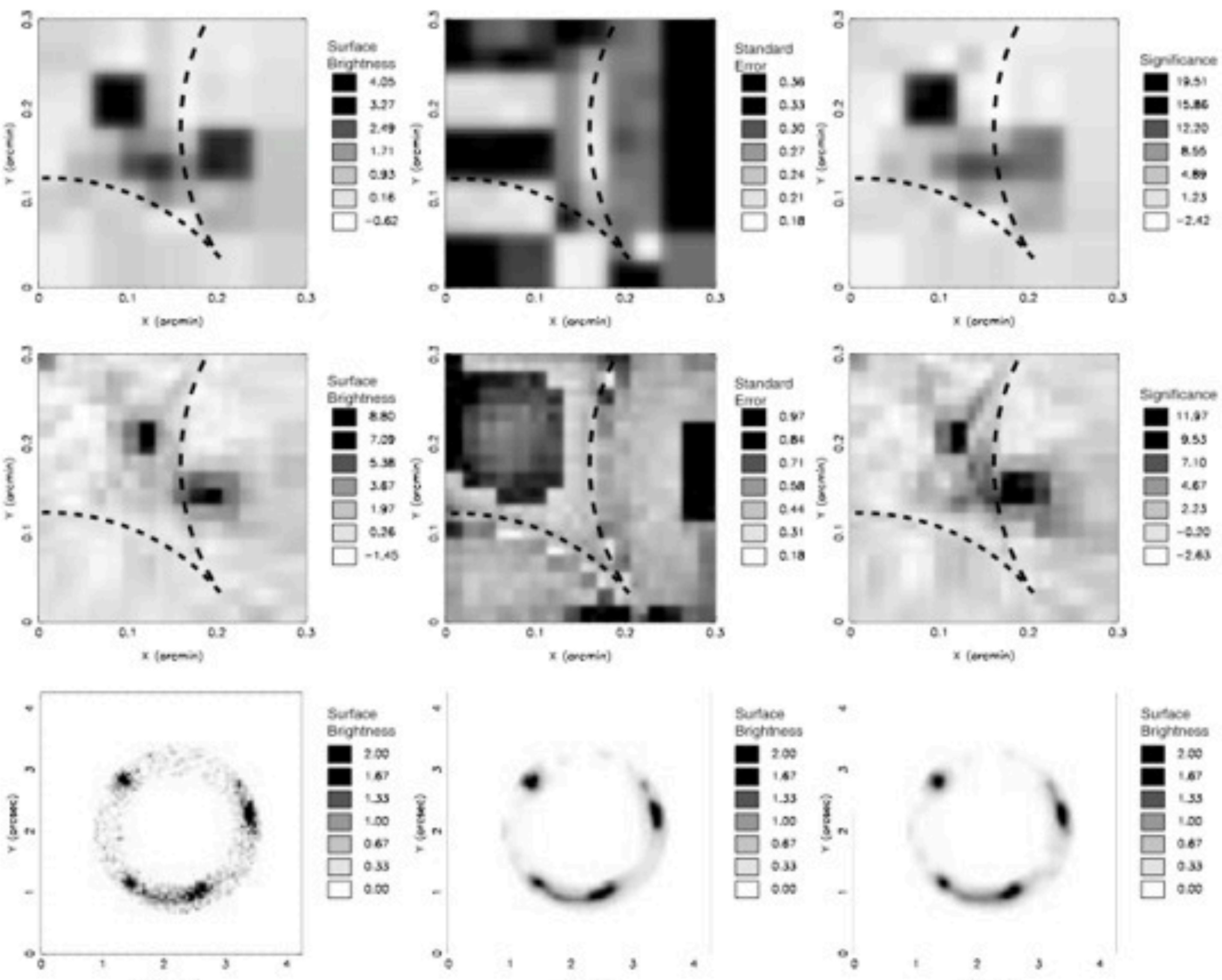

Dye & Warren 2005

Q0047-2808

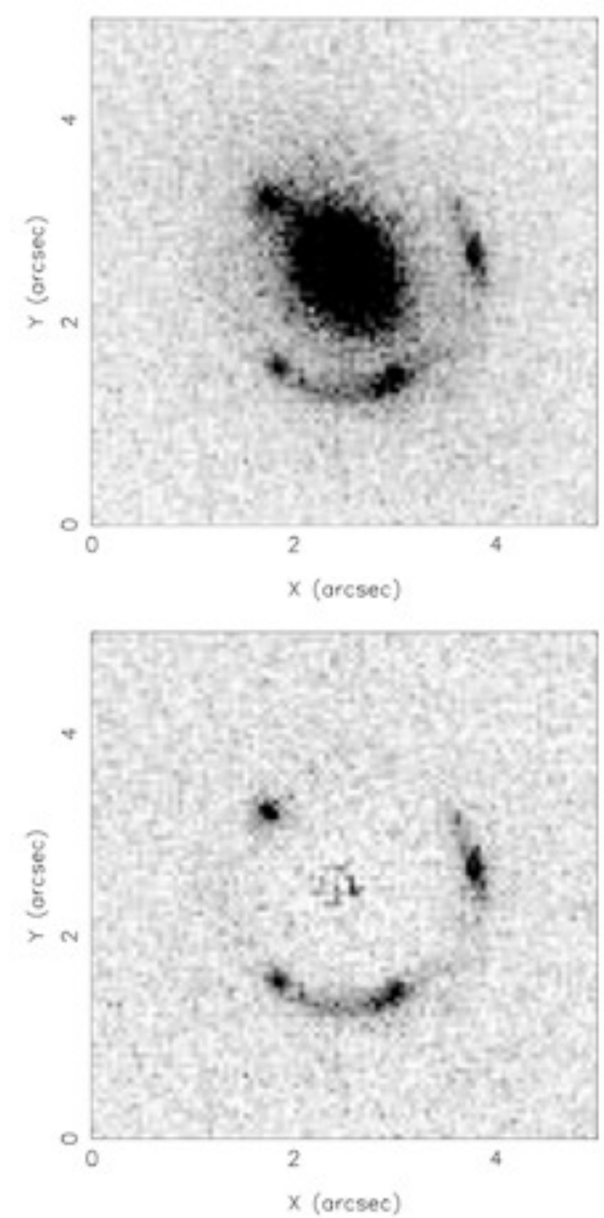

Two-Component Models: Stars + DM

Grid-based inversion of the lensed images makes use of all information: tight constraints on density profile

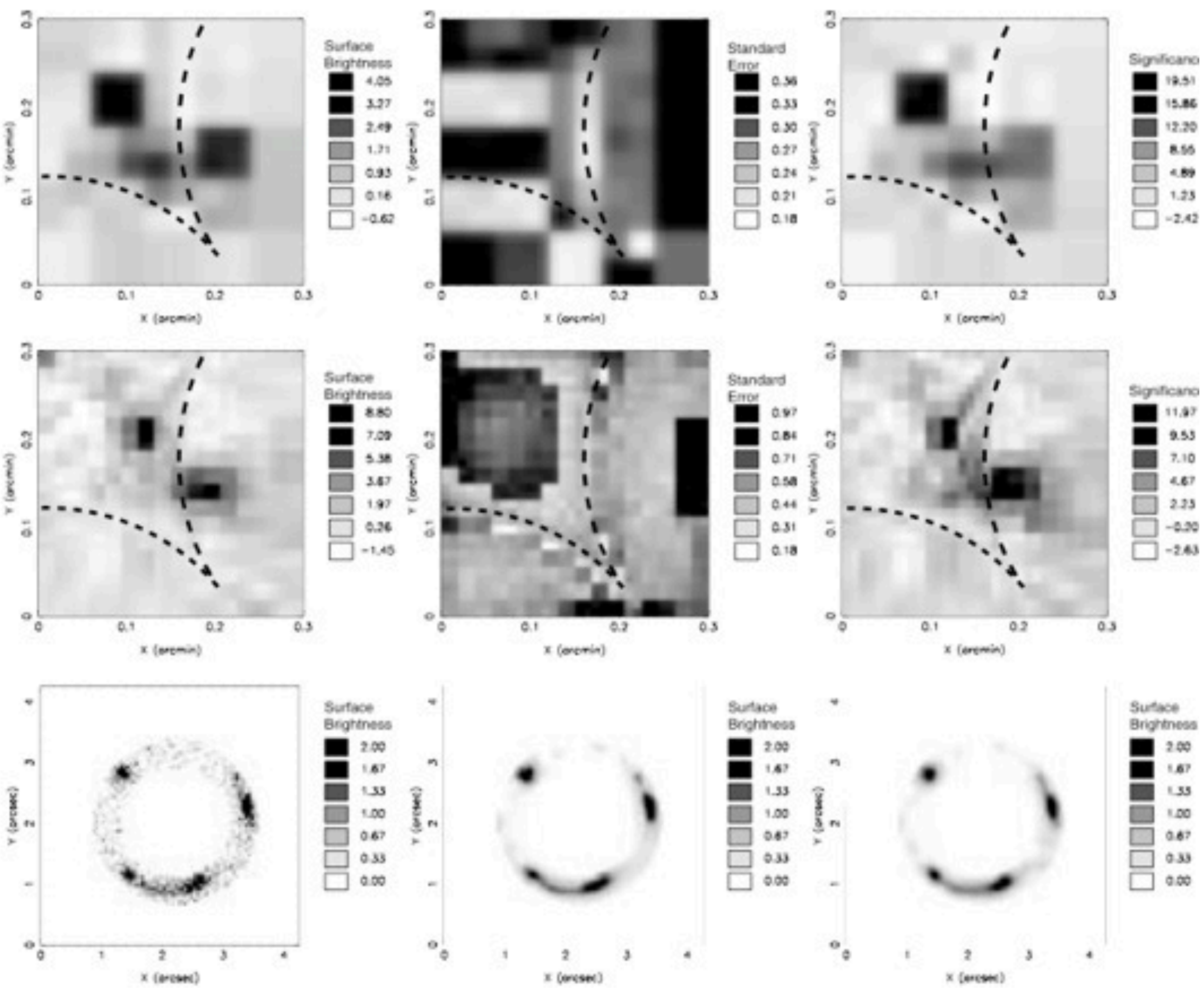

Dye & Warren 2005

Q0047-2808

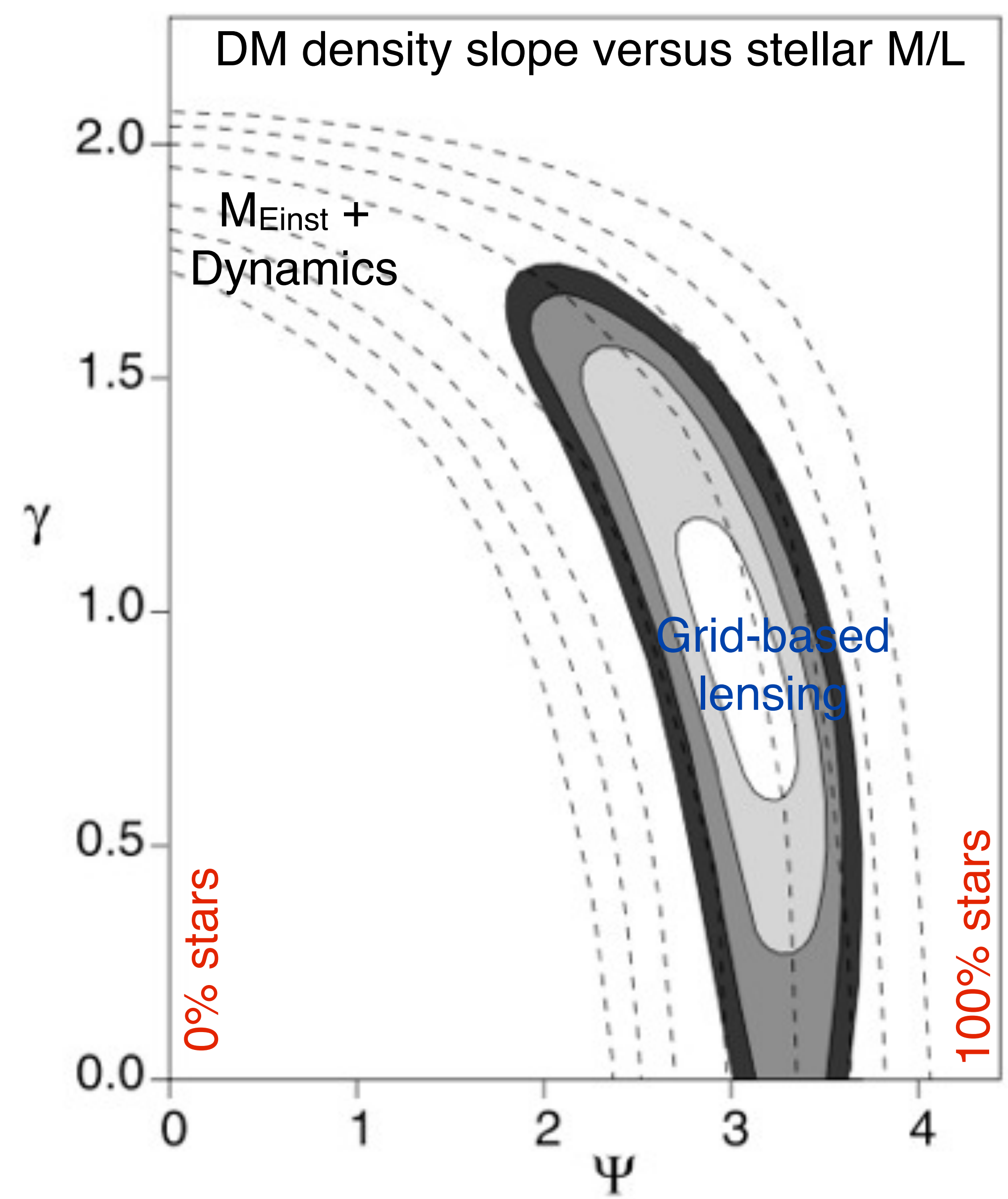

Single-Component Mass Models

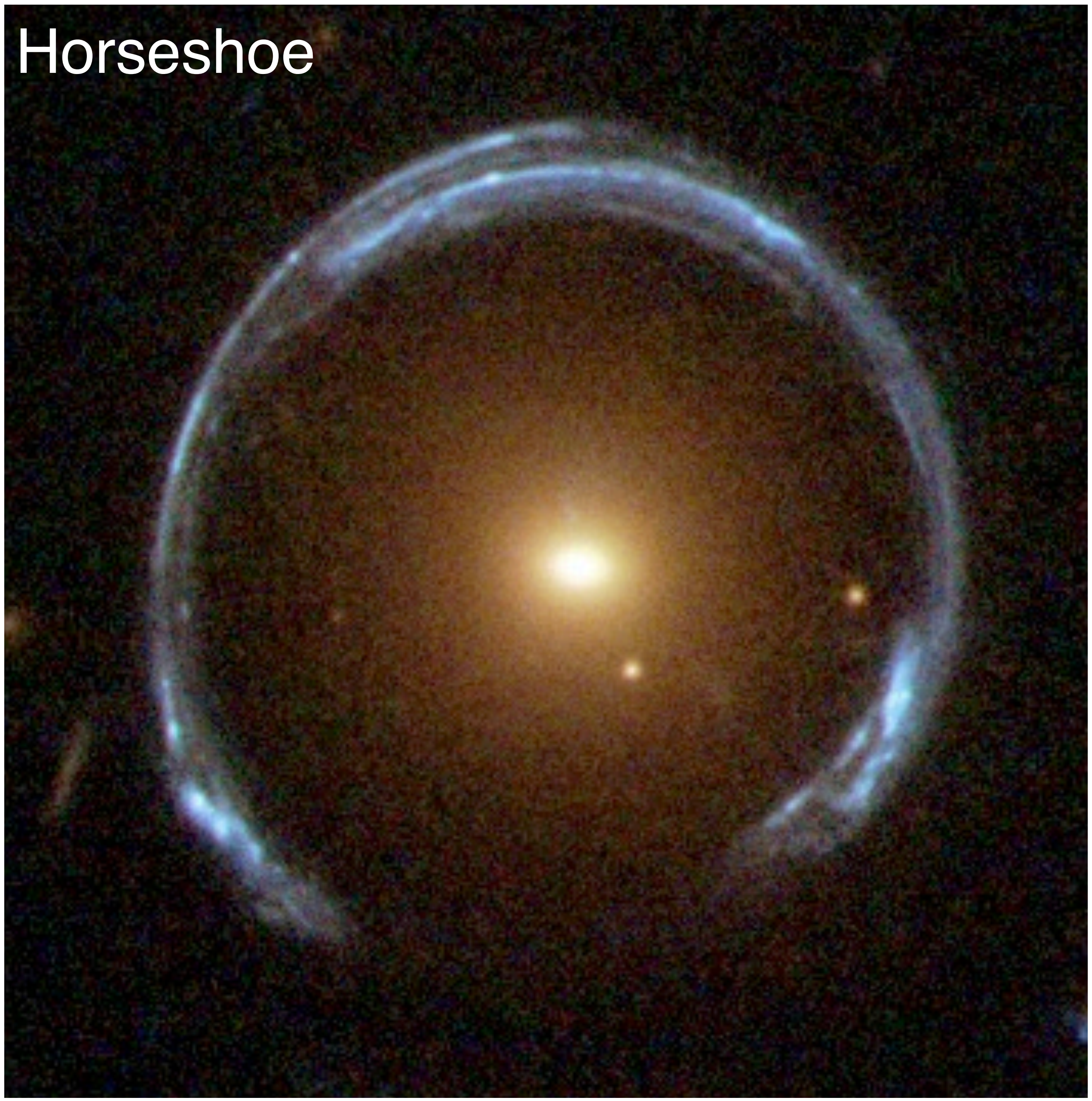

The Horseshoe system has a very large R_{einst}=30 kpc but only a single galaxy in the center suggesting an extremely massive DM halo.

Table 1. Properties of the cosmic Horseshoe[1].

	Parameter	Values
Lens Galaxy	RA	11h 48m 33.15s
	Dec	19° 30′ 03.″5
	Redshift	0.444
	Effective radii	$1.''96 \pm 0.''02$
	g_L	(20.84 ± 0.06) mag
	r_L	(19.00 ± 0.02) mag
	i_L	(18.22 ± 0.01) mag
	z_L	(17.75 ± 0.04) mag
	Axis ratio, g	0.8 ± 0.1
Source	Redshift[2]	2.38115 ± 0.00012
	Star formation rate	$\sim 100\, M_\odot\, \mathrm{yr}^{-1}$
	Dynamical mass	$M_{vir} \simeq 10^{10}\, M_\odot$
Ring	Diameter	$10.''2$
	Length	$\sim 300°$
	u_L	21.6 mag
	g_L	20.1 mag
	i_L	19.7 mag
	Mass enclosed[3]	$(5.02 \pm 0.09) \times 10^{12}\, M_\odot$

[1] Belokurov et al. (2007) measured the redshift of the source to be $z = 2.379$. We find a systematic shift that brings the source redshift to be $z = 2.3811$ in agreement with Quider et al. (2009).
[2] The mass within the Einstein radius or, more precisely, within the ring diameter, is taken from Dye et al. (2008).
[3] Parameters obtained from images taken with the 2.5 m Isaac Newton Telescope (INT). Magnitudes are taken from SDSS DR7. See Belokurov et al. (2007)

Single-Component Mass Models

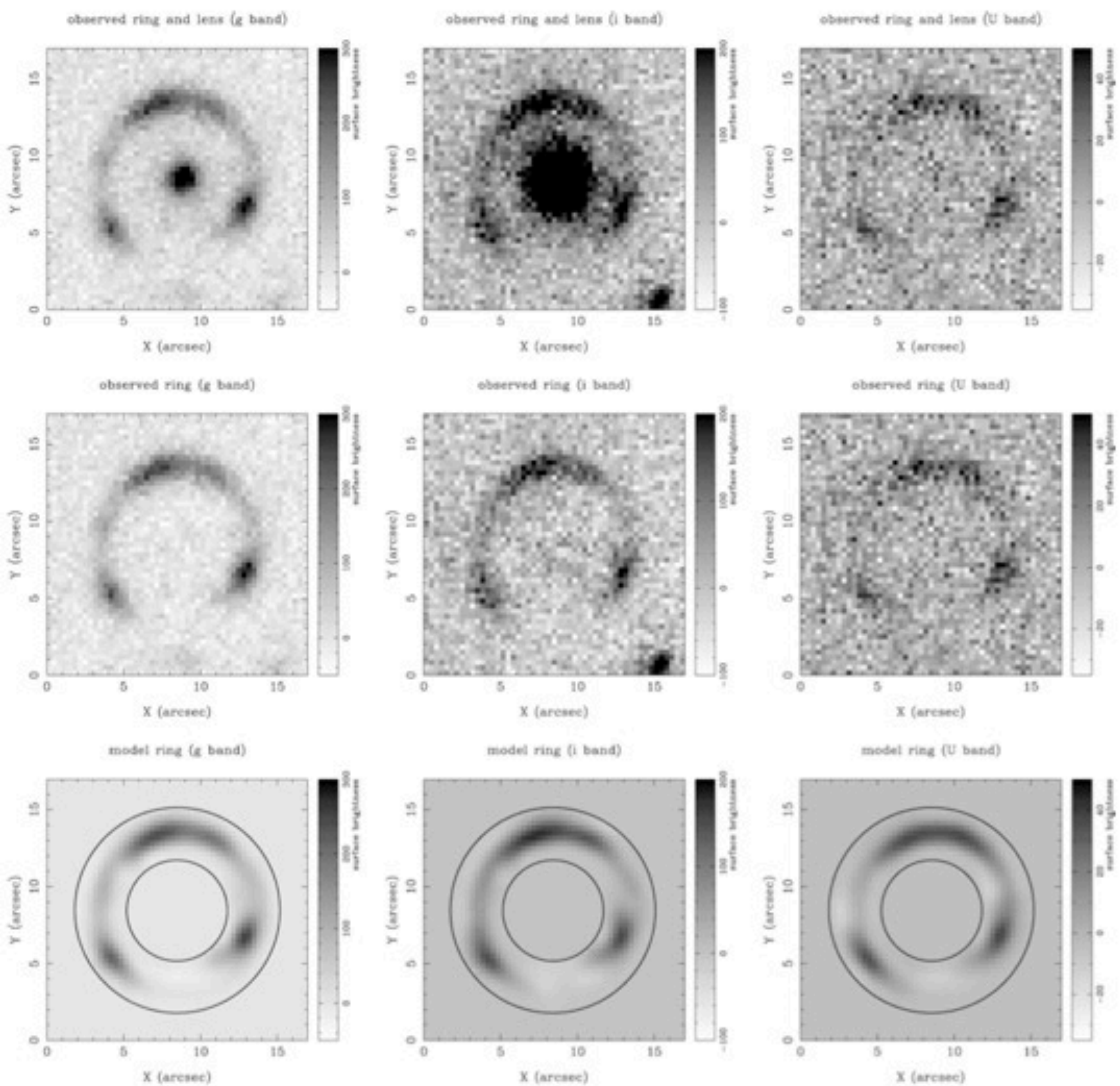

Dye et al. 2008

The Horseshoe system has a very large R_{einst}=30 kpc but only a single galaxy in the center suggesting an extremely massive DM halo.

Table 1. Properties of the cosmic Horseshoe[1].

	Parameter	Values
Lens Galaxy	RA	11h 48m 33.15s
	Dec	$19^\circ\ 30'\ 03''.5$
	Redshift	0.444
	Effective radii	$1''.96 \pm 0''.02$
	g_L	(20.84 ± 0.06) mag
	r_L	(19.00 ± 0.02) mag
	i_L	(18.22 ± 0.01) mag
	z_L	(17.75 ± 0.04) mag
	Axis ratio, g	0.8 ± 0.1
Source	Redshift[2]	2.38115 ± 0.00012
	Star formation rate	$\sim 100\, M_\odot\, \mathrm{yr}^{-1}$
	Dynamical mass	$M_{vir} \simeq 10^{10}\, M_\odot$
Ring	Diameter	$10''.2$
	Length	$\sim 300^\circ$
	u_L	21.6 mag
	g_L	20.1 mag
	i_L	19.7 mag
	Mass enclosed[3]	$(5.02 \pm 0.09) \times 10^{12}\, M_\odot$

[1] Belokurov et al. (2007) measured the redshift of the source to be $z = 2.379$. We find a systematic shift that brings the source redshift to be $z = 2.3811$ in agreement with Quider et al. (2009).
[2] The mass within the Einstein radius or, more precisely, within the ring diameter, is taken from Dye et al. (2008).
[3] Parameters obtained from images taken with the 2.5 m Isaac Newton Telescope (INT). Magnitudes are taken from SDSS DR7. See Belokurov et al. (2007)

Single-Component Mass Models

Parameter	SIE	NFW	PL
κ_0	2.50 ± 0.03	0.118 ± 0.002	2.30 ± 0.03
θ	46.5 ± 2.7	55.5 ± 3.1	49.2 ± 3.0
q	0.76 ± 0.03	0.89 ± 0.02	0.78 ± 0.03
x_c	-0.12 ± 0.04 arcsec	-0.10 ± 0.04 arcsec	-0.11 ± 0.04 arcsec
y_c	0.05 ± 0.03 arcsec	0.04 ± 0.03 arcsec	0.02 ± 0.03 arcsec
α	–	–	1.96 ± 0.02
$\ln \epsilon$	-4237.7	-4262.7	-4235.4
Param.	SIE+γ	NFW+γ	PL+γ
κ_0	2.58 ± 0.03	0.116 ± 0.002	2.37 ± 0.03
θ	49.8 ± 2.7	47.9 ± 3.1	50.8 ± 3.1
q	0.81 ± 0.02	0.86 ± 0.02	0.83 ± 0.02
x_c	-0.10 ± 0.04 arcsec	-0.09 ± 0.04 arcsec	-0.11 ± 0.04 arcsec
y_c	0.03 ± 0.03 arcsec	0.04 ± 0.03 arcsec	0.04 ± 0.03 arcsec
α	–	–	1.95 ± 0.02
γ	0.017 ± 0.005	0.011 ± 0.006	0.020 ± 0.005
θ_γ	38.2 ± 9.4	46.1 ± 12.4	37.7 ± 8.6
$\ln \epsilon$	-4239.0	-4272.0	-4240.2

Residuals: SIE NFW Power-law

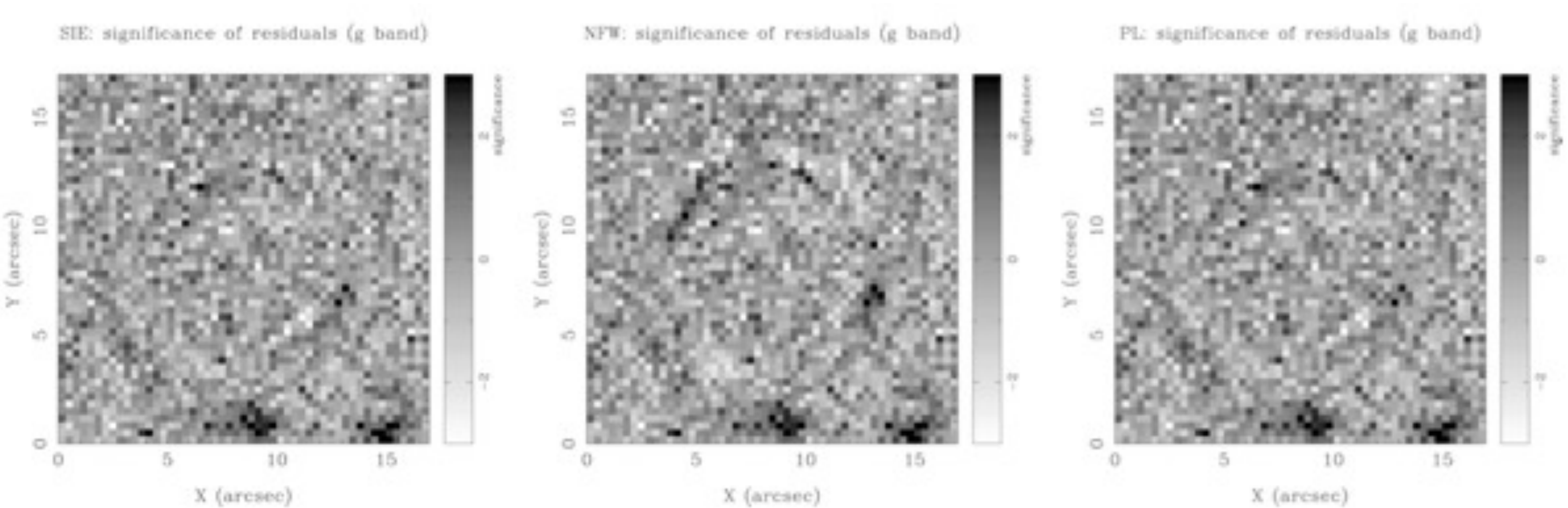

Dye et al. 2008

Different models can be compared via the Bayesian Evidence:

$$\mathcal{E} \approx \mathcal{L}_{\max} \times \frac{V_{\rm post}}{V_{\rm prior}}$$

i.e. the marginalization over all model-parameters of the posterior PDF: Probability of the data, given the model-family

A SIE/PL model leaves nearly no residuals and has an evidence exceeding that of the NFW model [this is a massive group-like system]

Two-Component L&D Mass Models

Spiniello et al 2011

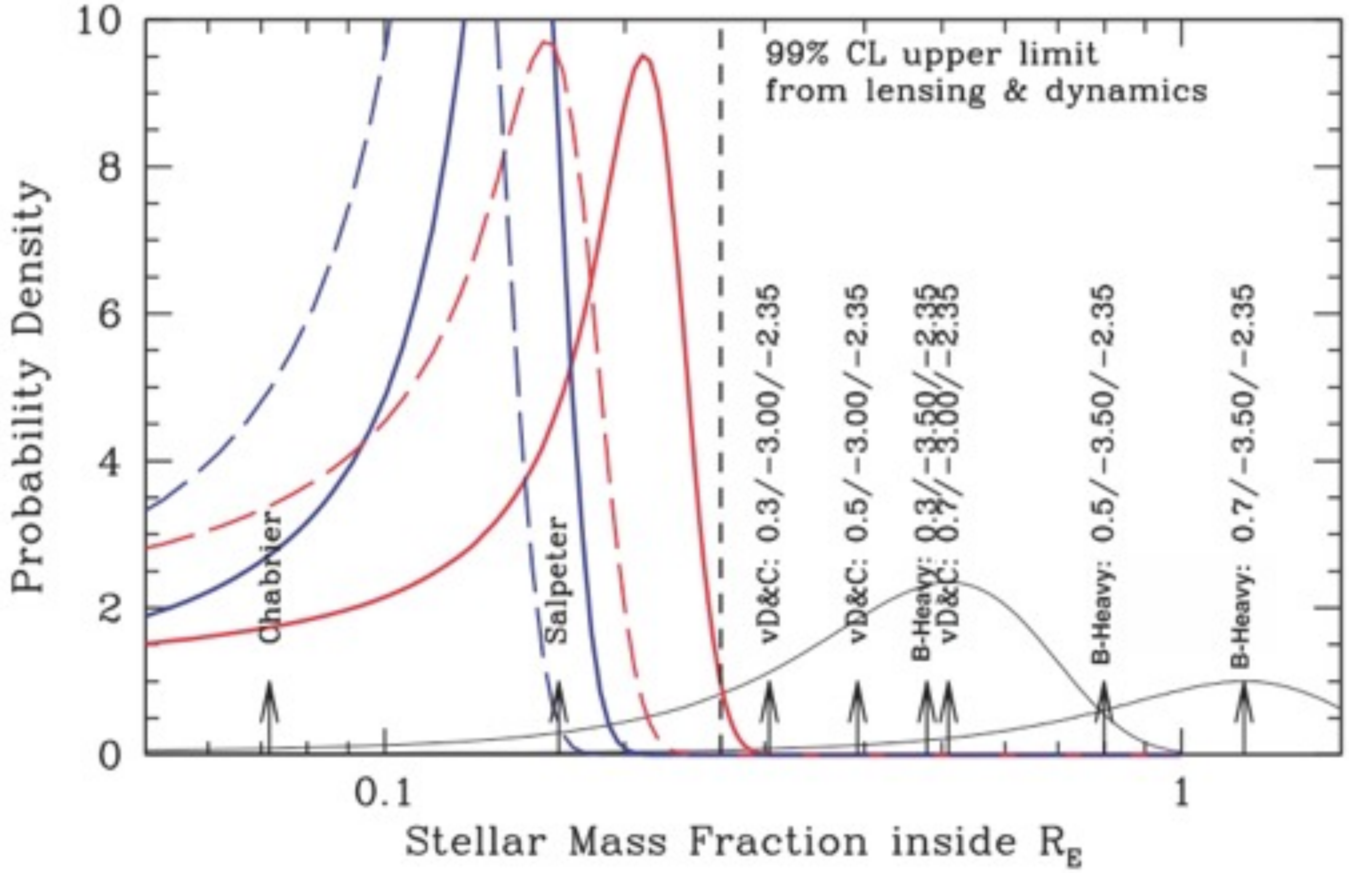

When the mass inside R_{einst} is combined with an extended kinematic profile, only a small subset of models still fits the data.

For a Hernquist (β=0) stellar component embedded in a gNFW DM halo, the posterior PDF for M_{star} gives:

$$f_{\rm DM}(< R_{\rm eff}) = 0.60^{+0.15}_{-0.06} \pm 0.1$$

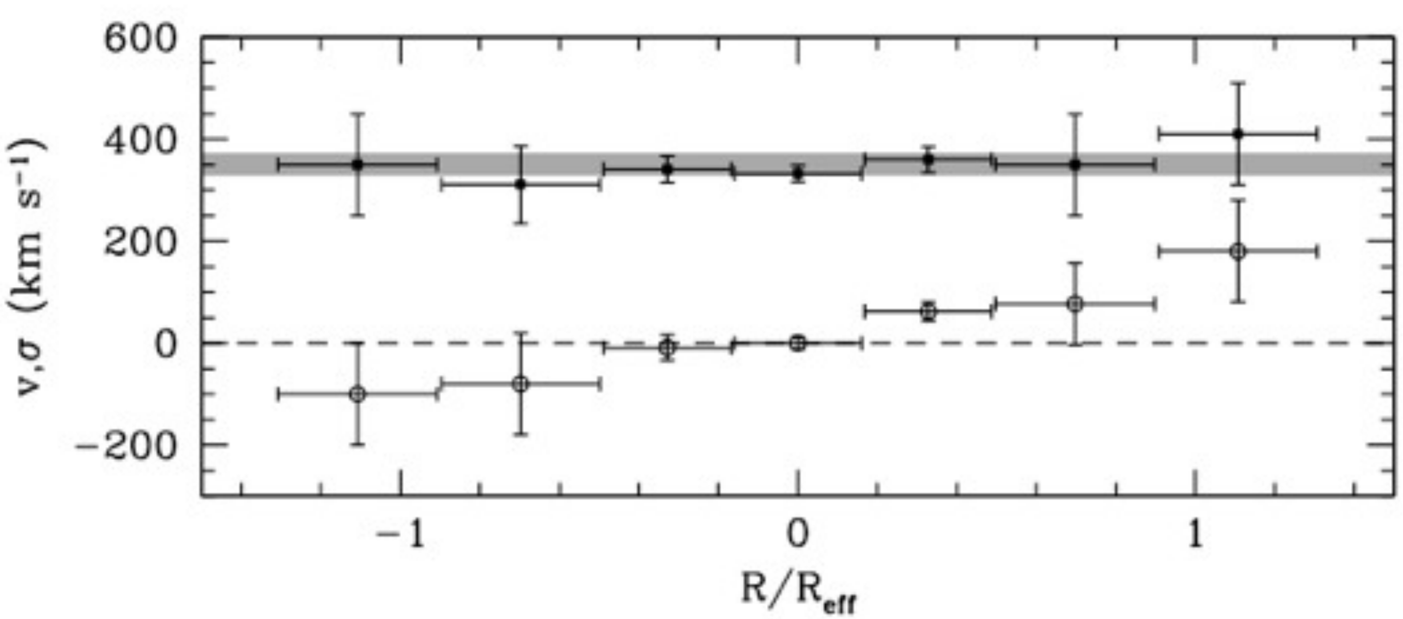

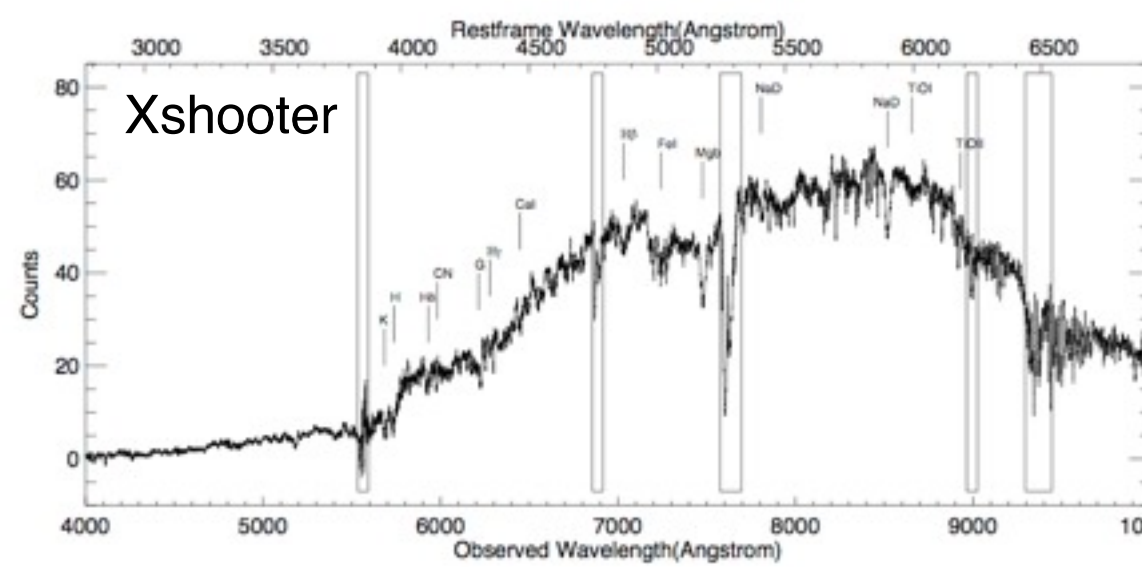

Scaling Relations versus Constant Stellar M/L Models

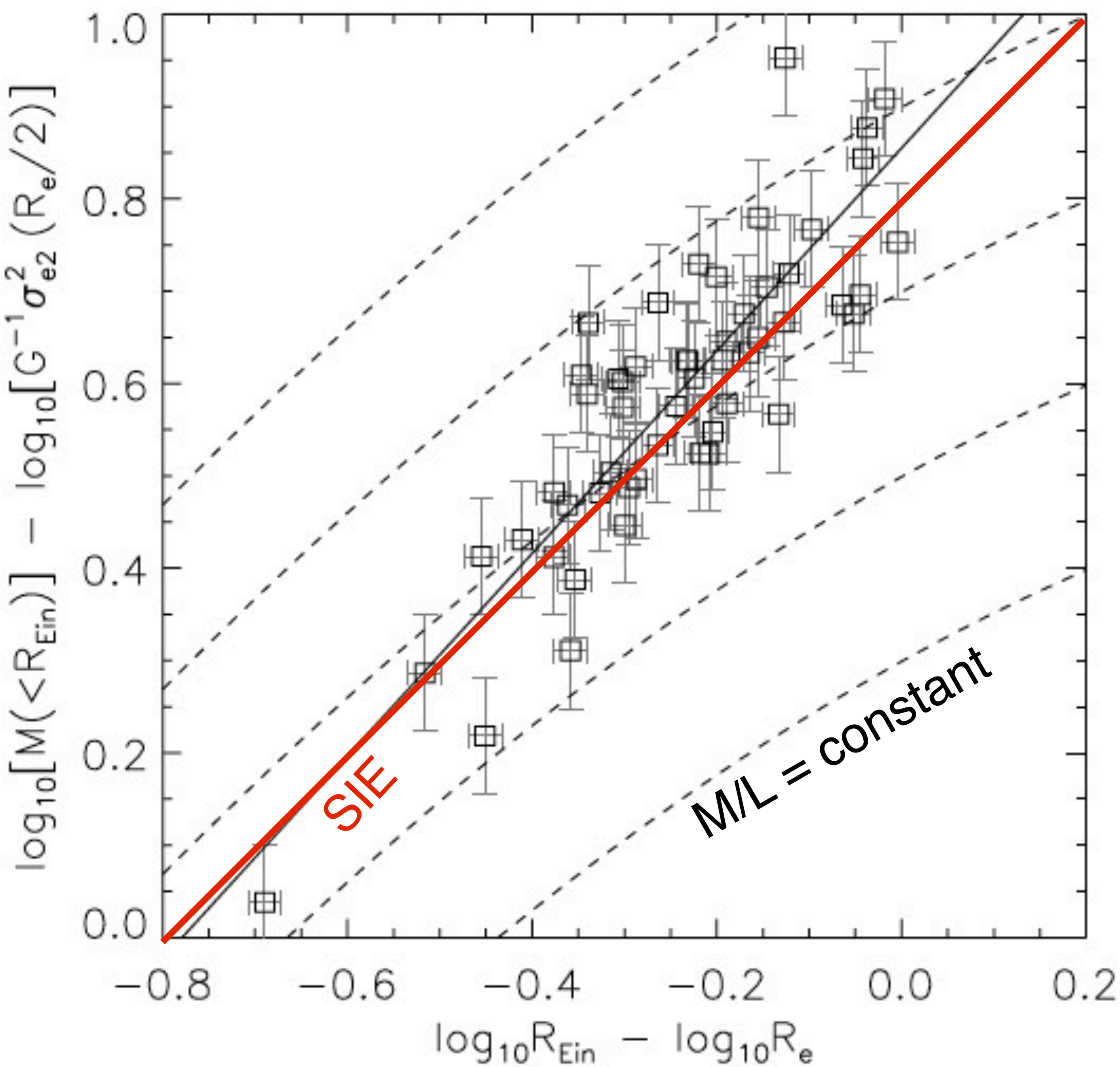

Under homology conditions, one can rescale (i) R_{Einst}/R_{eff} and (ii) $M_{einst}/(\sigma^2 R_{eff})$.

One finds that lenses follow a power-law density distribution.

Constant M/L models can be excluded at >99.9% CL and $<f_{DM}>$=0.38+-0.07 (68%) inside R_{eff}.

Bolton et al. 2008; also Koopmans et al. 2009

DM Density Slopes inside $R_{Einst/eff}$

Combination with Stellar Dynamics

Constant M/L model versus SIS

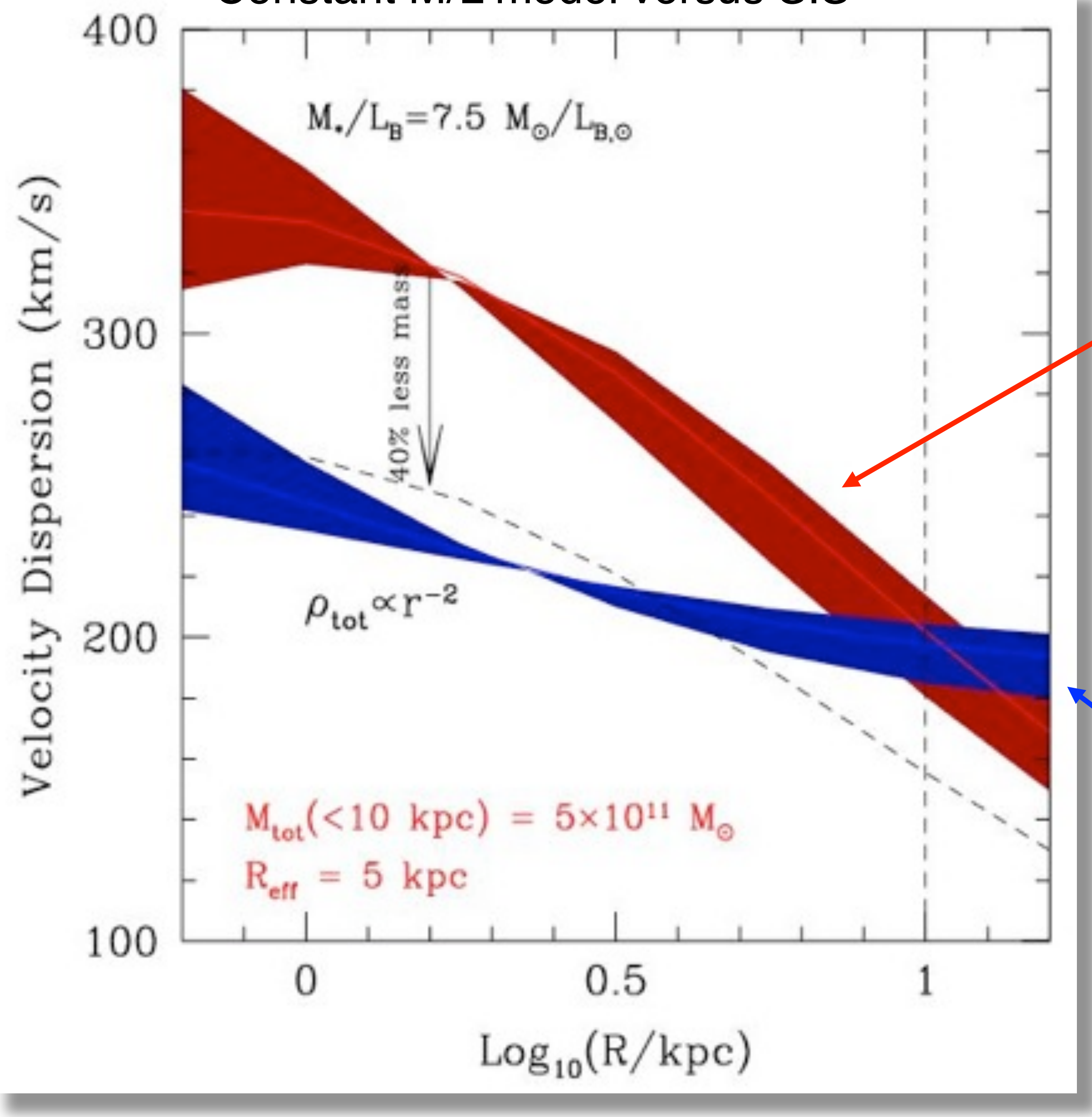

$$\langle v_{||}^2 \rangle (\leq R_{\rm A}) = \frac{1}{\pi} \left[\frac{G M_{\rm E}}{R_{\rm E}} \right] f(\gamma', \delta, \beta) \times \left(\frac{R_{\rm A}}{R_{\rm E}} \right)^{2-\gamma'}$$

$R^{1/4}$ constant M/L density profile

Lensing mass is the same

SIS density profile with stellar M/L=0

DM: Lensing & Dynamics

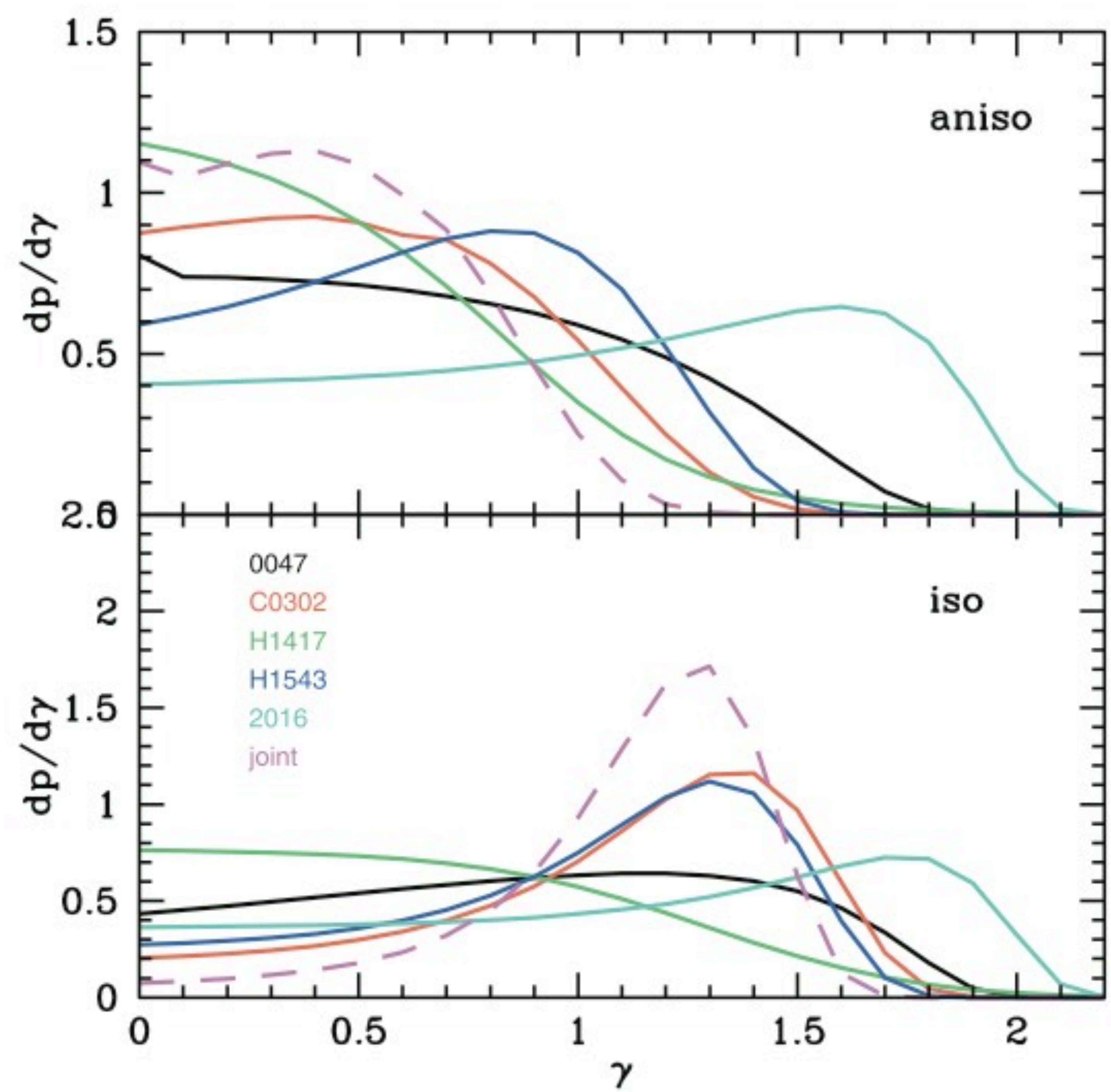

Treu & Koopmans 2004

Applying this technique through the spherical Jeans equations (w/β<>0) to five lens systems with lensing and kinematics (from Keck) at z~0.5-1.0, it was found for two-component models (HQ/JF+gNFW) that for β=0.

$$\langle\gamma_{\rm DM}\rangle = 1.3^{+0.2}_{-0.4} \quad (68\%{\rm CL})$$

$$f_{\rm DM} = 0.15 - 0.65 \quad {\rm inside}\ {\rm R}_{\rm eff}$$

And for Osipkov-Merritt model with $r_i = R_{eff}$

$$\langle\gamma_{\rm DM}\rangle < 0.6 \quad (68\%{\rm CL})$$

[Slope total mass is 0.45-0.90 steeper]

Adiabatic Contraction

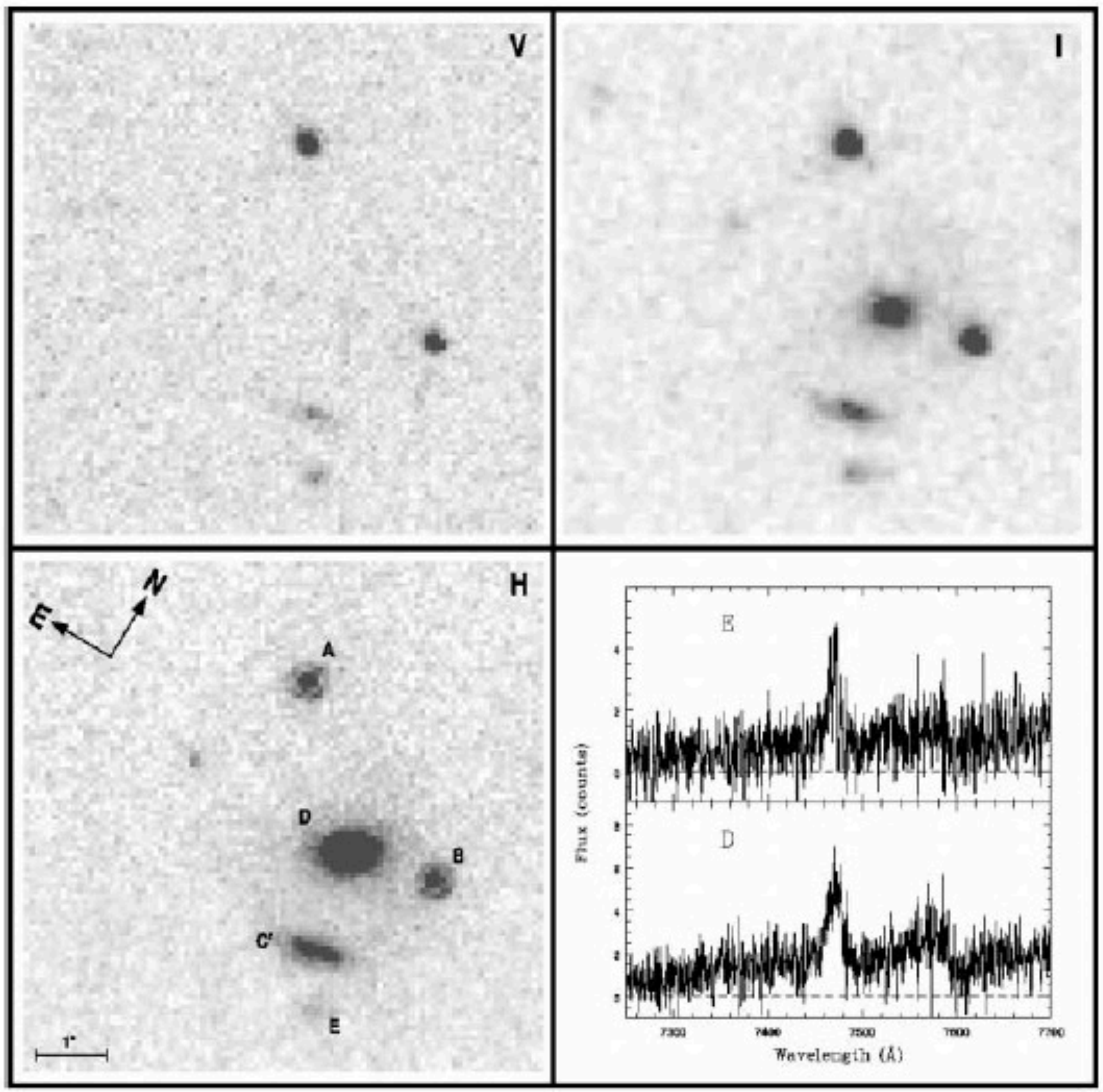

Treu & Koopmans 2002

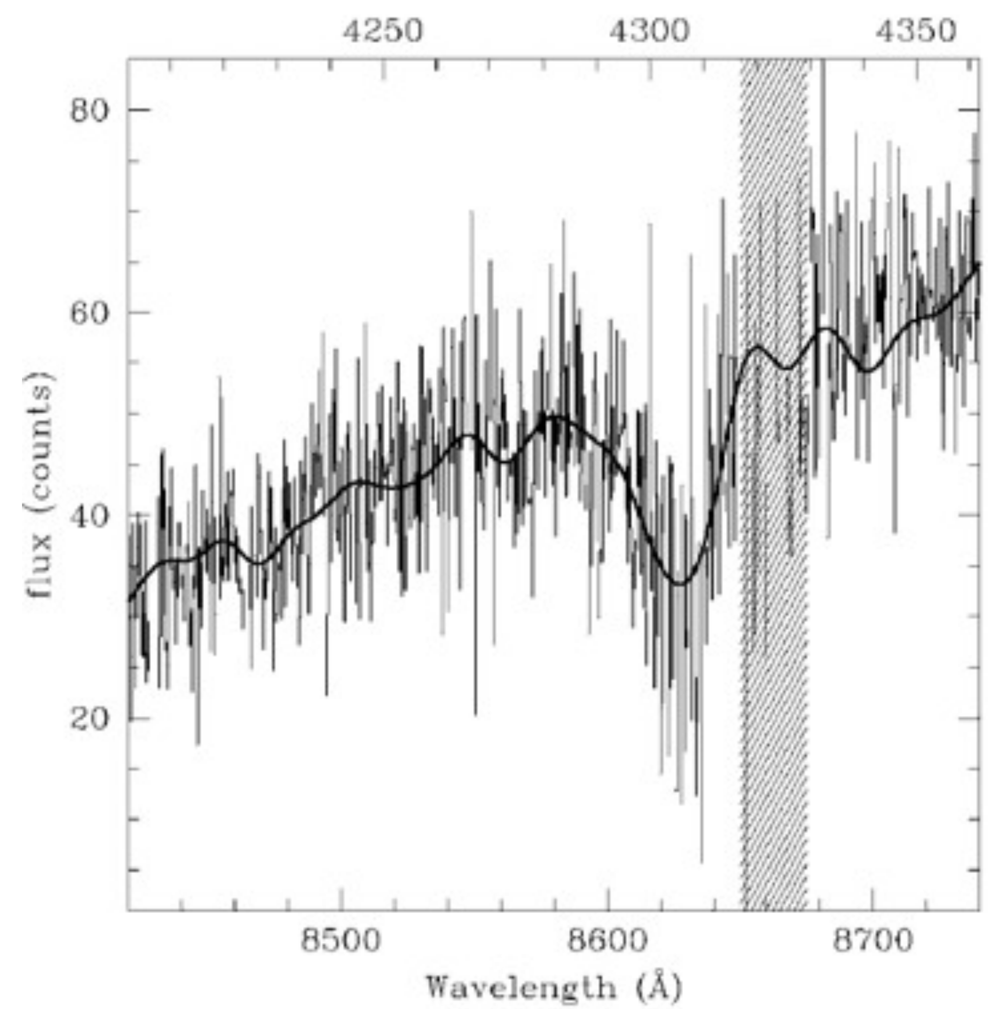

MG2016+112: ETG at z=1.01. R_{eff}~2.7 kpc; Stellar dispersion of 330+-32 km/s; 80% DM inside R_{Einst}~14 kpc

Adiabatic Contraction

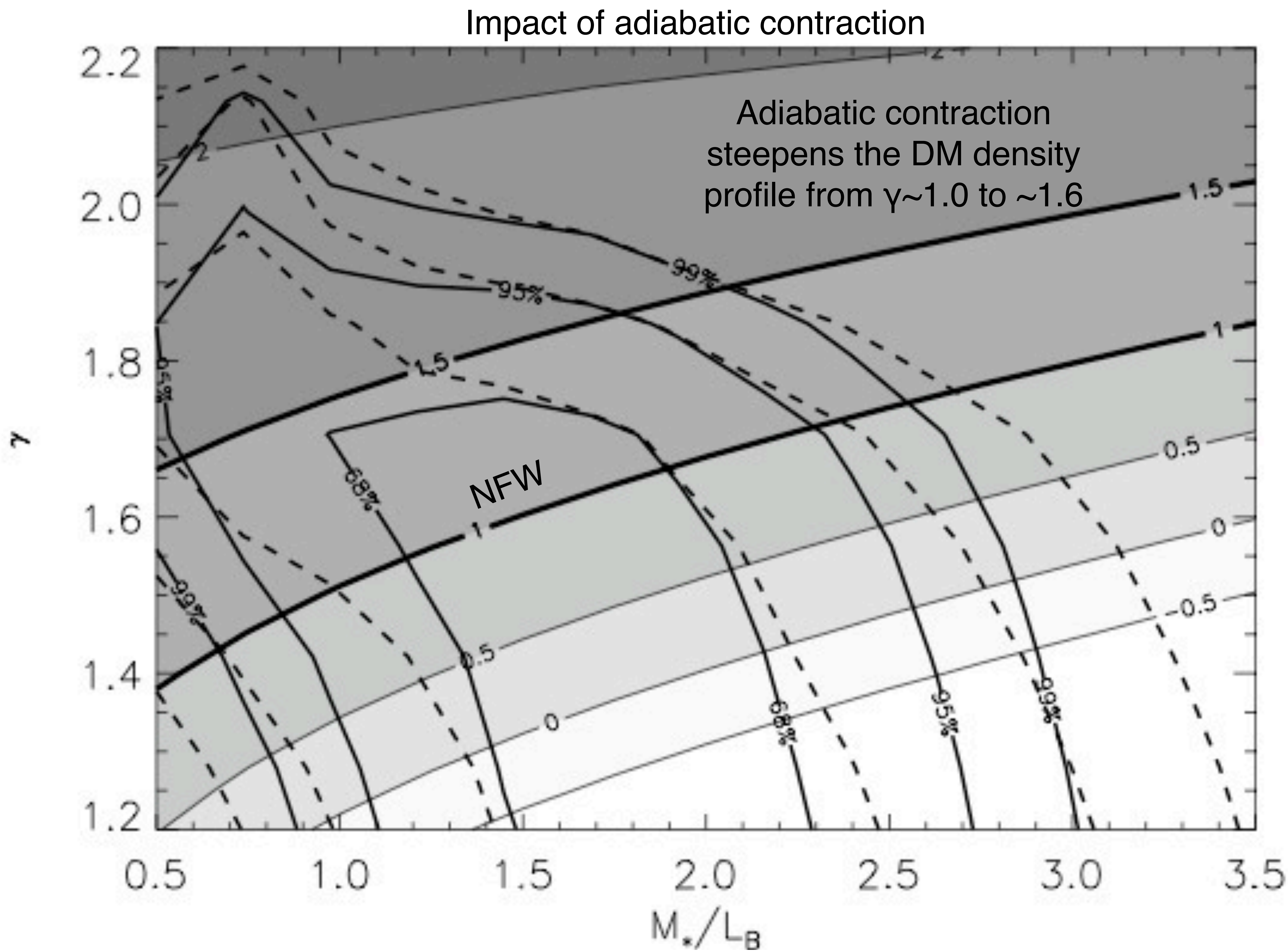

Adiabatic Contraction

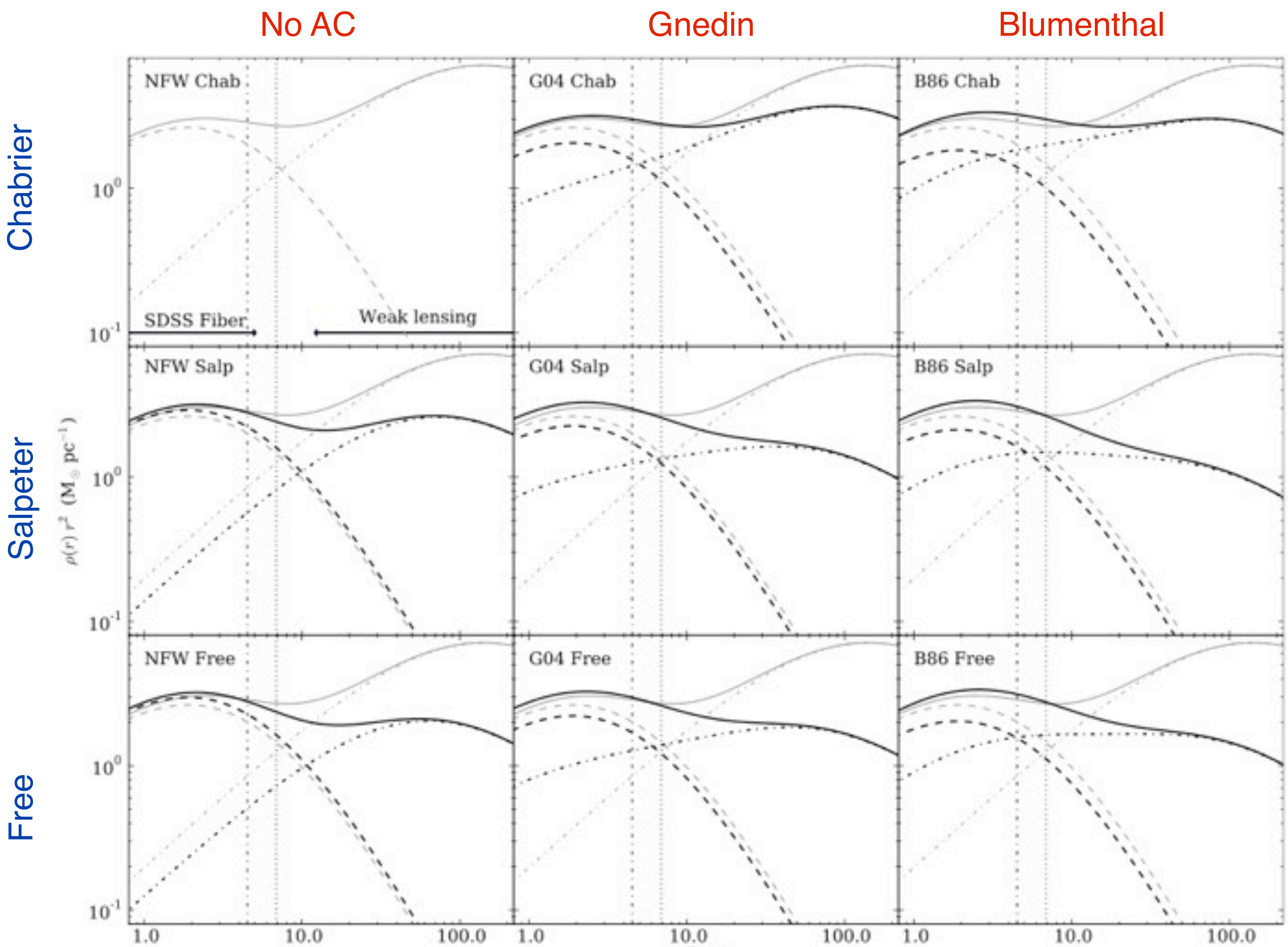

Contraction & IMF have major impact on the halo shape and required halo mass.

Constraints from WL, SL and dynamics prefer a heavy Salpeter-like IMF with some moderate AC.

Auger et al. 2010

Similarly: Scaling Relations for DM

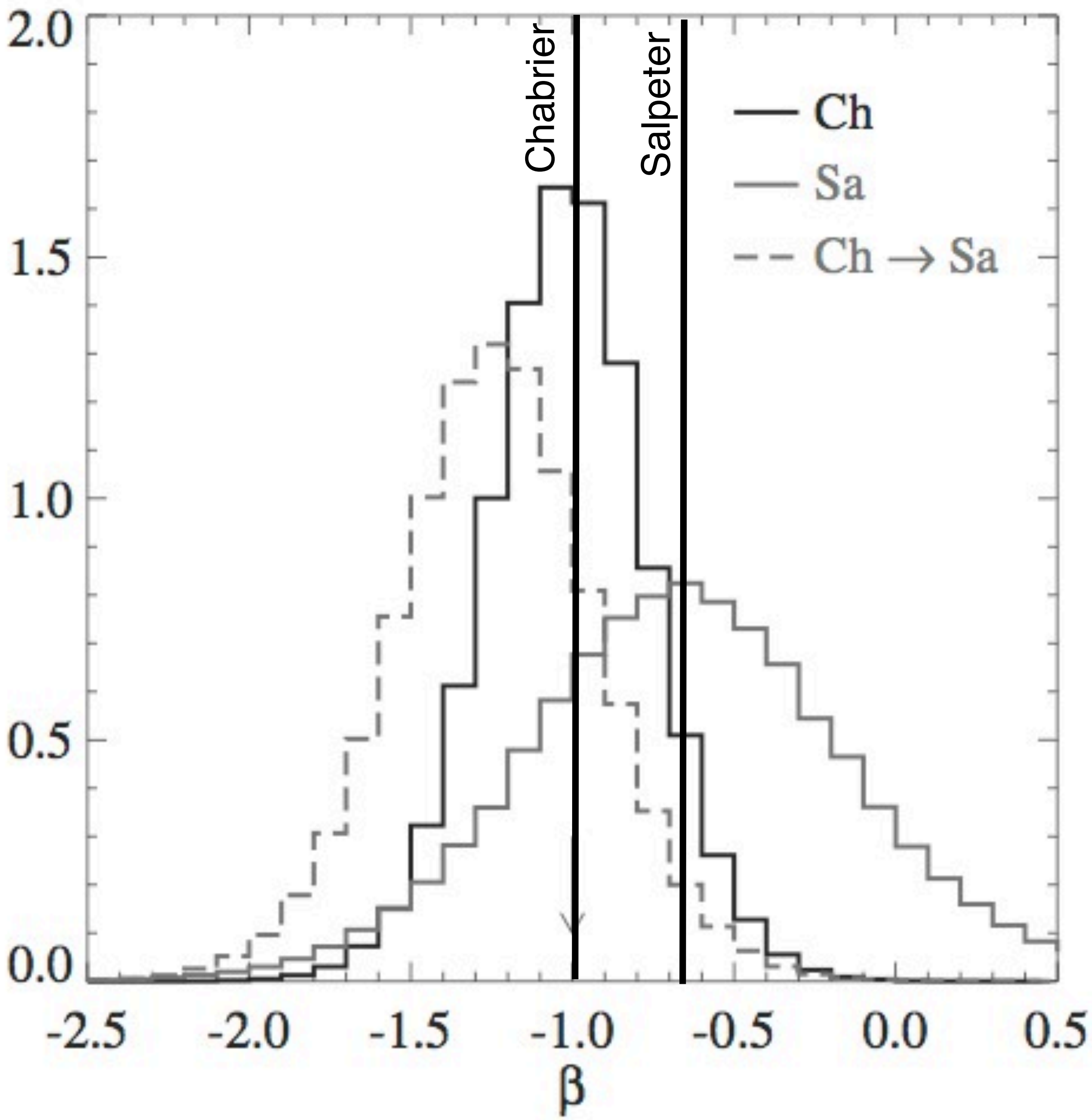

Rescaling lenses to a common DM mass-scale (substracting stellar mass) as function of R_{einst}/R_{eff} allows its density profile to be inferred.

Chabrier IMFs leads to low stellar masses and DM profiles close to γ'=1.7 (SIE), whereas Salpeter IMFs lead to more stellar mass and a more shallow DM profile (γ_{DM}=1.7), consistent with TK04.

Grillo et al. 2012

The Double Einstein Ring

If strong lensing provides M_{Einst} accurately inside R_{Einst}, then having two rings provides the density profile inside the two rings w/o hardly any assumption.

Color Composite

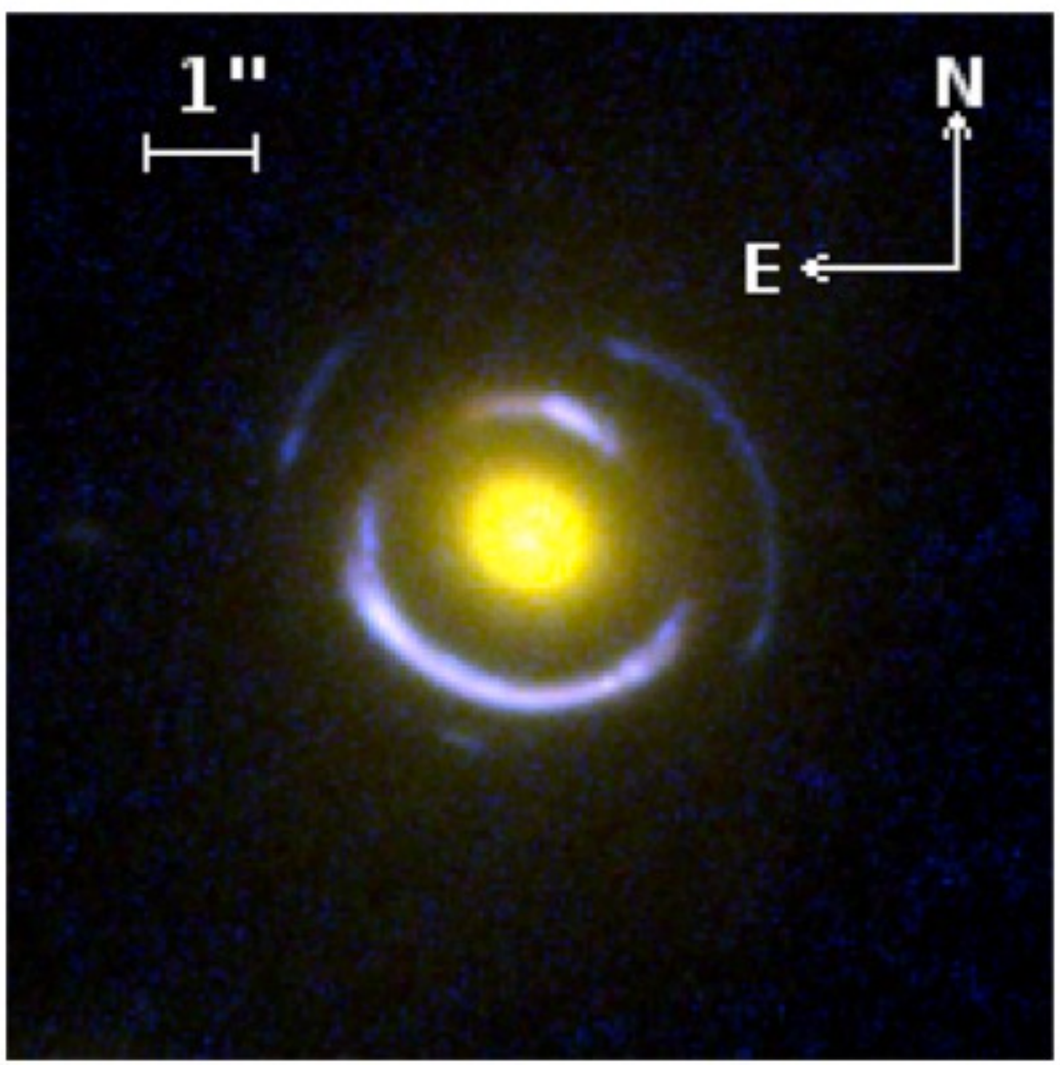

Multi-color HST data

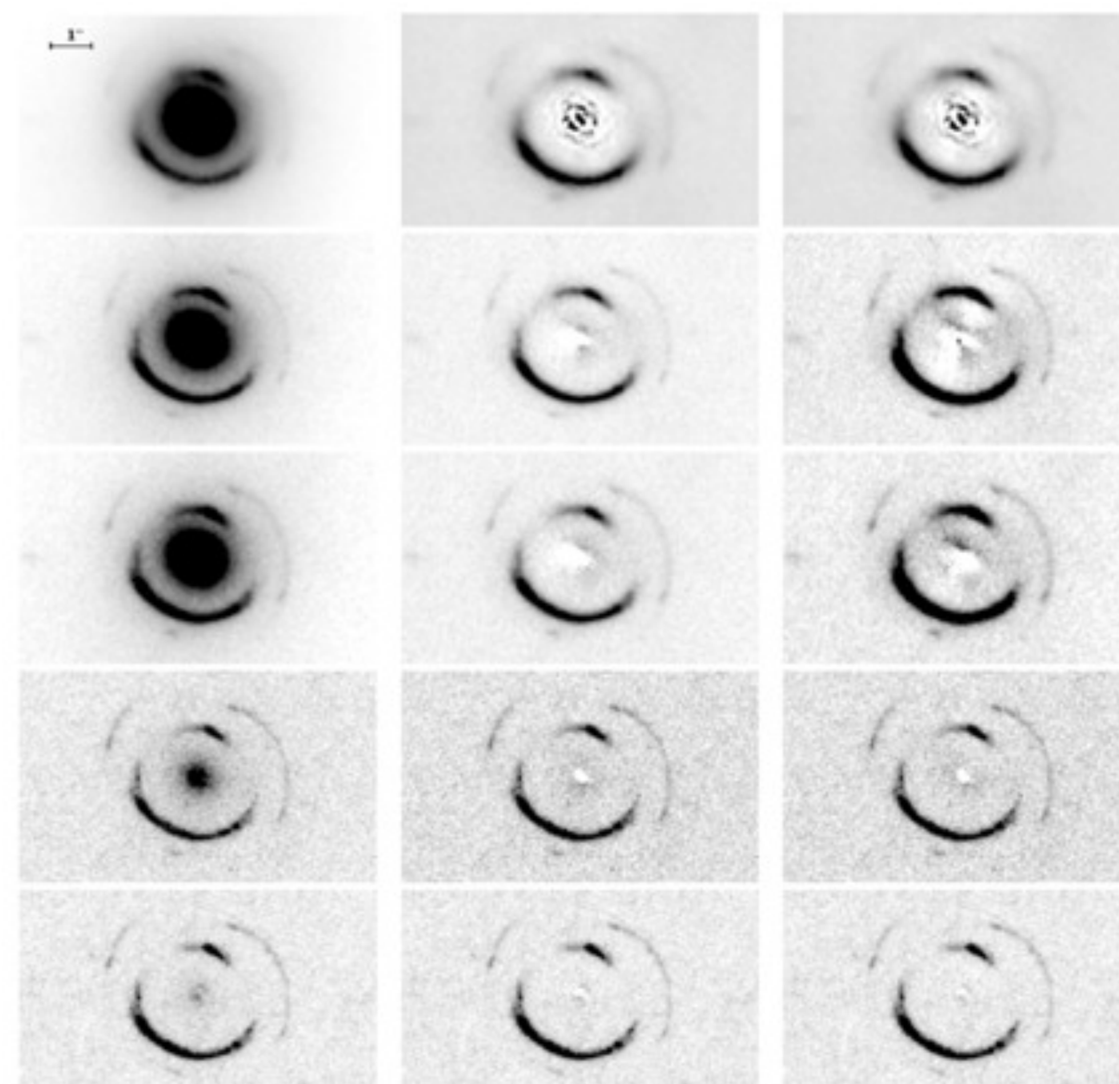

Sonnenfeld et al. 2012

The Double Einstein Ring

If strong lensing provides M_{Einst} accurately inside R_{Einst}, then having two rings provides the density profile inside the two rings w/o hardly any assumption.

Color Composite

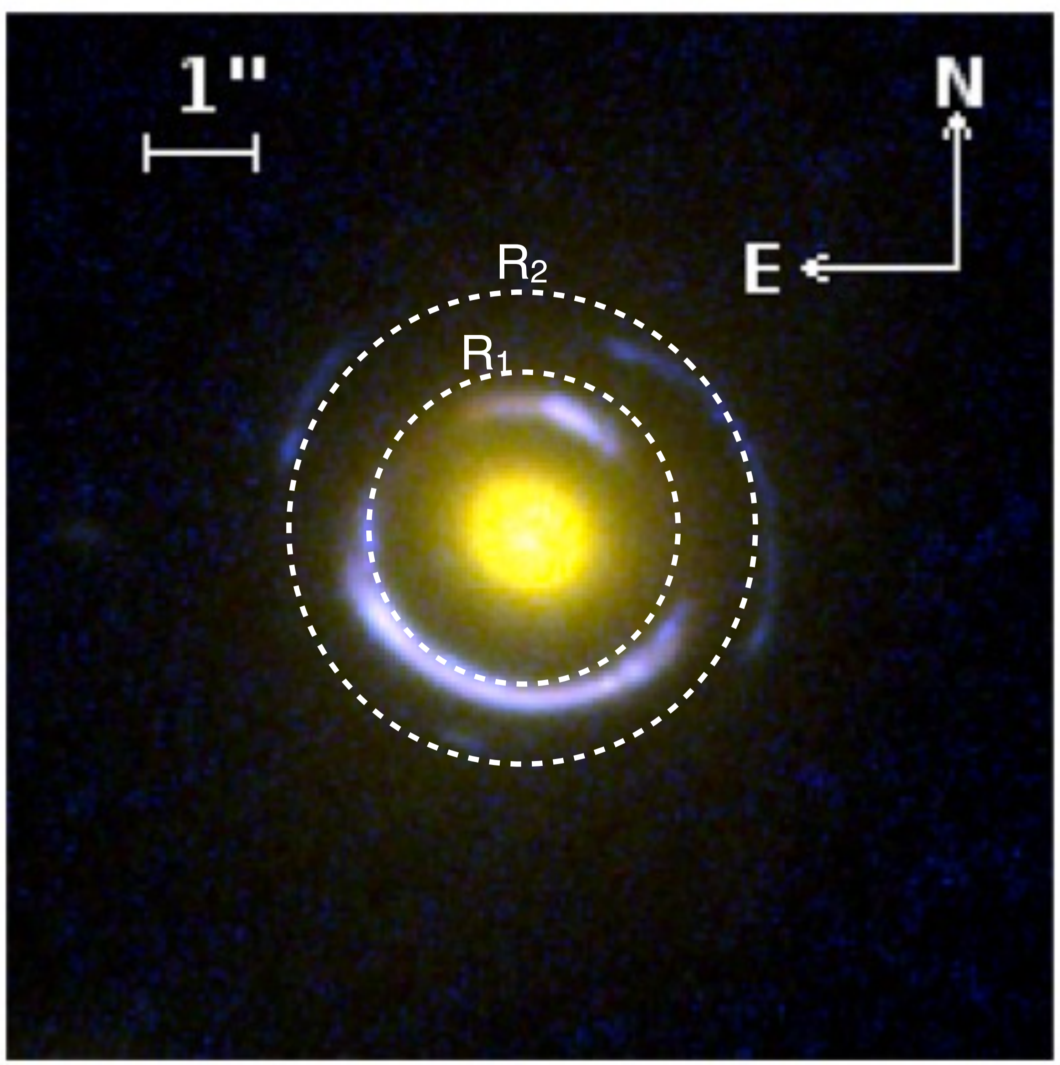

Multi-color HST data

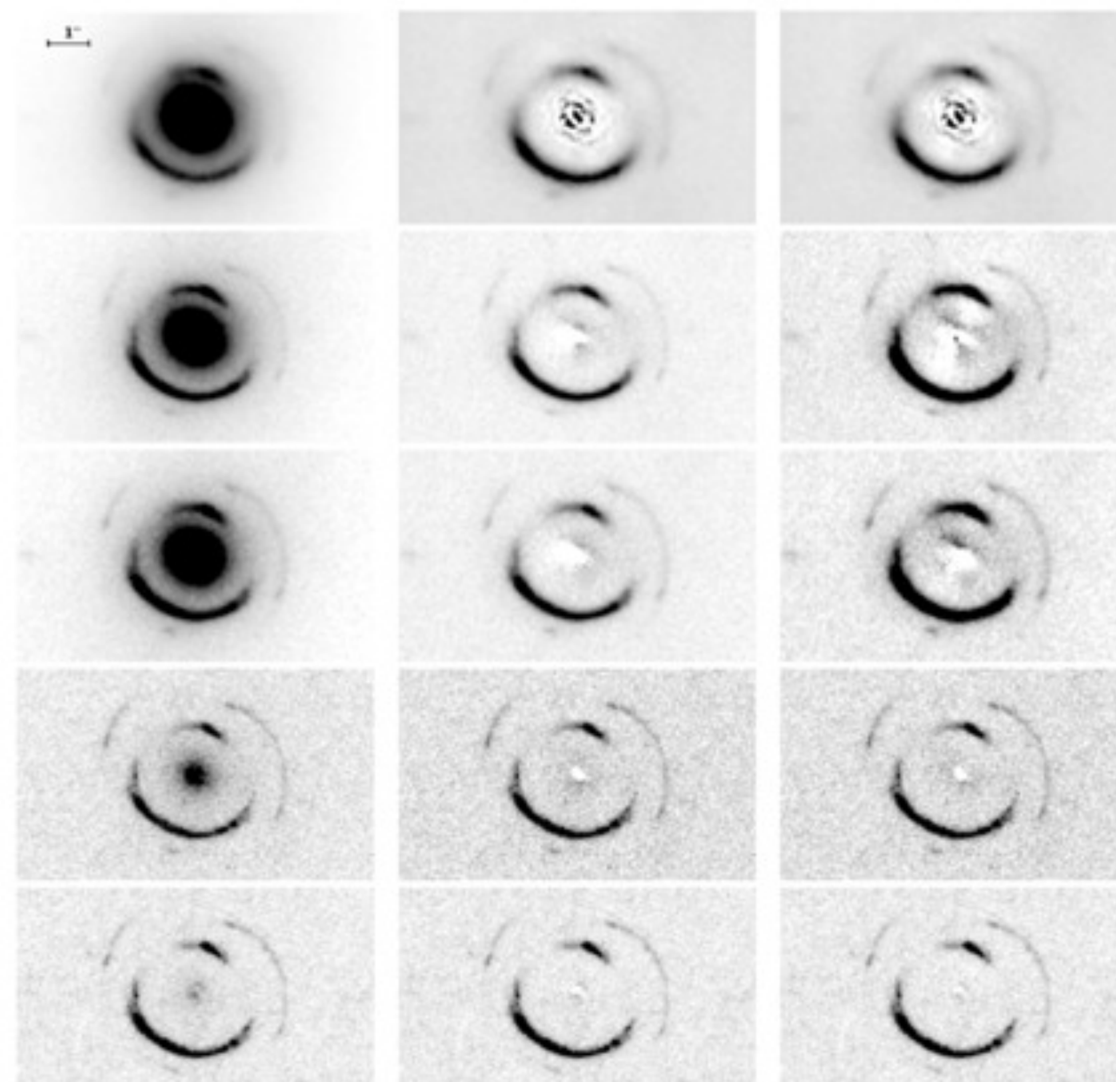

Sonnenfeld et al. 2012

The Double Einstein Ring

If strong lensing provides M_{Einst} accurately inside R_{Einst}, then having two rings provides the density profile inside the two rings w/o hardly any assumption.

Color Composite

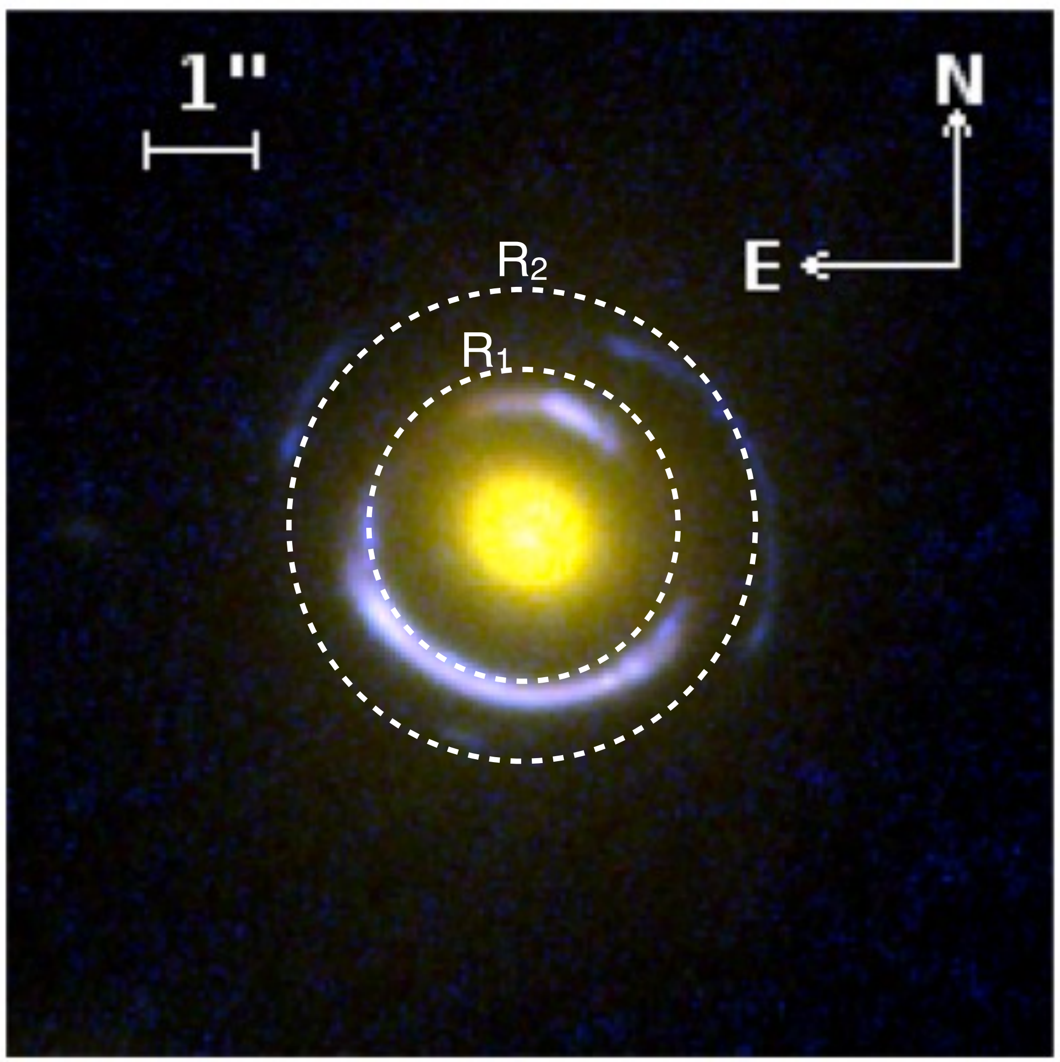

Multi-color HST data

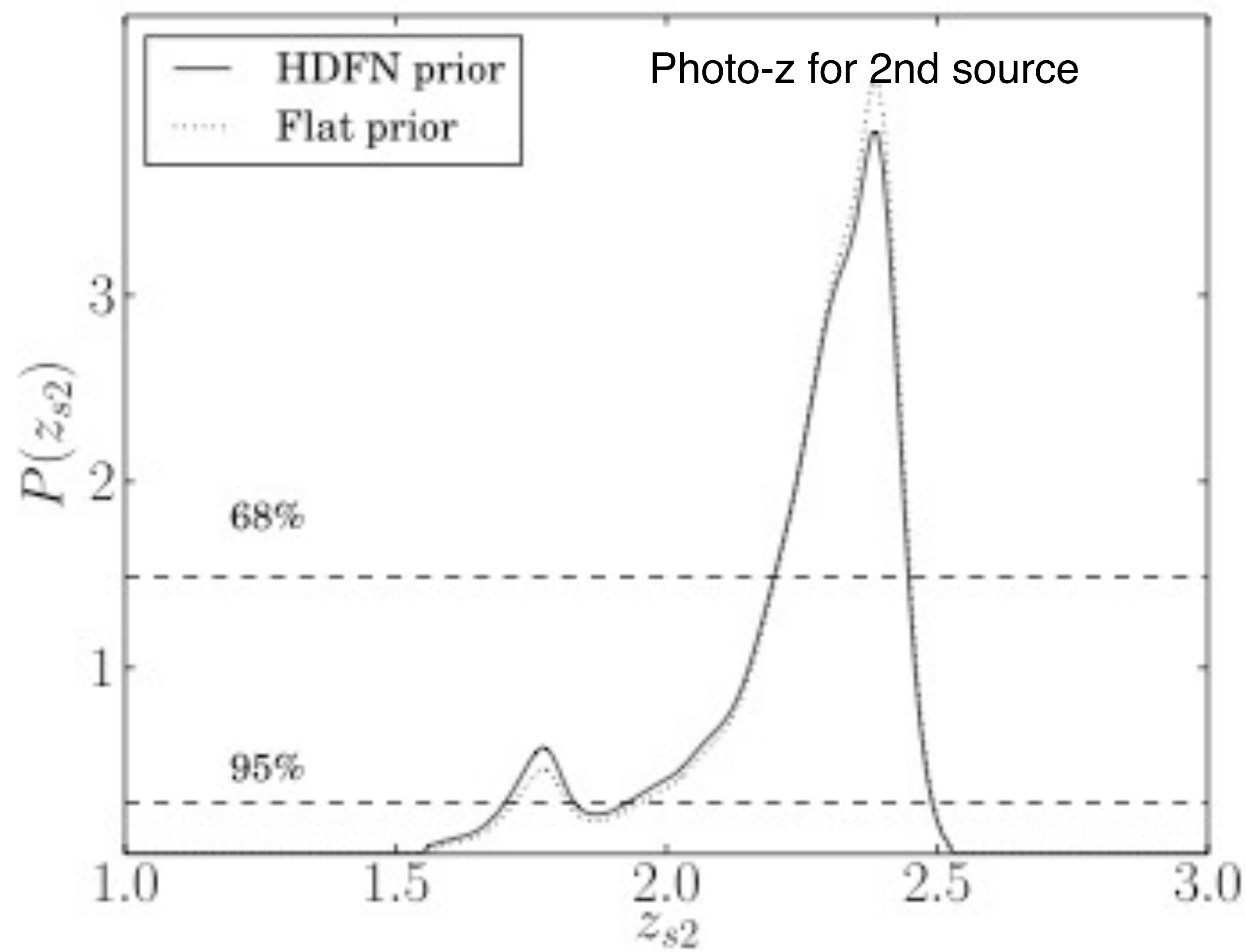

Sonnenfeld et al. 2012

The Double Einstein Ring

Combining the double Einstein ring data with an extended kinematic profile breaks the old single-ring-only degeneracy

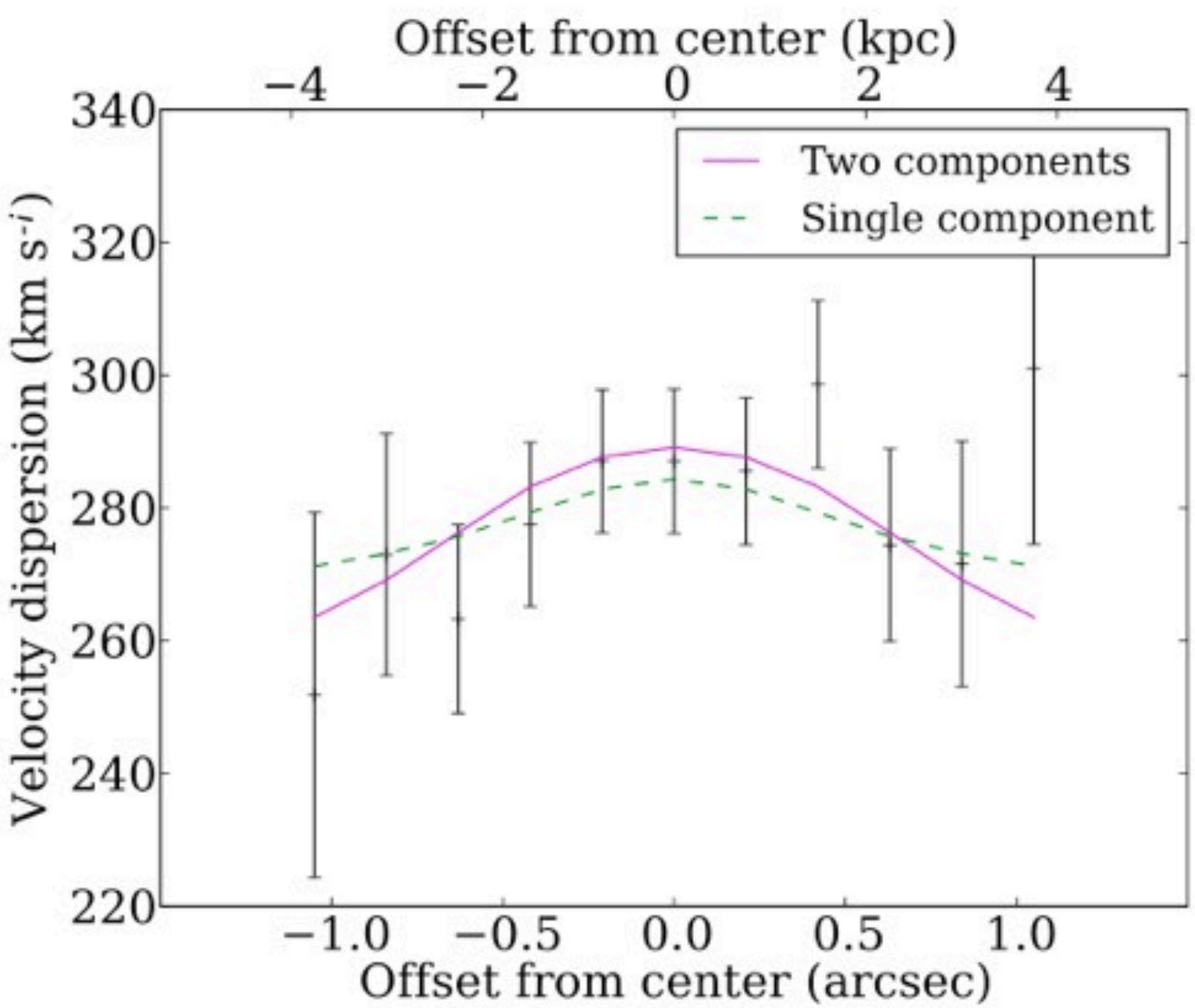

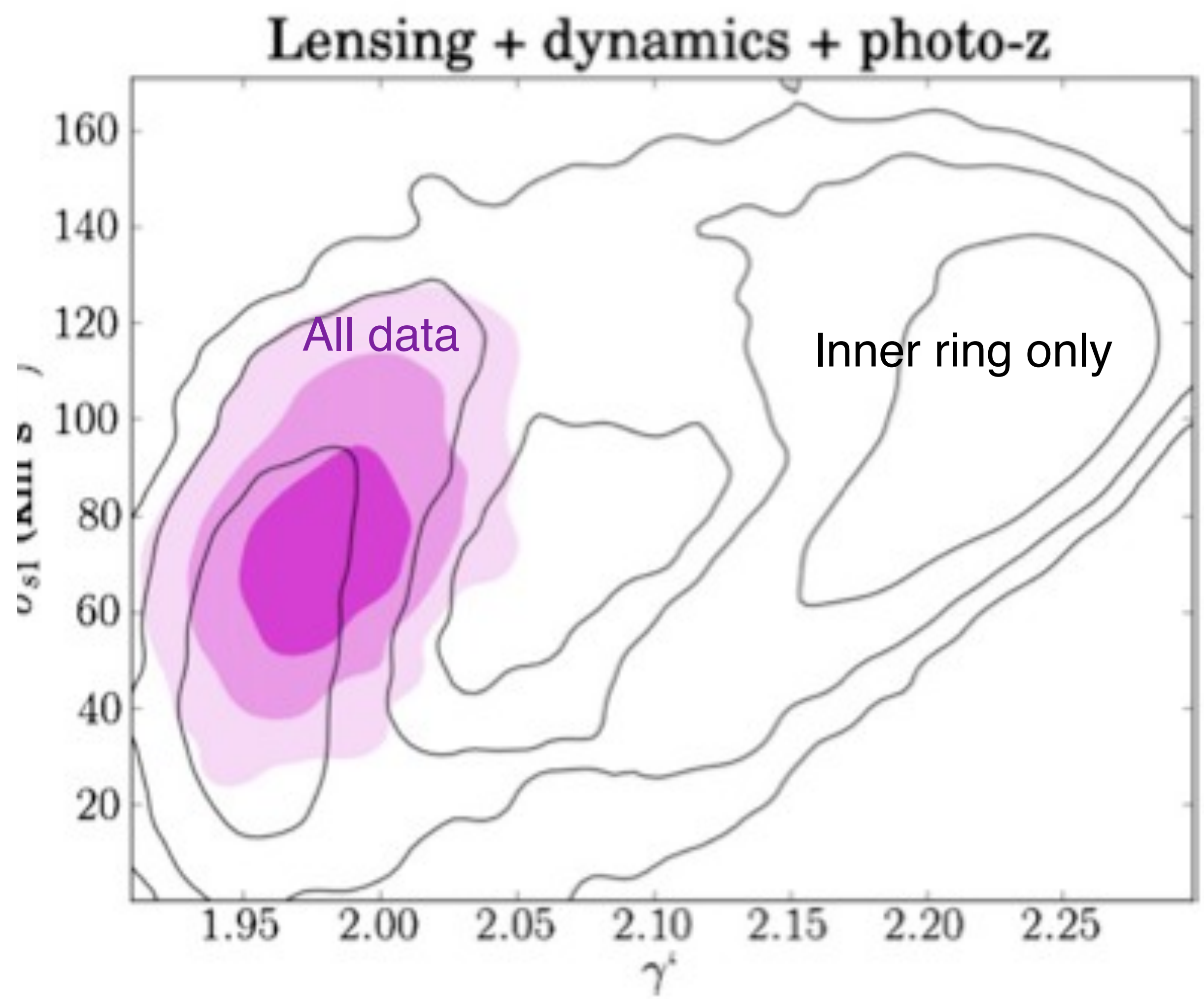

Sonnenfeld et al. 2012

The Double Einstein Ring

Full Bayesian MCMC exploration of parameter space:

γ_{DM}=1.7 ± 0.2

Sonnenfeld et al. 2012

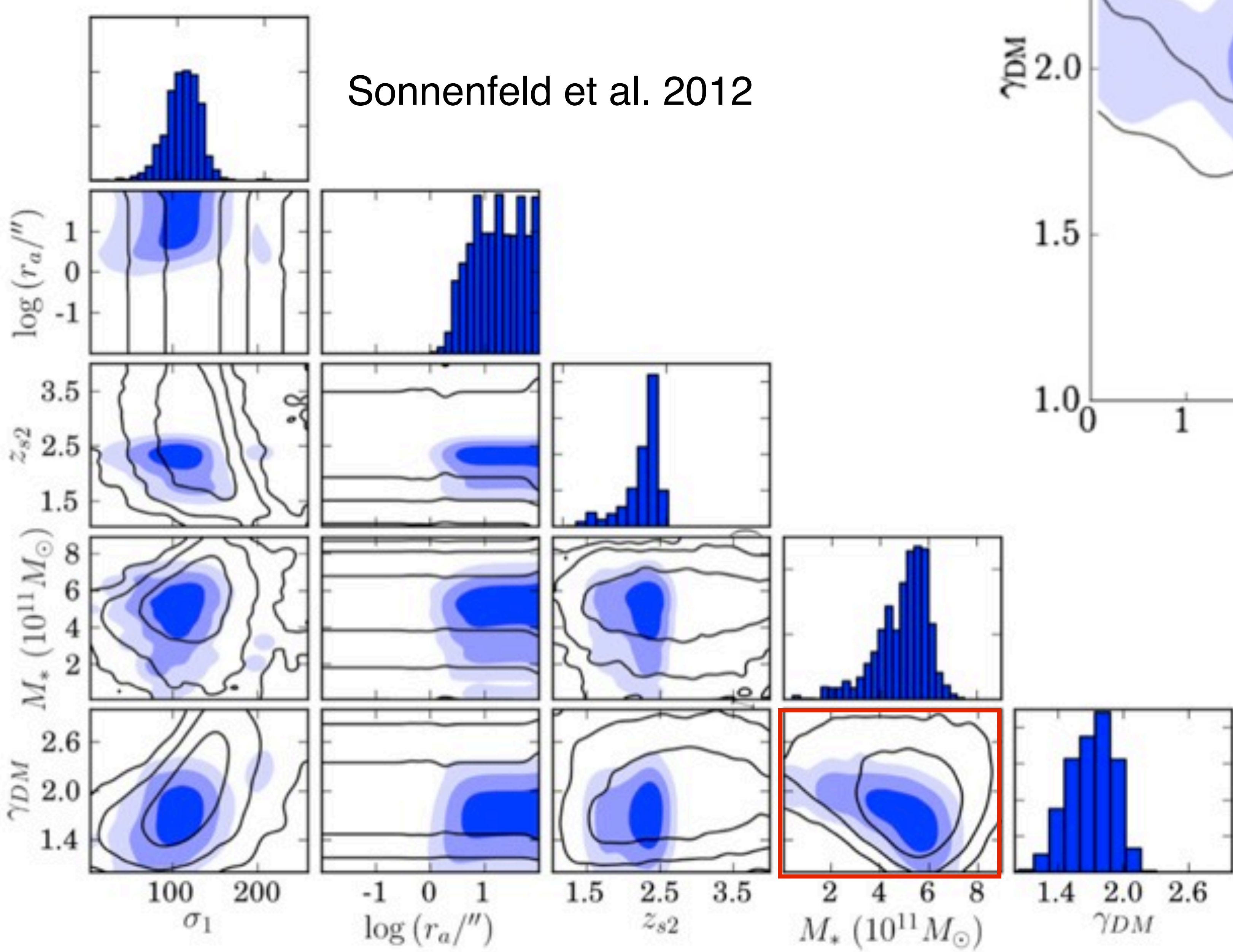

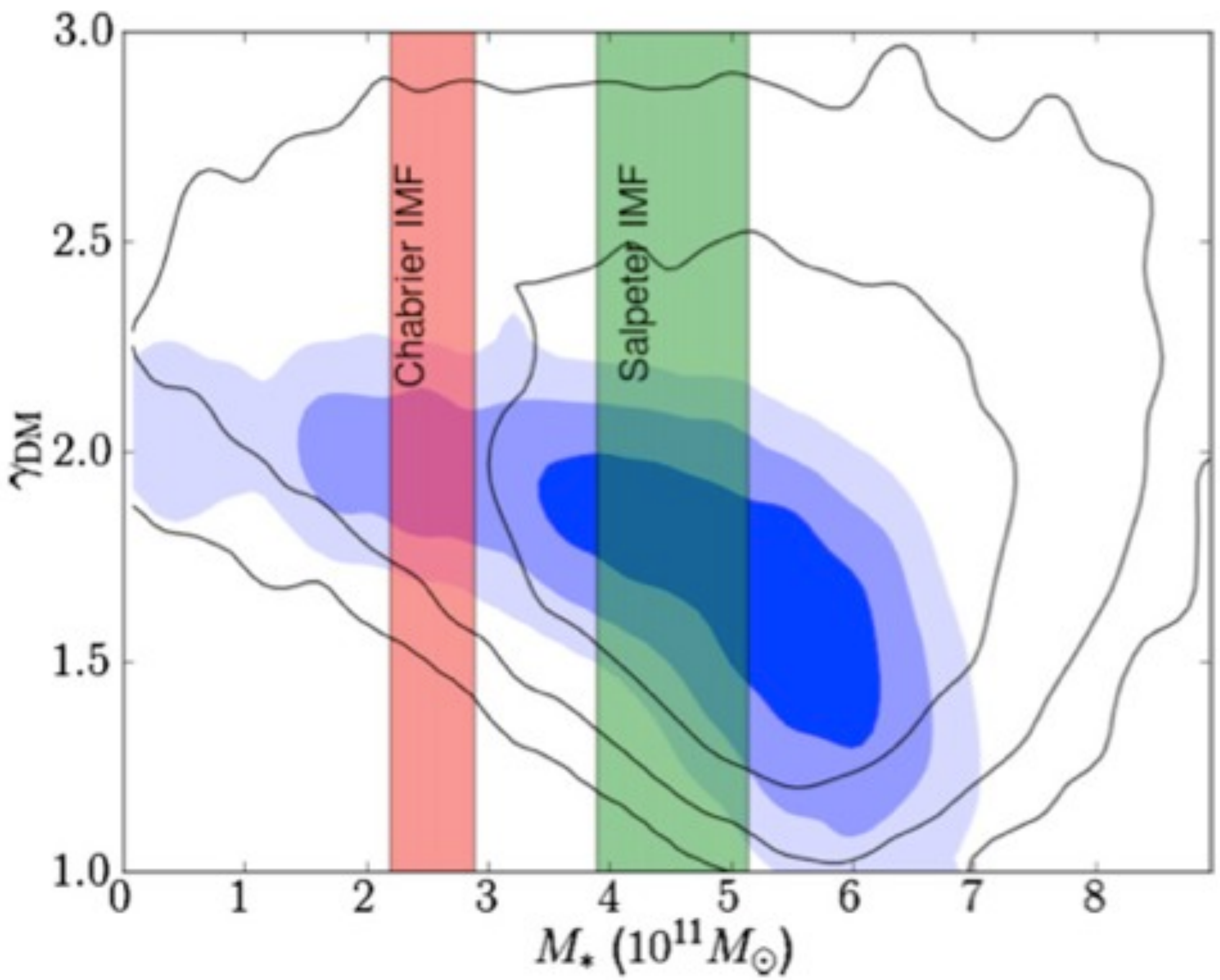

SPS models (B&C) based on broad-band colors from all HST filters.

Salpeter IMF is preferred

Self-consistent 2D L&D

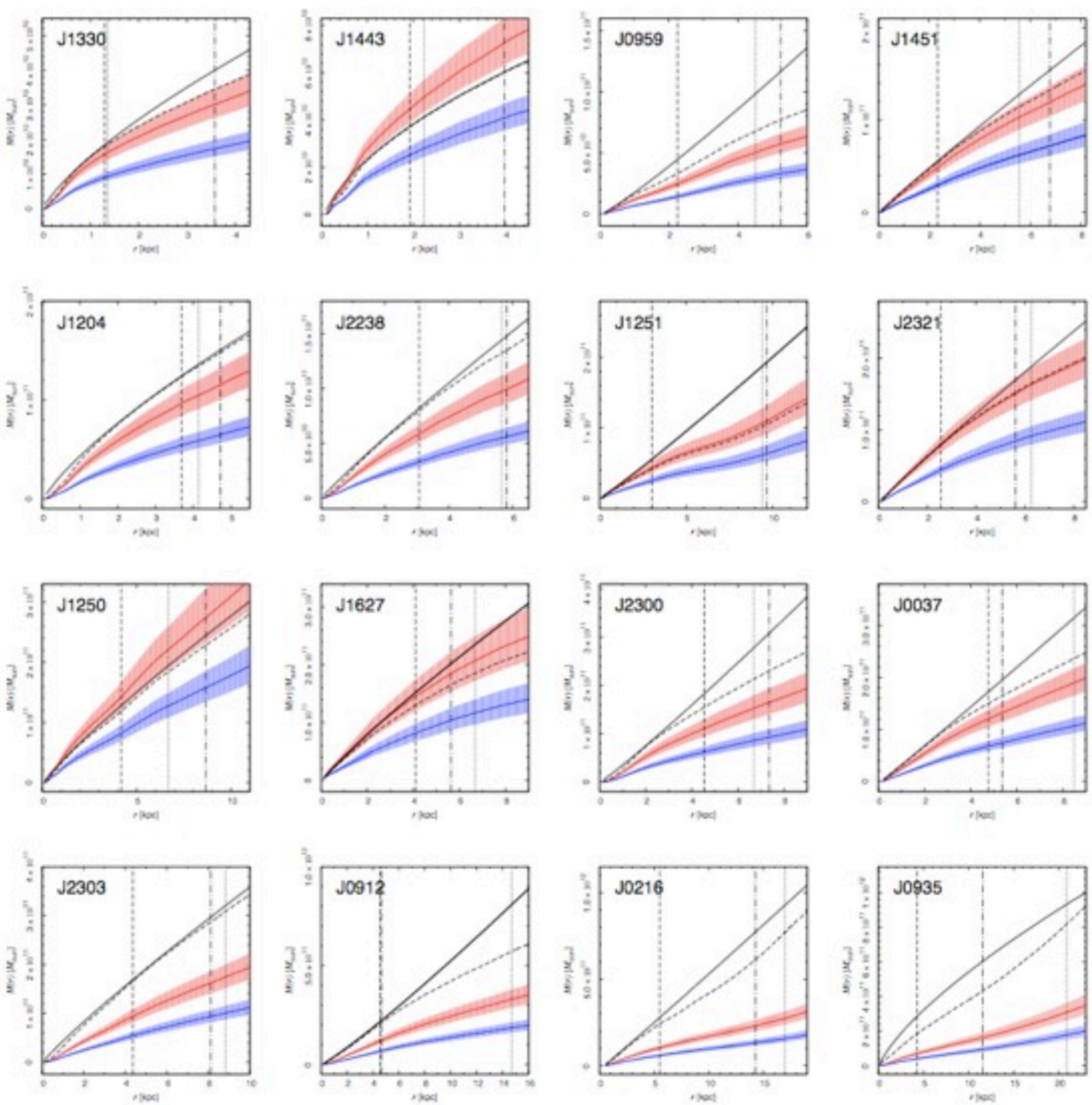

Barnabe et al. 2011

Fully self-consistent L&D sets very tight constraints on the density profiles using all information from 2D lensing and 2D kinematic data.

DM fraction f_{DM} increases rapidly with ETG mass/dispersion

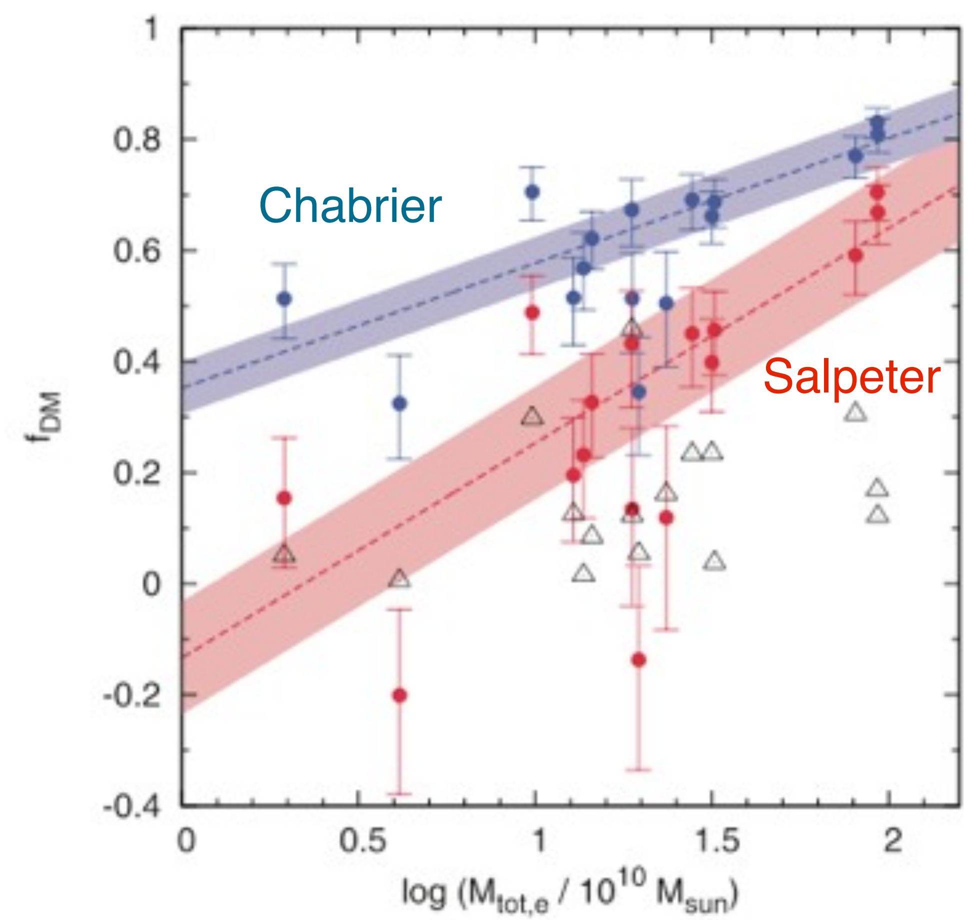

Extended Halos: 1-100 R_{eff}

Connection between SL & WL

Weak Lensing of Strong Lenses

Shear field after PSF correction using 22 SLACS ETGs

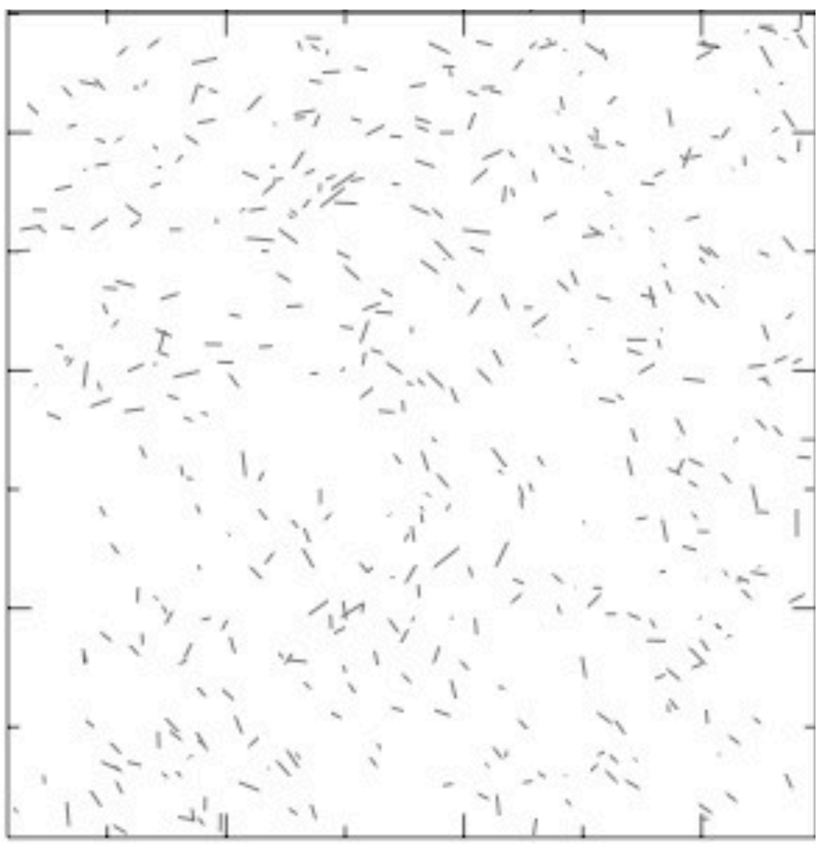

Gavazzi et al. 2007

SLACS galaxies are centered in the middle of the upper CCD of ACS

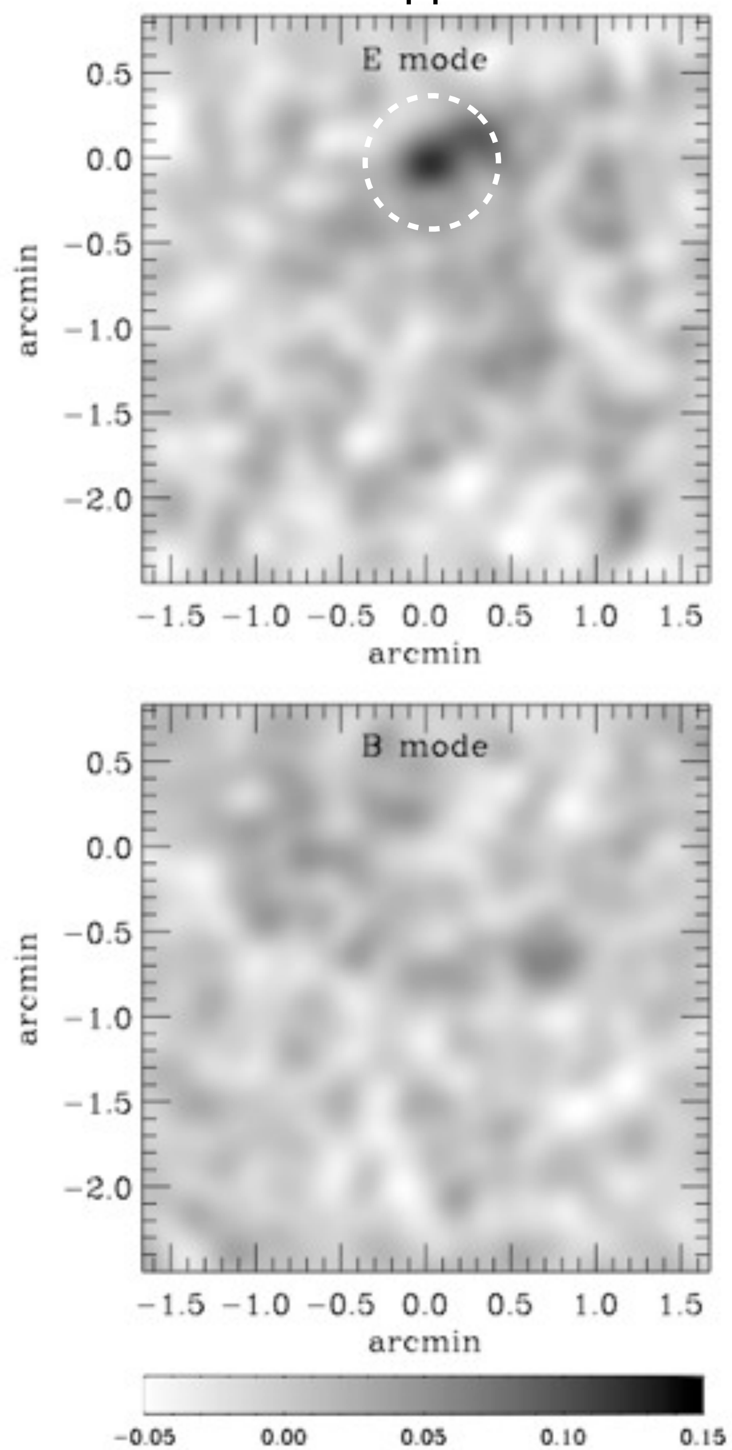

All lens galaxies are centered at the same position on the CCD and the shear signals can be stacked to obtain a mass-averaged convergence map.

Systematics (B-modes) seem under control

Weak Lensing of Strong Lenses

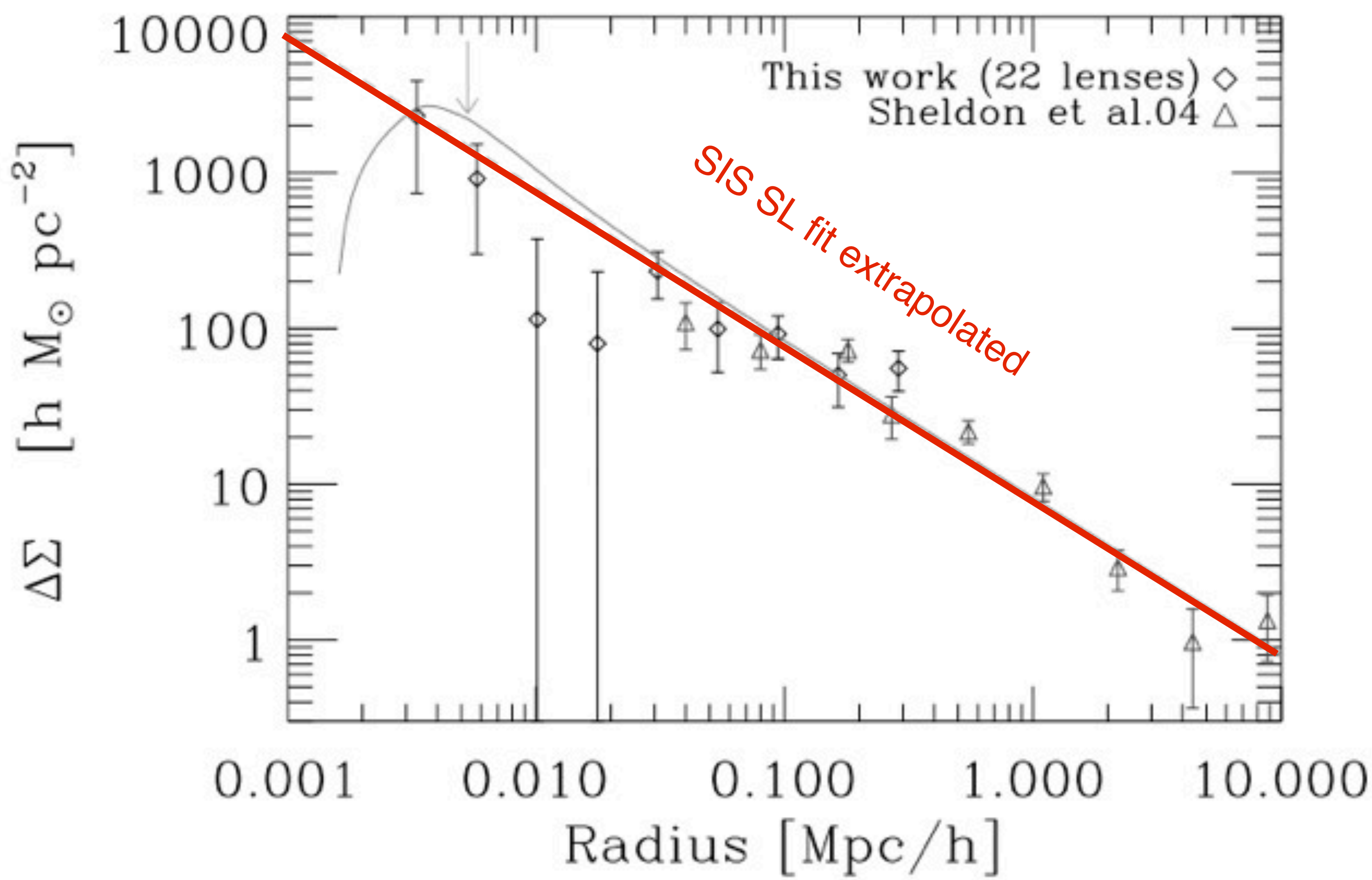

The best SL-SIS model can fit the WL data all the way over 1-100 $R_{eff.}$

Gavazzi et al. 2007

Weak Lensing of Strong Lenses

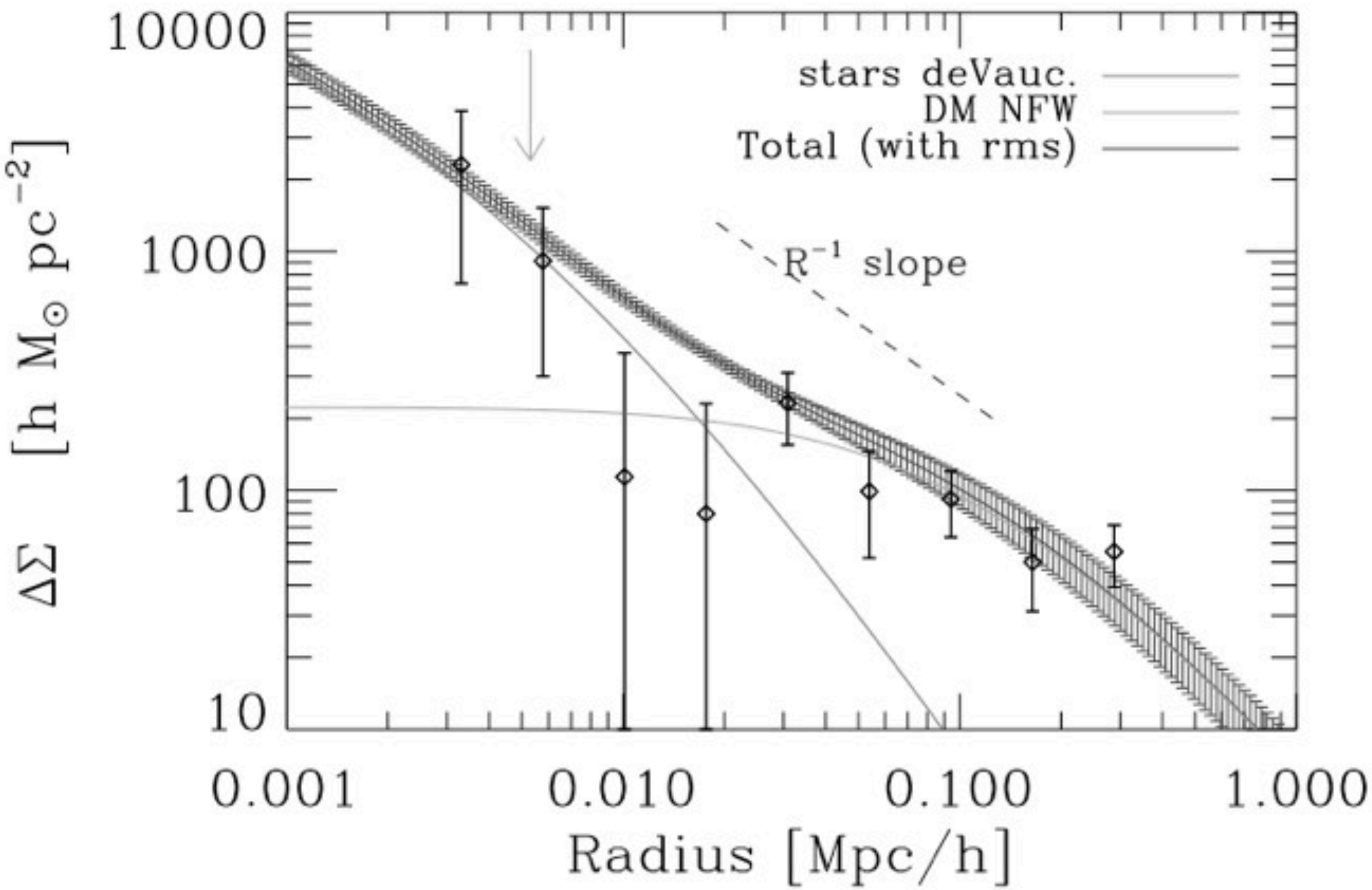

The best SL-SIS model can fit the WL data all the way over 1-100 $R_{eff.}$

Two-component mass model: deV+NFW with stellar M/L and M_{vir} as the only free parameters:

M_*/L_V=4.5±0.5 h
M_{vir}/L_V=250±95 h

$f_{DM}(<R_{vir})$ = 0.02 ± 0.01
$f_{DM}(R_{eff})$ = 0.27 ± 0.04

Gavazzi et al. 2007

The Inclusion of Stellar Population Synthesis:

Impact on DM inferences

Multi-color SLACS Sample

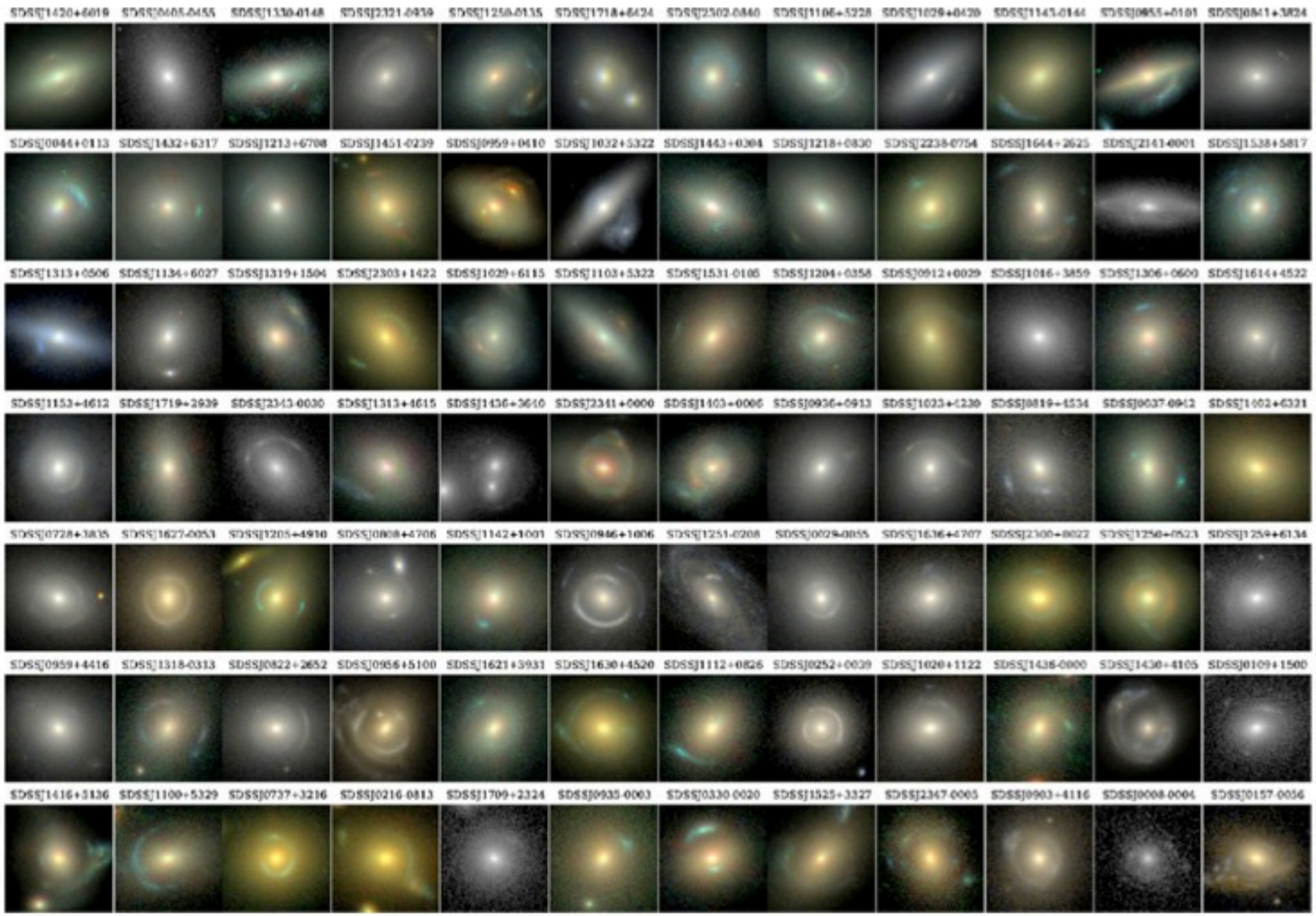

Auger et al. 2009

V, I & H-band HST data allow one to measure stellar masses using SPS and subtract this from the total lensing mass inside $R_{Einst/eff}$

SPS codes: B&C03, MIUSCAT, CvD12, etc

CSP Constraints on Stellar Mass

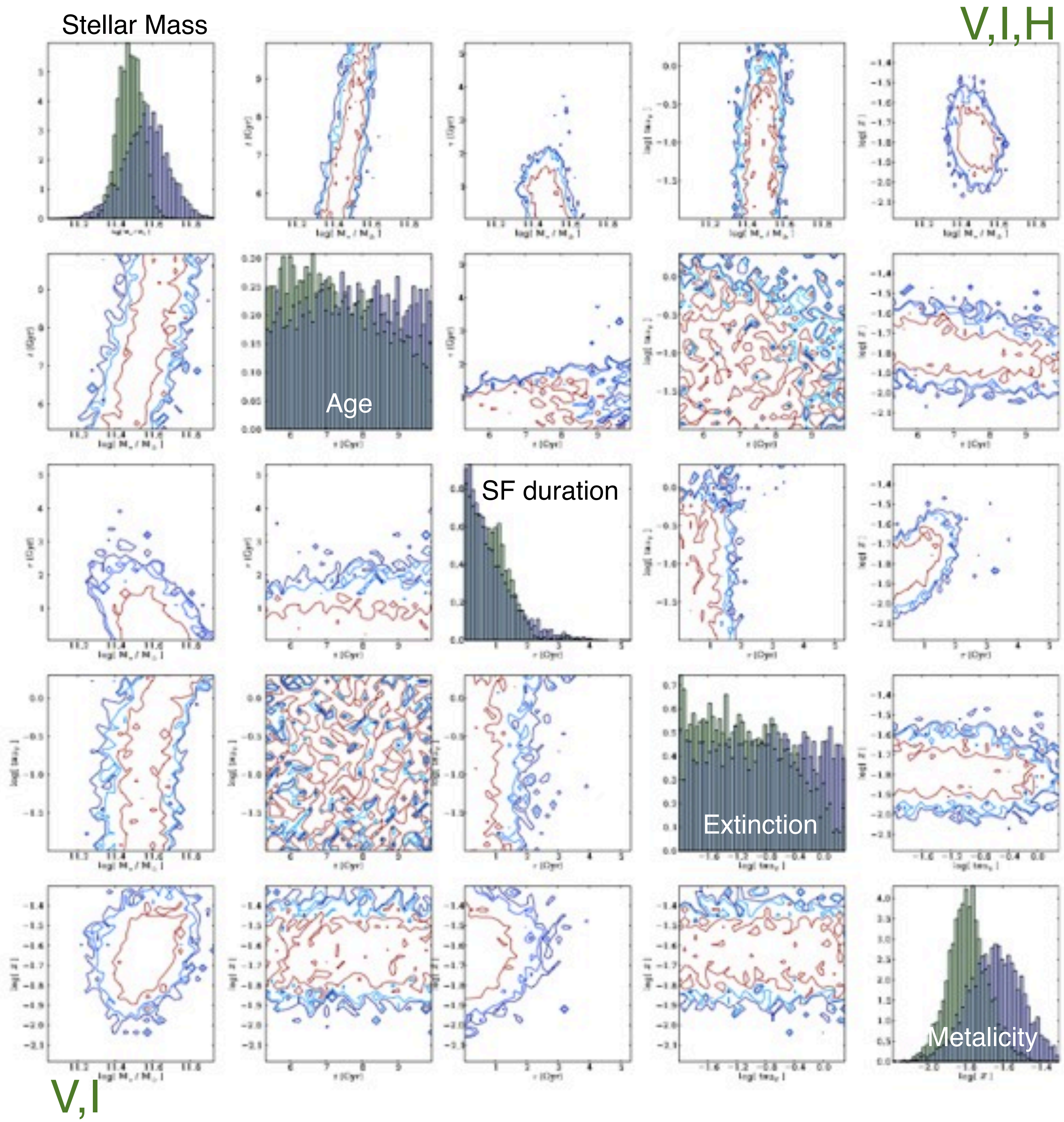

B&C03 SPS models provides strong constraints on the stellar mass PROVIDED the IMF is given (e.g. Chabrier, Salpeter)

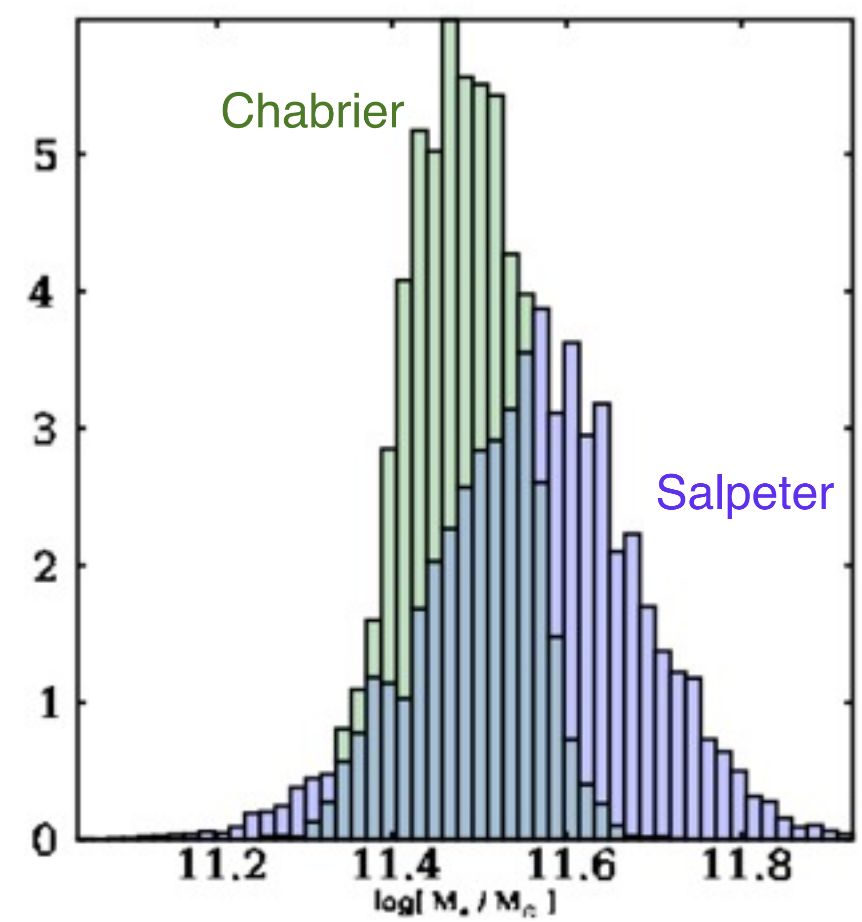

Auger et al. 2009

Dark-Matter Fraction versus Mass

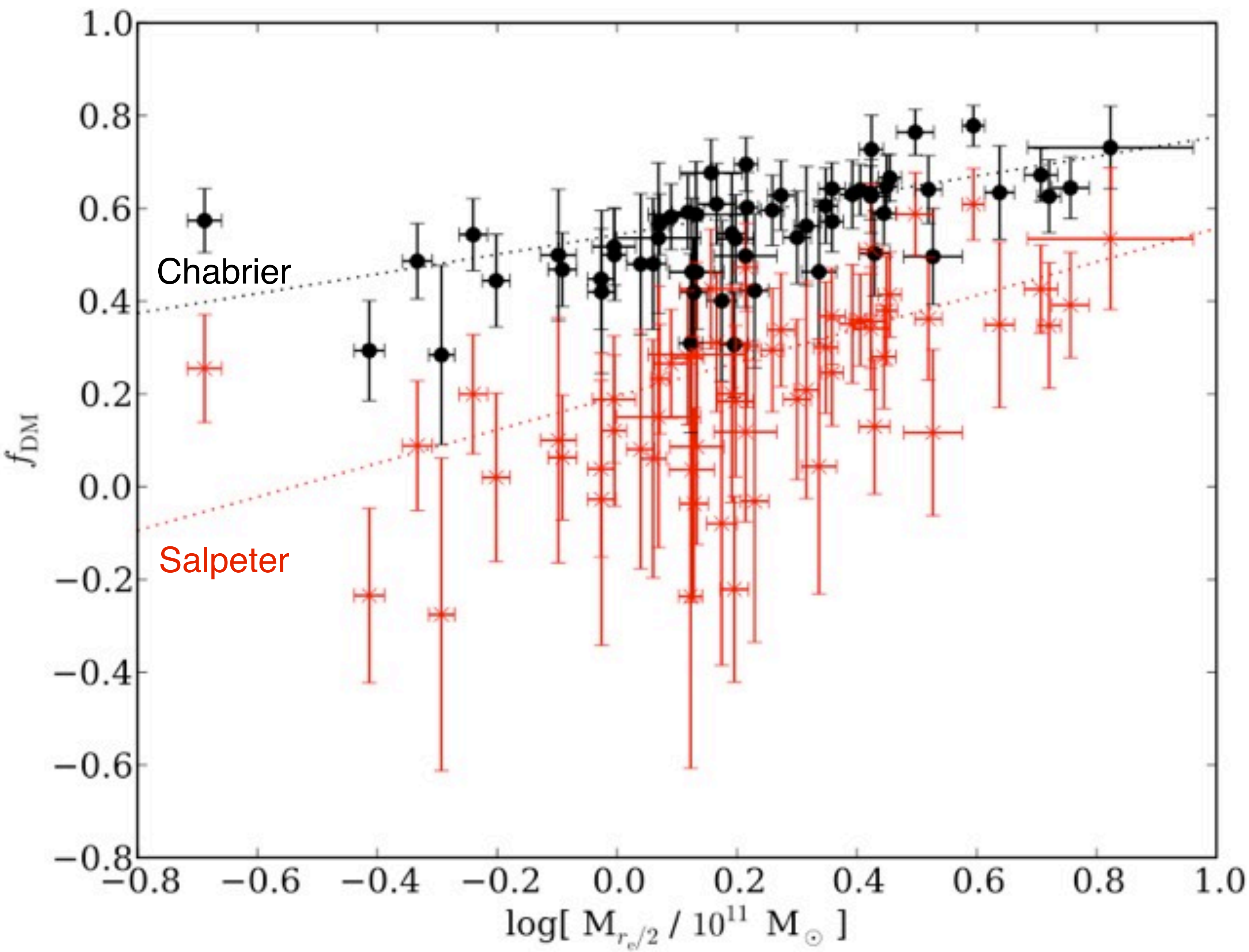

Auger et al. 2010

Subtracting the SPS stellar mass from the mass inside $R_{eff/2}$~R_{Einst}, suggests that the DM fraction in ETG increases with galaxy mass, assuming a fixed IMF.

This has implications for feedback models in ΛCDM, increasing as galaxies get more massive.

However! Impact of IMF variations on the inference of DM in ETGs

A full SPS modeling of SDSS galaxies suggest a trend in the IMF slope between 150-300 km/s, doubling the stellar M/L over this range. If confirmed (e.g. Conroy et al. 2013), this implies a tilting of the f_{DM} trend with galaxy mass

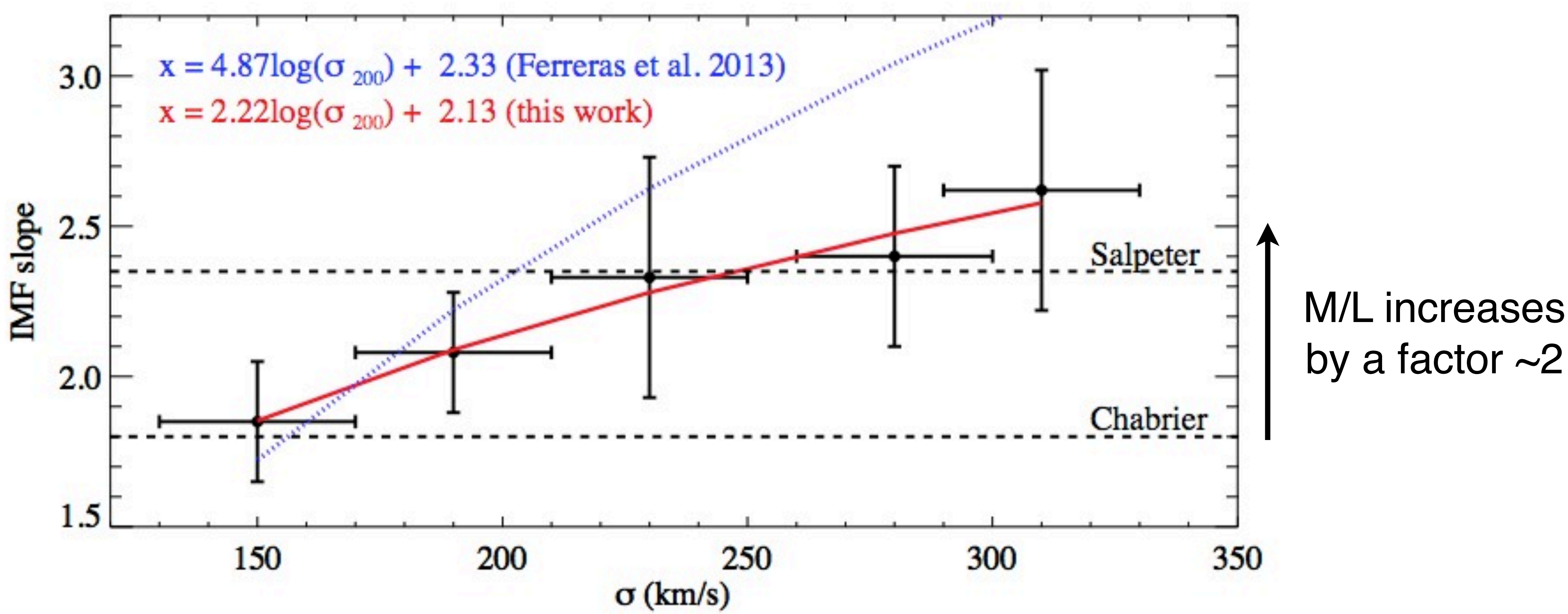

Spiniello et al. 2013

Impact of IMF variations on the inference of DM in ETGs

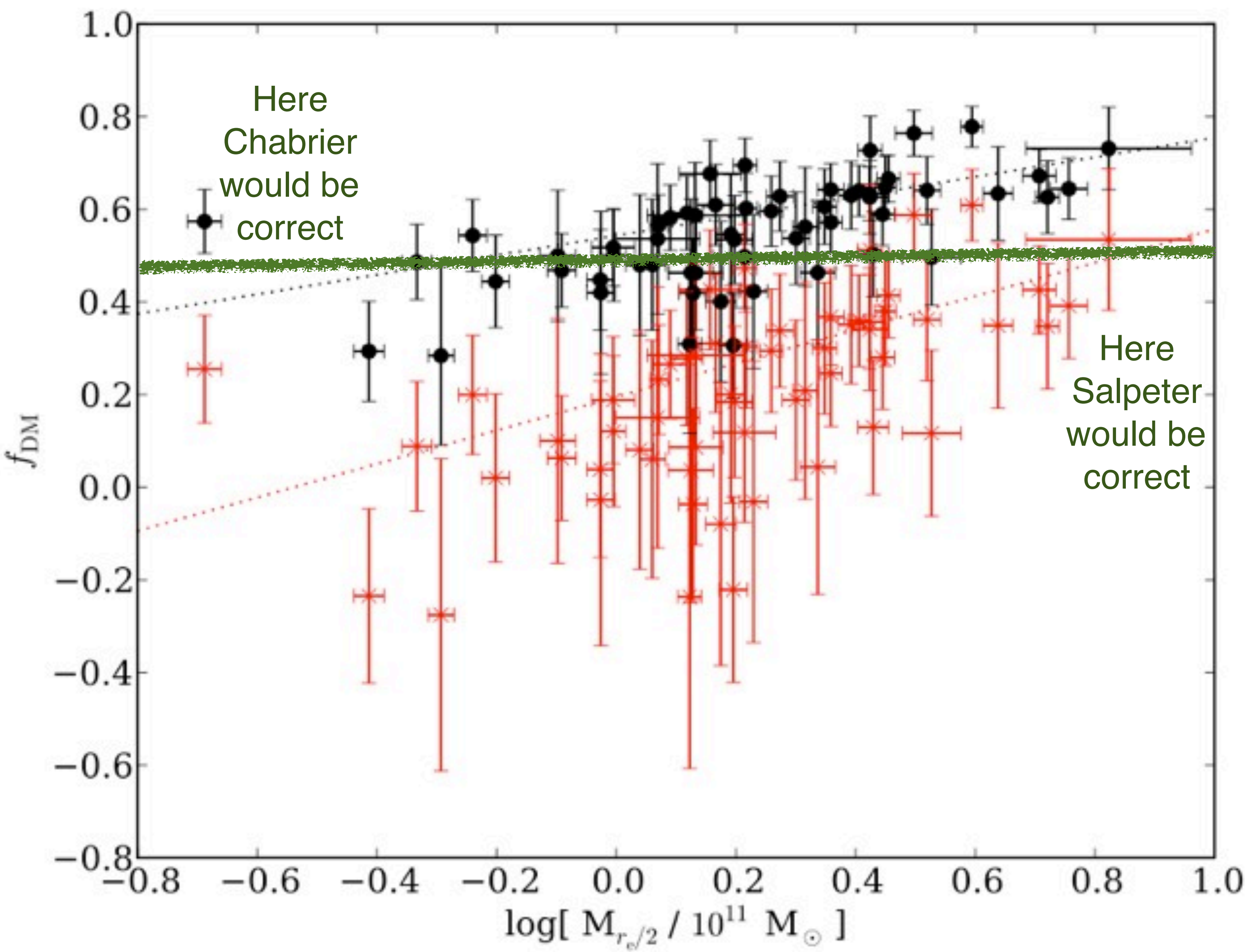

Auger et al. 2010

The amazing conclusion seems to be that f_{DM} does NOT depend on galaxy mass anymore and is constant over 150-300 km/s.

And f_{DM}~0.5 inside $R_{eff}/2$.

Spiniello et al. 2013, in prep.

The Slope and Lower Mass Limit of the IMF from L&D+SSP.

(see talk Barnabe)

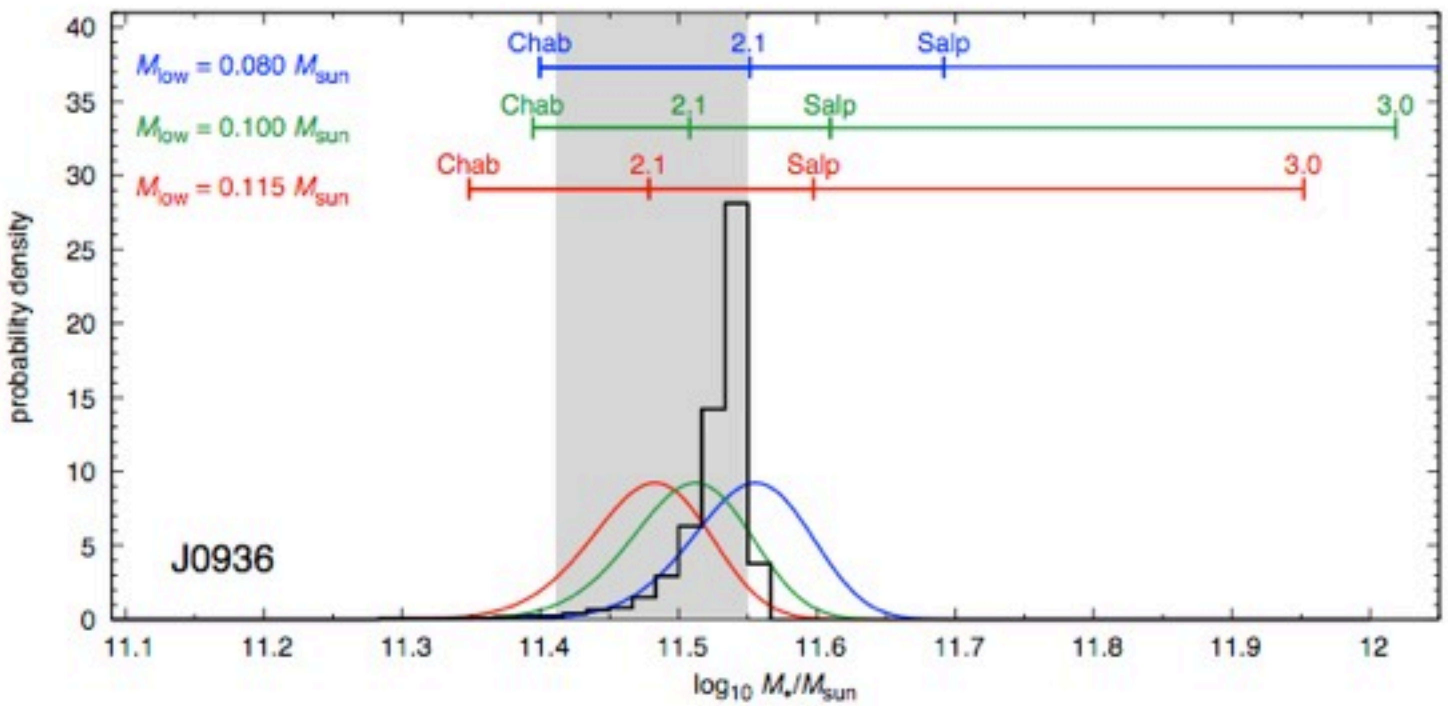

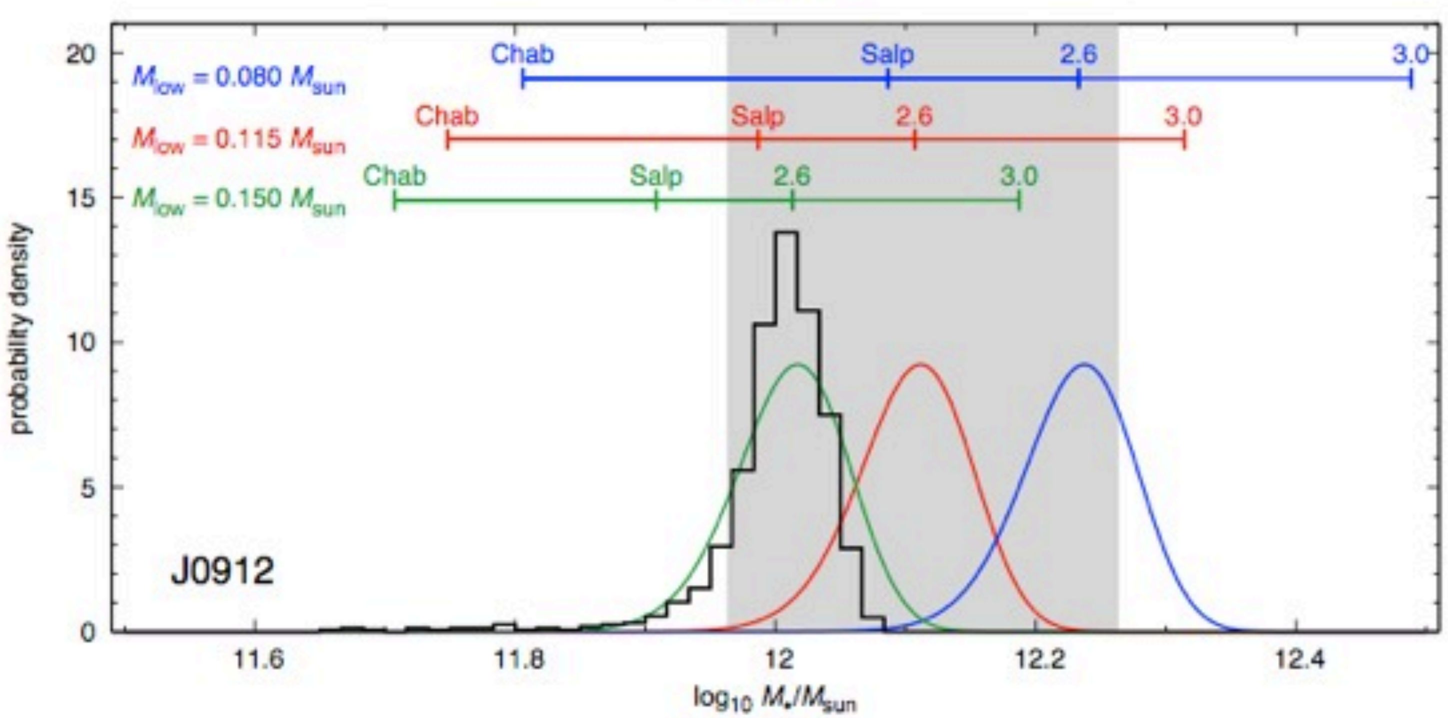

Barnabe et al. 2013

L&D provides an excellent constraint on the stellar mass independent of M/L.

SSP provides a slope, but no lower mass cutoff. Combined M_{low} of the IMF can be determined.

IMF M_{low} = $0.12 \pm 0.03\ M_{sun}$
IMF slope = 2.21 ± 0.14

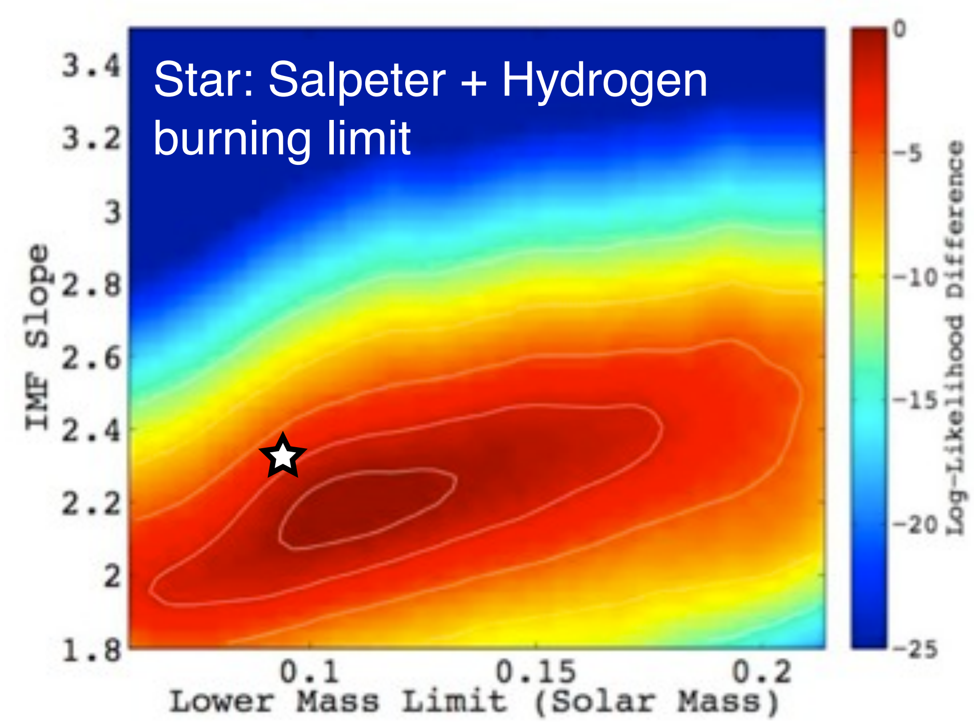

Disk/Spiral Lens Galaxies

B1933+503: A disk-galaxy at z=0.76

Power-law models fit best. Only deV with R_{eff}=19 kpc h^{-1} fits, but that is much larger than observed.

2 quads + double

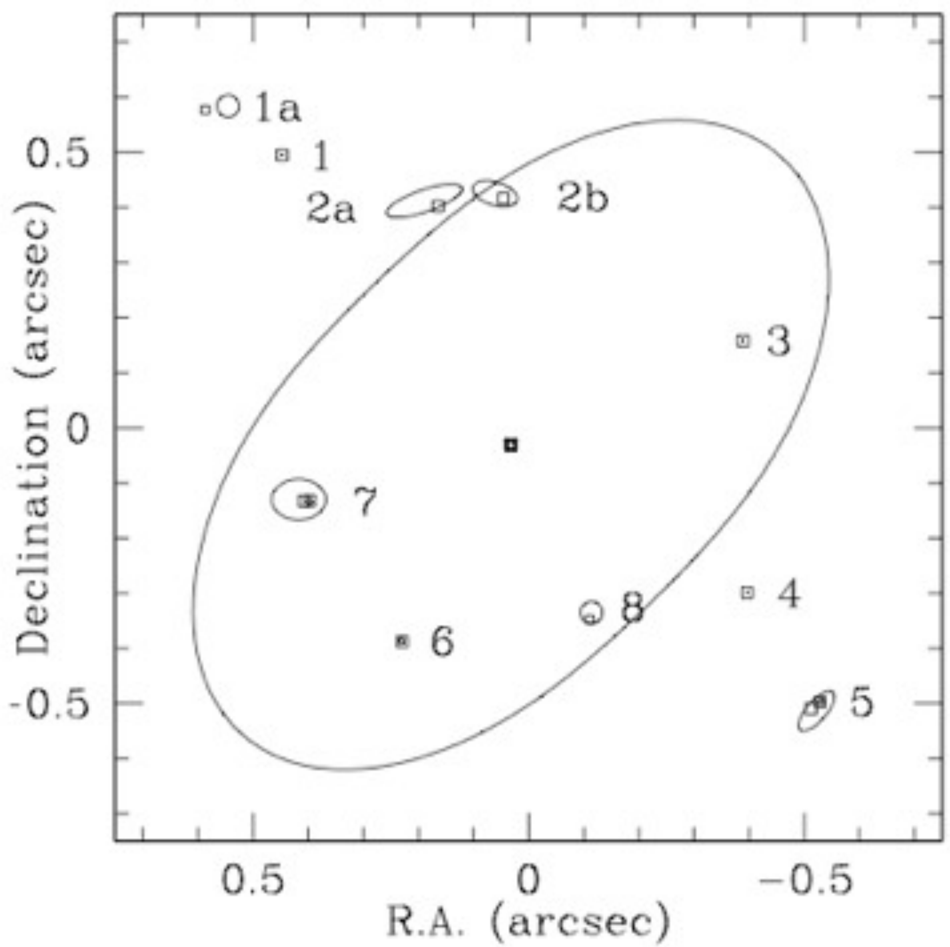

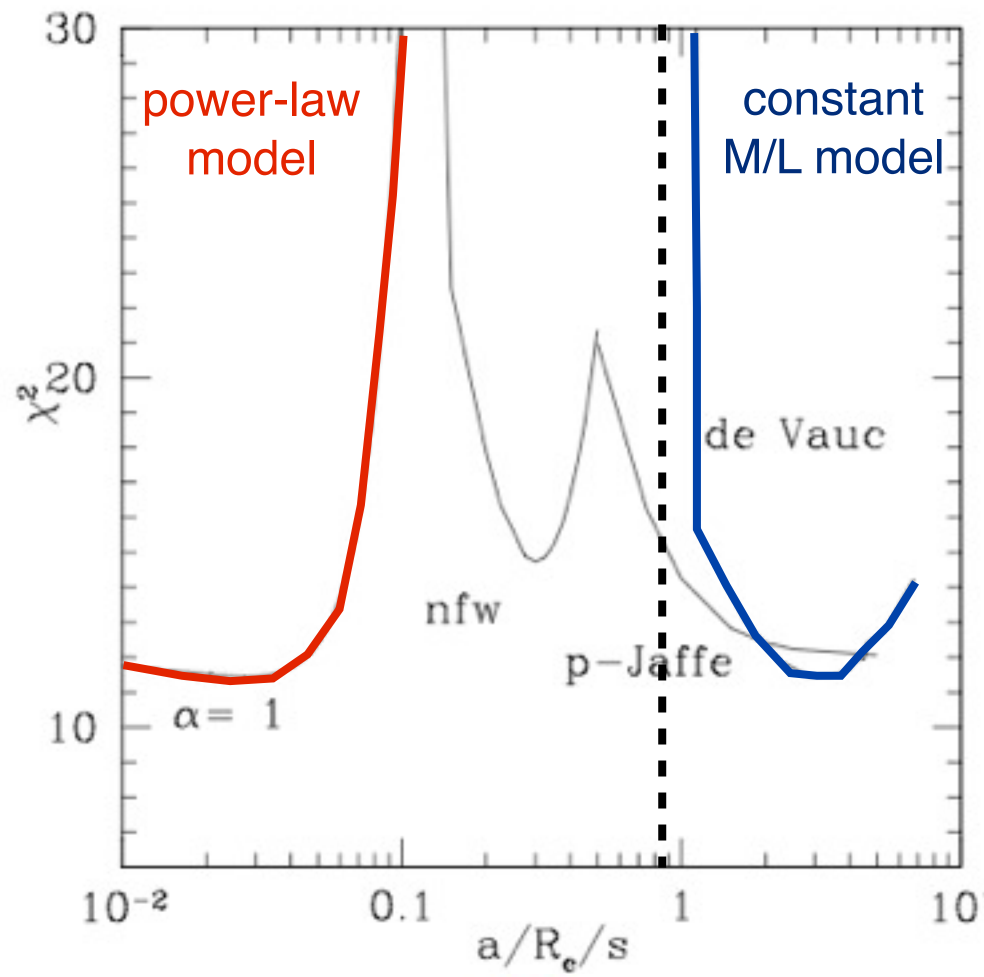

Cohn et al. 2001

Table 2
Lens Galaxy Light

	ΔR.A. (arcsec)	ΔDecl. (arcsec)	R_e (arcsec)	n_{sersic}	q	ϕ (°)
Disk	0.040 ± 0.005	-0.036 ± 0.005	0.85 ± 0.05	$\equiv 1$	0.63 ± 0.06	138.0 ± 1.5
Bulge	0.040 ± 0.005	-0.036 ± 0.005	0.055 ± 0.006	$\equiv 1$	0.41 ± 0.02	147 ± 3

B1933+503: A disk-galaxy at z=0.76

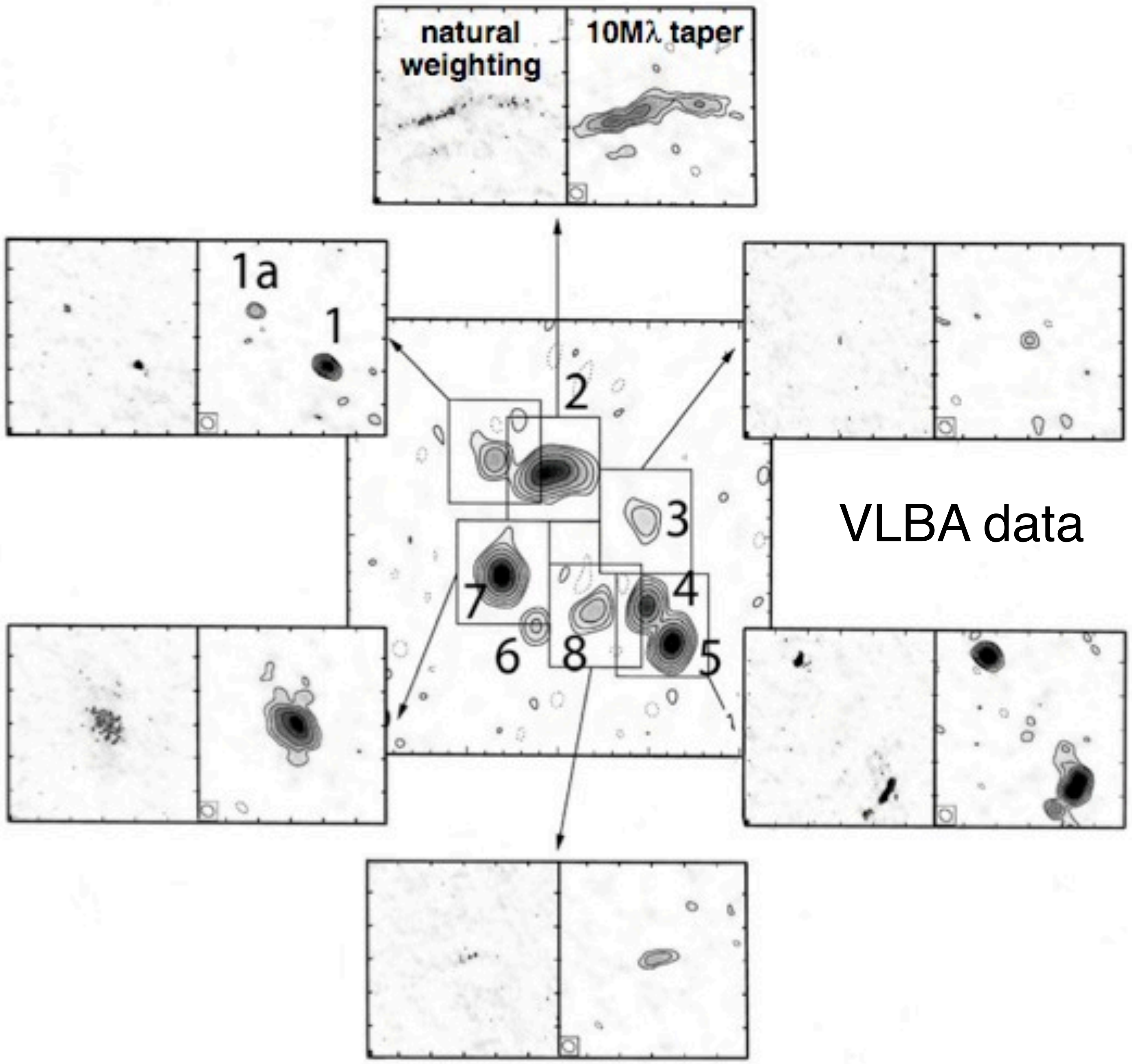

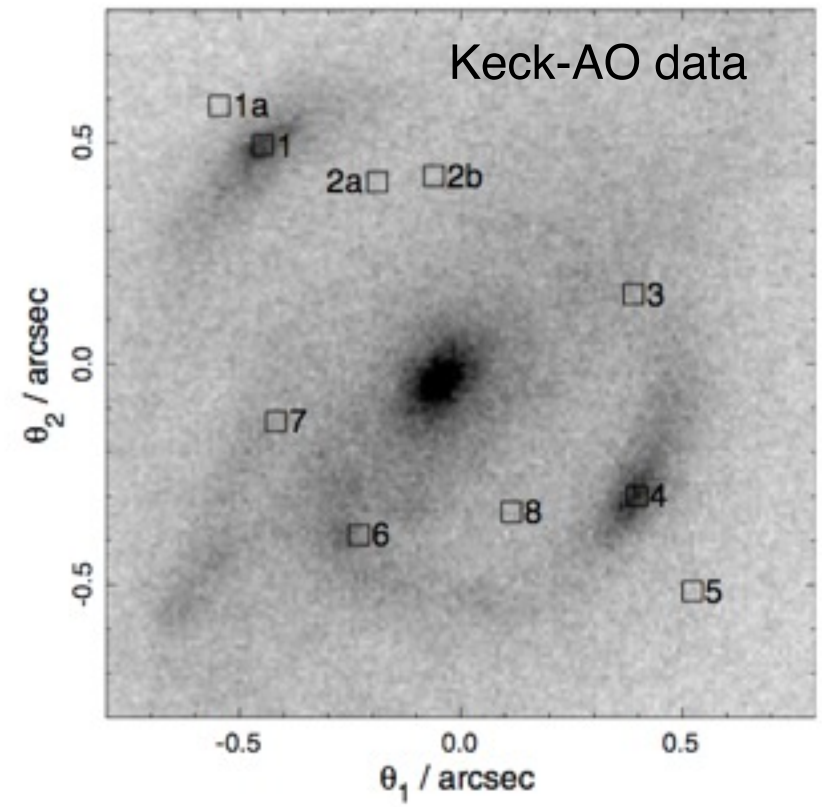

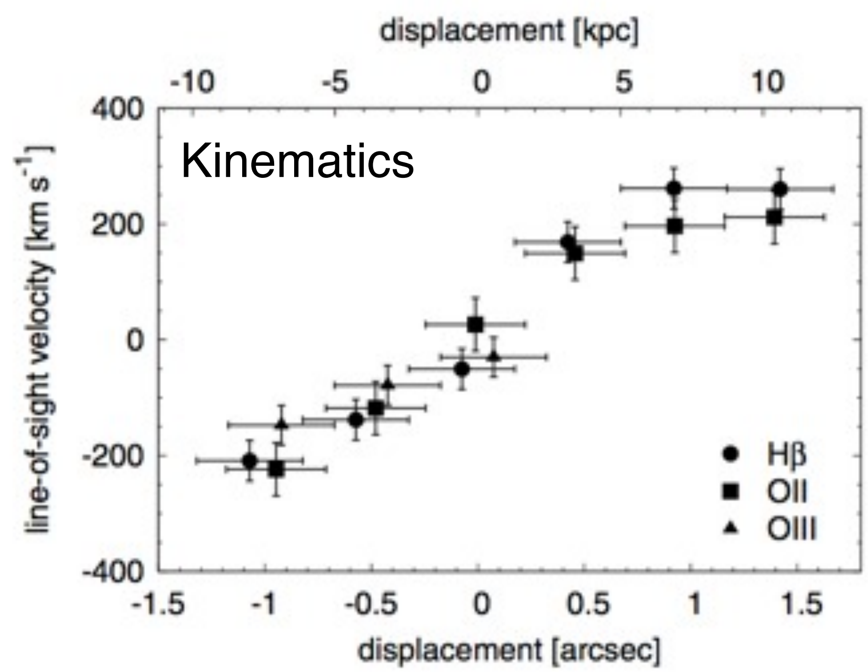

Suyu et al. 2012

B1933+503: A disk-galaxy at z=0.76

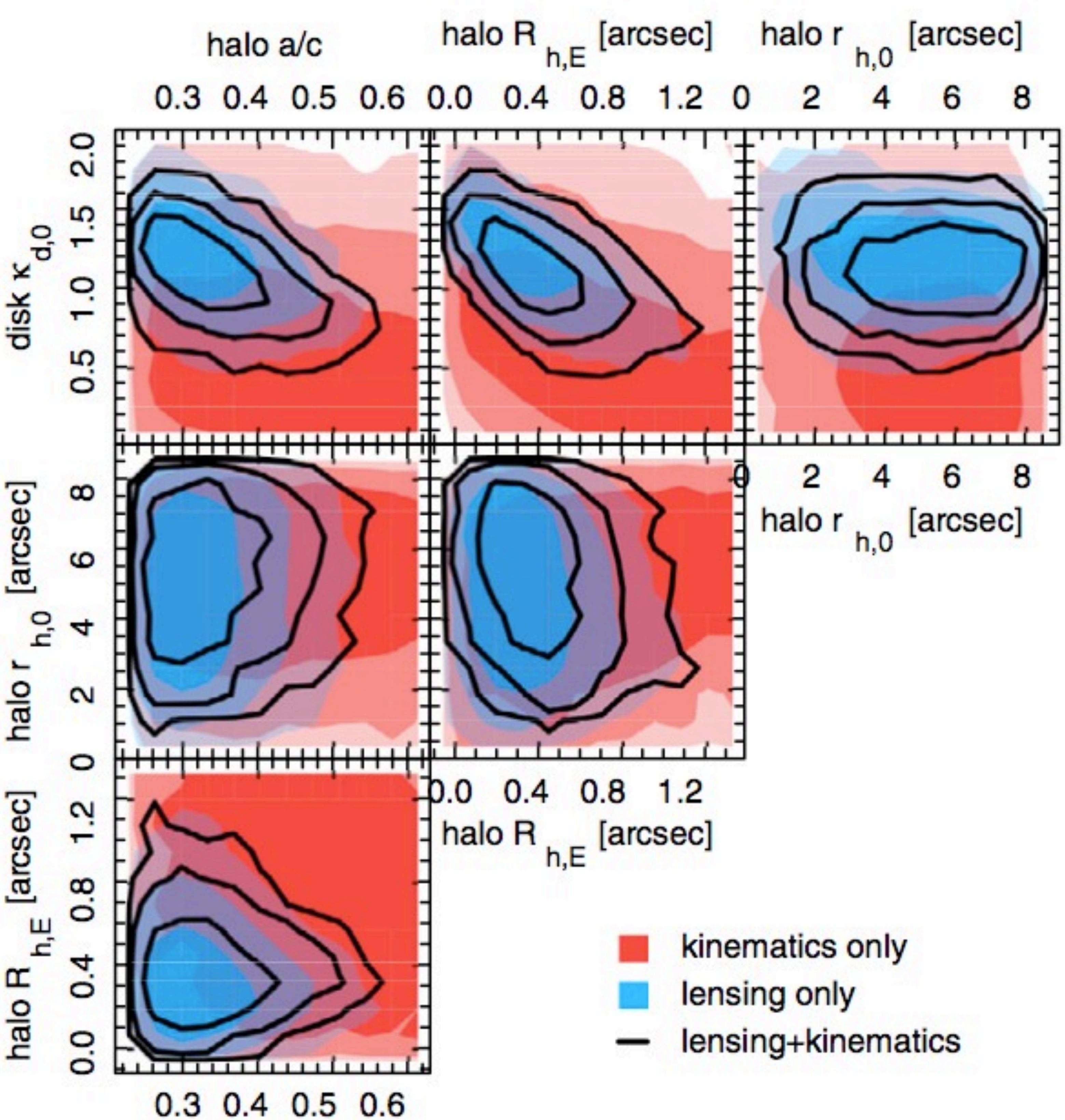

Given both high-resolution VLBA and Keck-AO data plus kinematics, a disk+bulge+halo model can be constructed.

When marginalizing over disk+bulge one finds:

(1) Disk contributed 0.76±0.05 to V at 2.2 R_d and hence is marginally sub-max.
(2) f_{DM} = 0.43/0.37 ± 0.09 inside $2.2R_d/R_{eff}$
(3) (c/a)=0.3 and $r_{h,0}$>16 kpc
(4) Chabrier IMF is preferred over Salpeter by 7.2 LH ratio.

$$\rho_h(r) = \frac{\rho_{h,0}}{(r/r_{h,0})(1+r/r_{h,0})^2},$$

$$r^2 = c^2\left(\frac{x^2}{a^2}+\frac{y^2}{b^2}+\frac{z^2}{c^2}\right), \quad a \leqslant b \leqslant c.$$

Suyu et al. 2012

B1933+503: A disk-galaxy at z=0.76

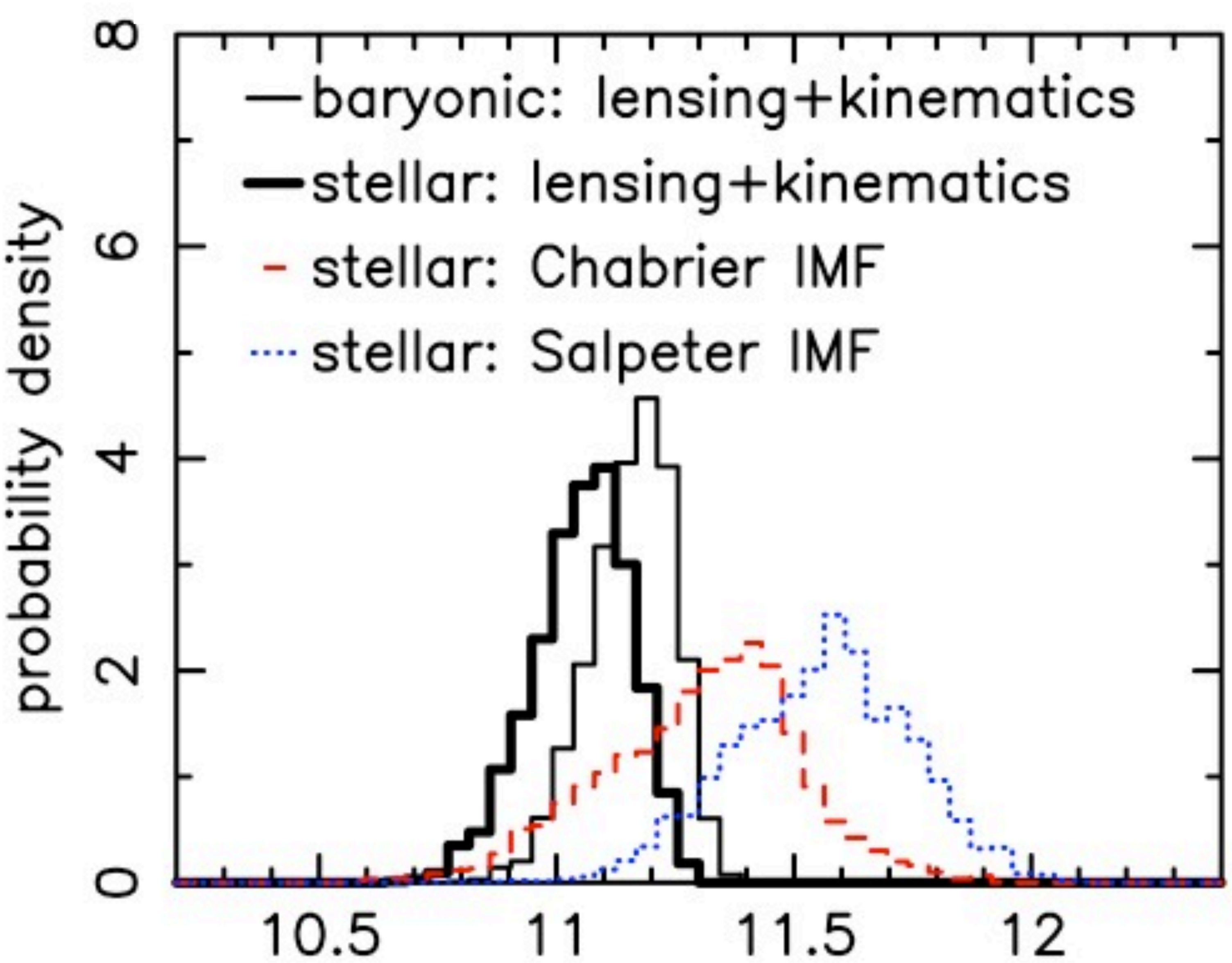

Given both high-resolution VLBA and Keck-AO data plus kinematics, a disk+bulge+halo model can be constructed.

When marginalizing over disk+bulge one finds:

(1) Disk contributed 0.76±0.05 to V at 2.2 R_d and hence is marginally sub-max.
(2) f_{DM} = 0.43/0.37 ± 0.09 inside 2.2R_d/R_{eff}
(3) (c/a)=0.3 and $r_{h,0}$>16 kpc
(4) Chabrier IMF is preferred over Salpeter by 7.2 LH ratio.

$$\rho_h(r) = \frac{\rho_{h,0}}{(r/r_{h,0})(1+r/r_{h,0})^2},$$

$$r^2 = c^2\left(\frac{x^2}{a^2}+\frac{y^2}{b^2}+\frac{z^2}{c^2}\right), \quad a \leqslant b \leqslant c.$$

Suyu et al. 2012

Q2237+0305: A disk-galaxy at z=0.04

The Einstein Cross is a spiral galaxy with a lensing bulge. DM should (in principle) play a minor role in the inner regions of this system

HST data

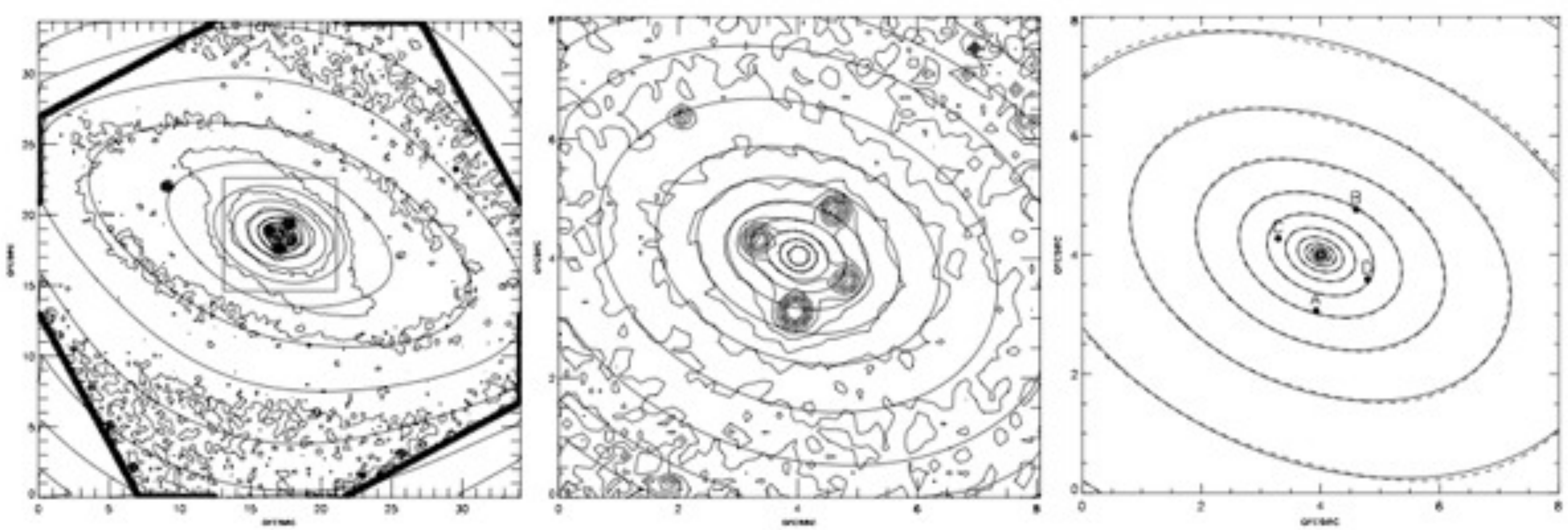

Sauron data

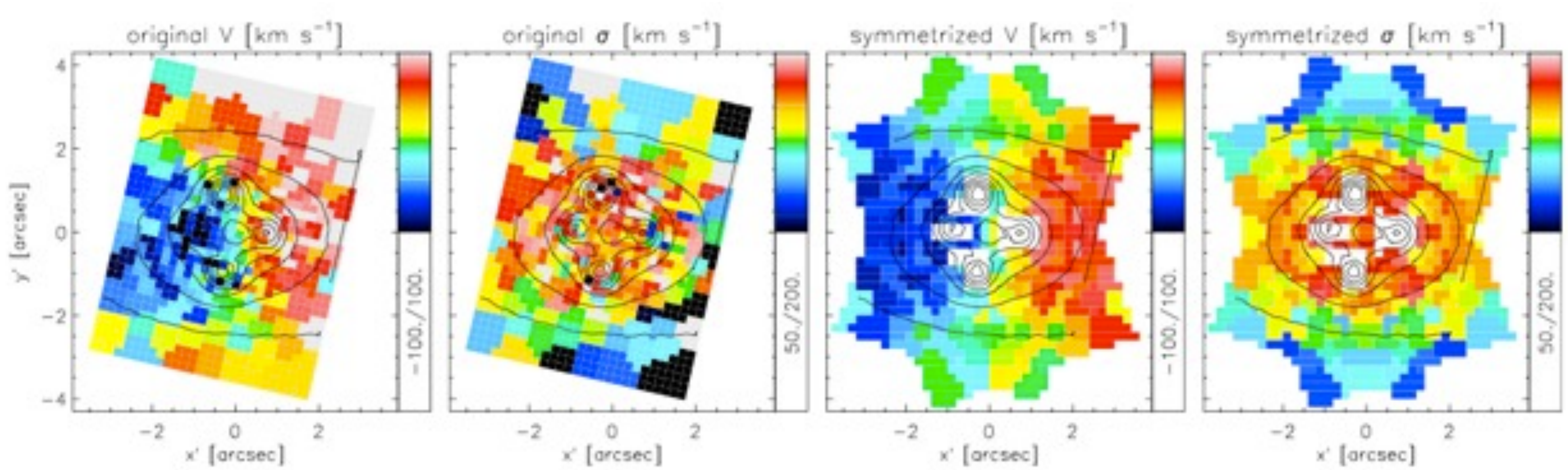

van de Ven et al. 2010

Q2237+0305: A disk-galaxy at z=0.04

Very little dark matter (<20%) in the bulge:
a sanity check on methodology.

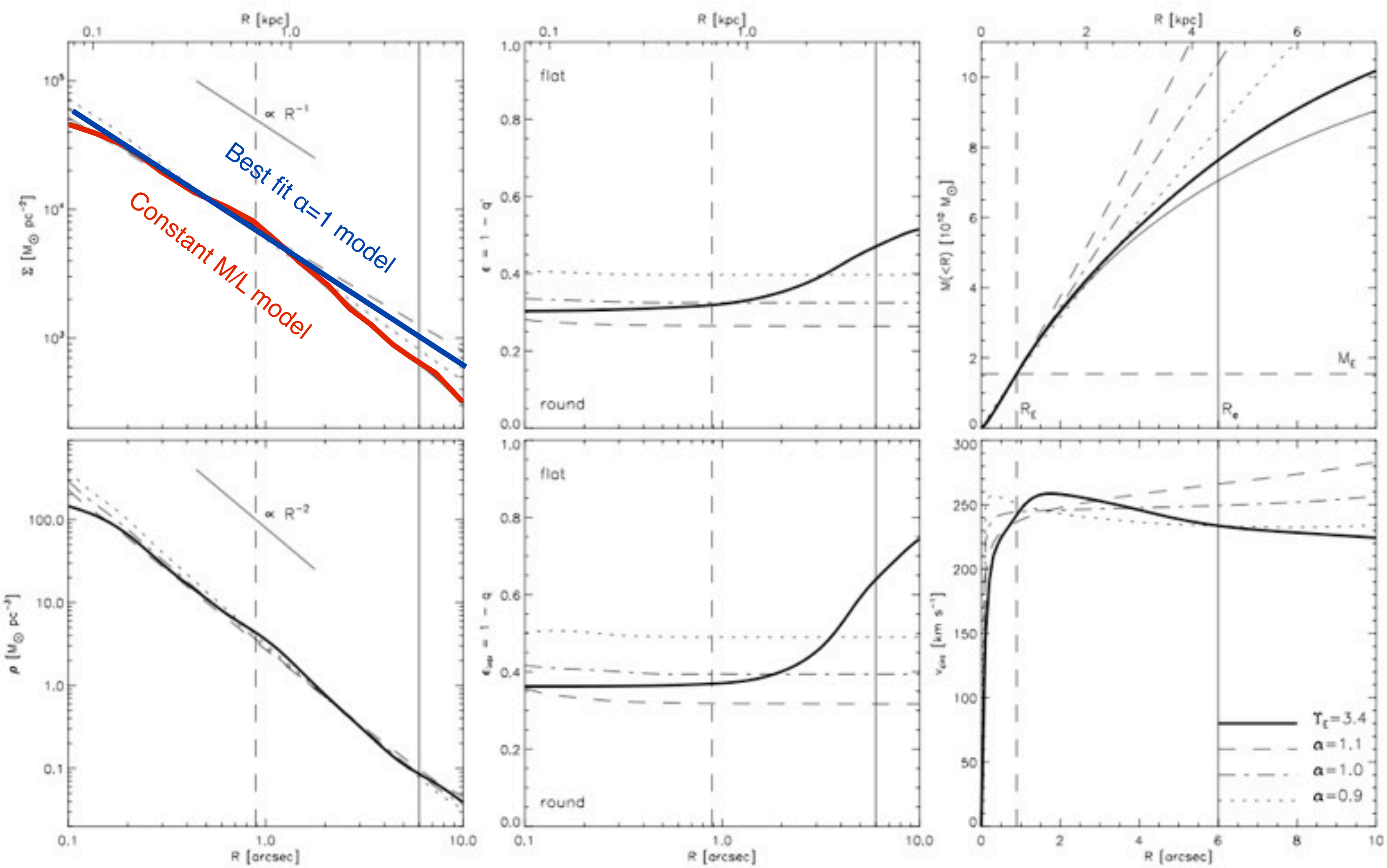

van de Ven et al. 2010

The SWELLS Survey - Disk-Galaxy Lenses

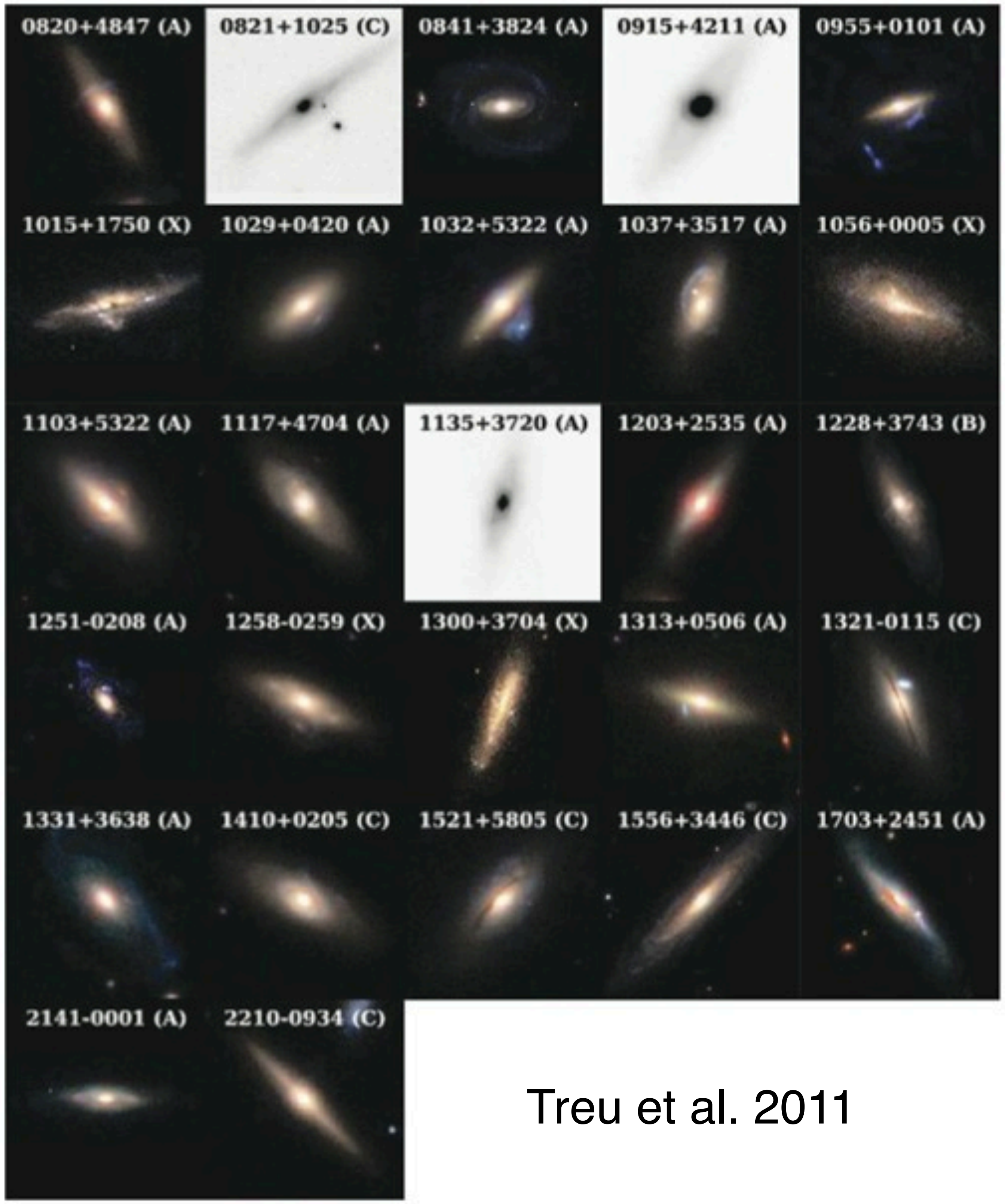

Highly-inclined disk galaxies selected from SDSS. Follow-up with HST, Keck-AO and Keck-spectroscopy.

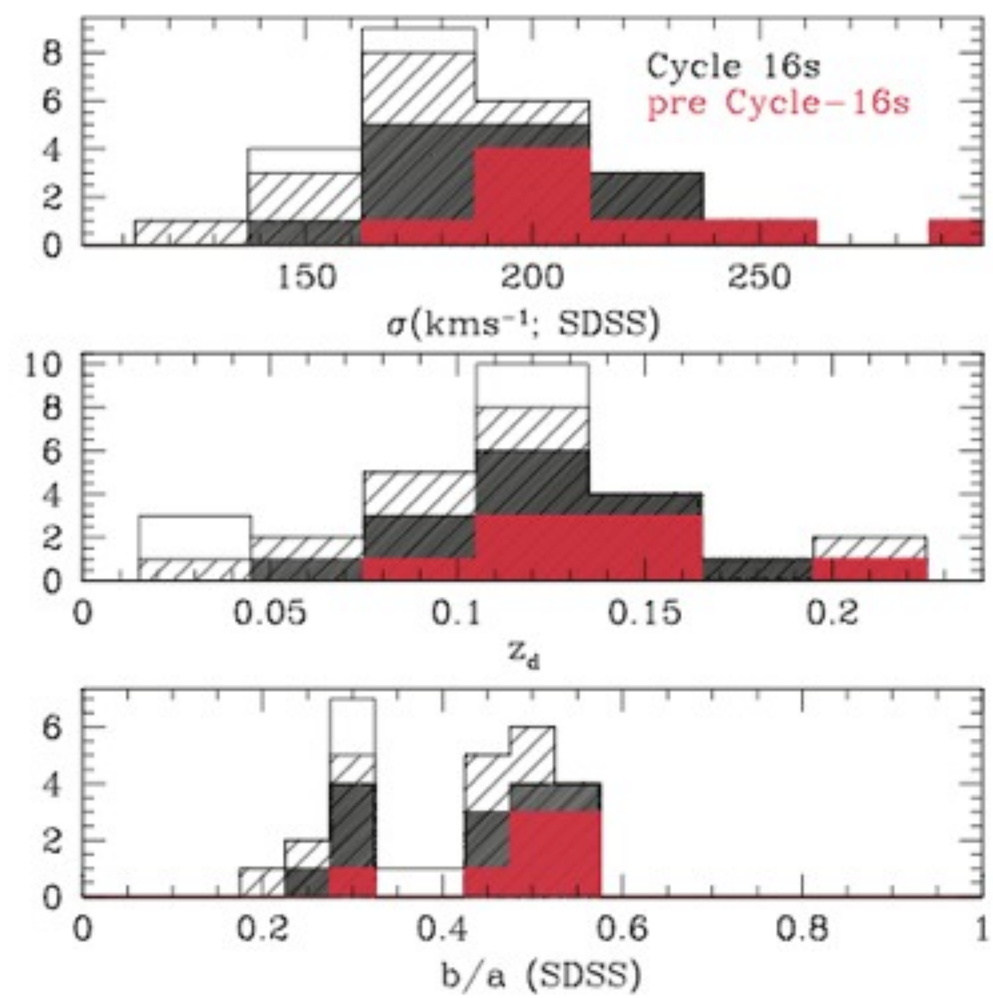

Treu et al. 2011

The SWELLS Survey - Disk-Galaxy Lenses

Joint lensing & dynamical provide a stellar mass for the disk and the bulge. SPS modeling predict M/L value.

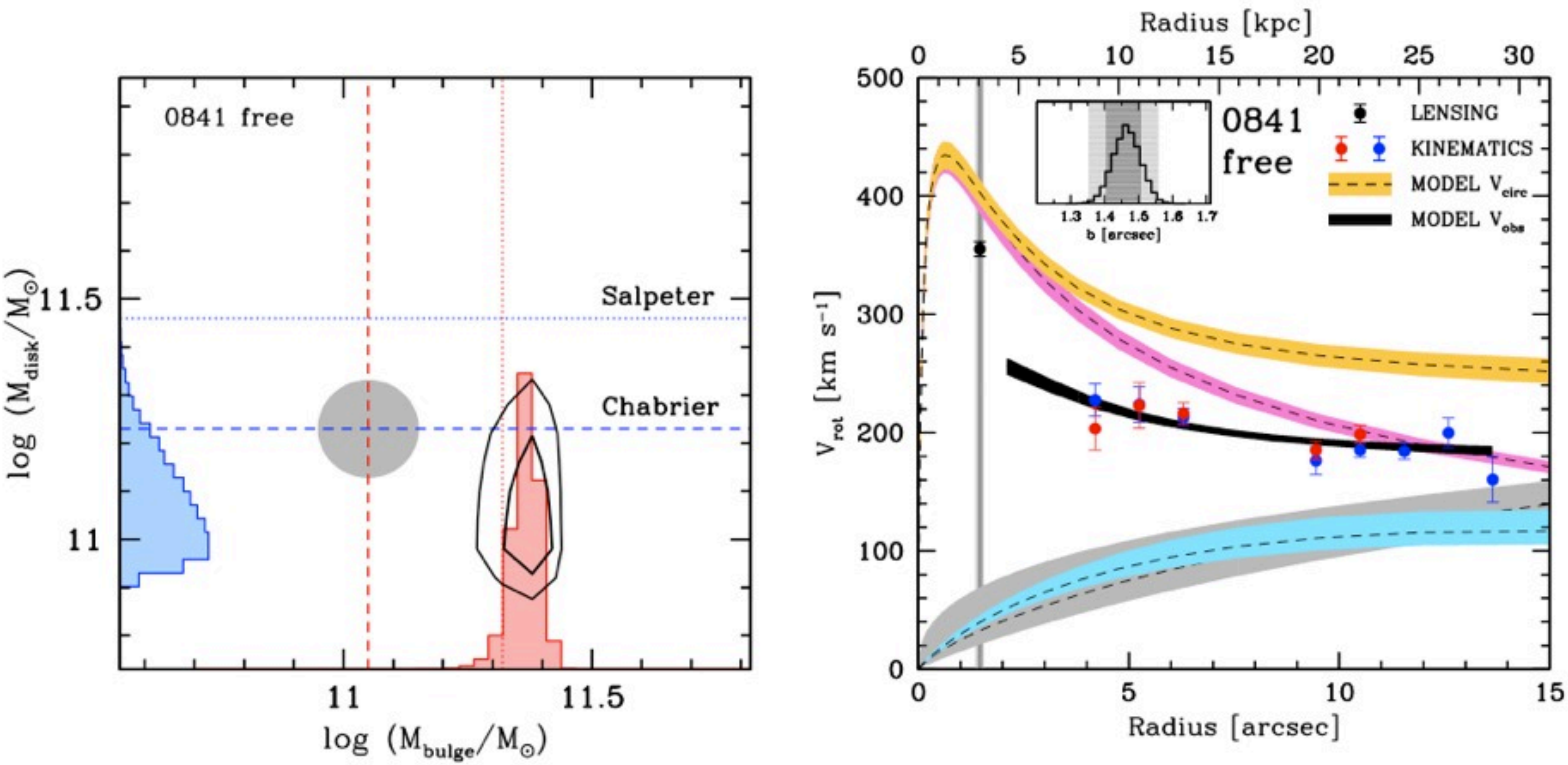

Dutton et al. 2012

The SWELLS Survey - Disk-Galaxy Lenses

Constraints on the bulge are quite tight and show a Salpeter IMF.
Disk masses are less well measured but jointly Chabrier is preferred.

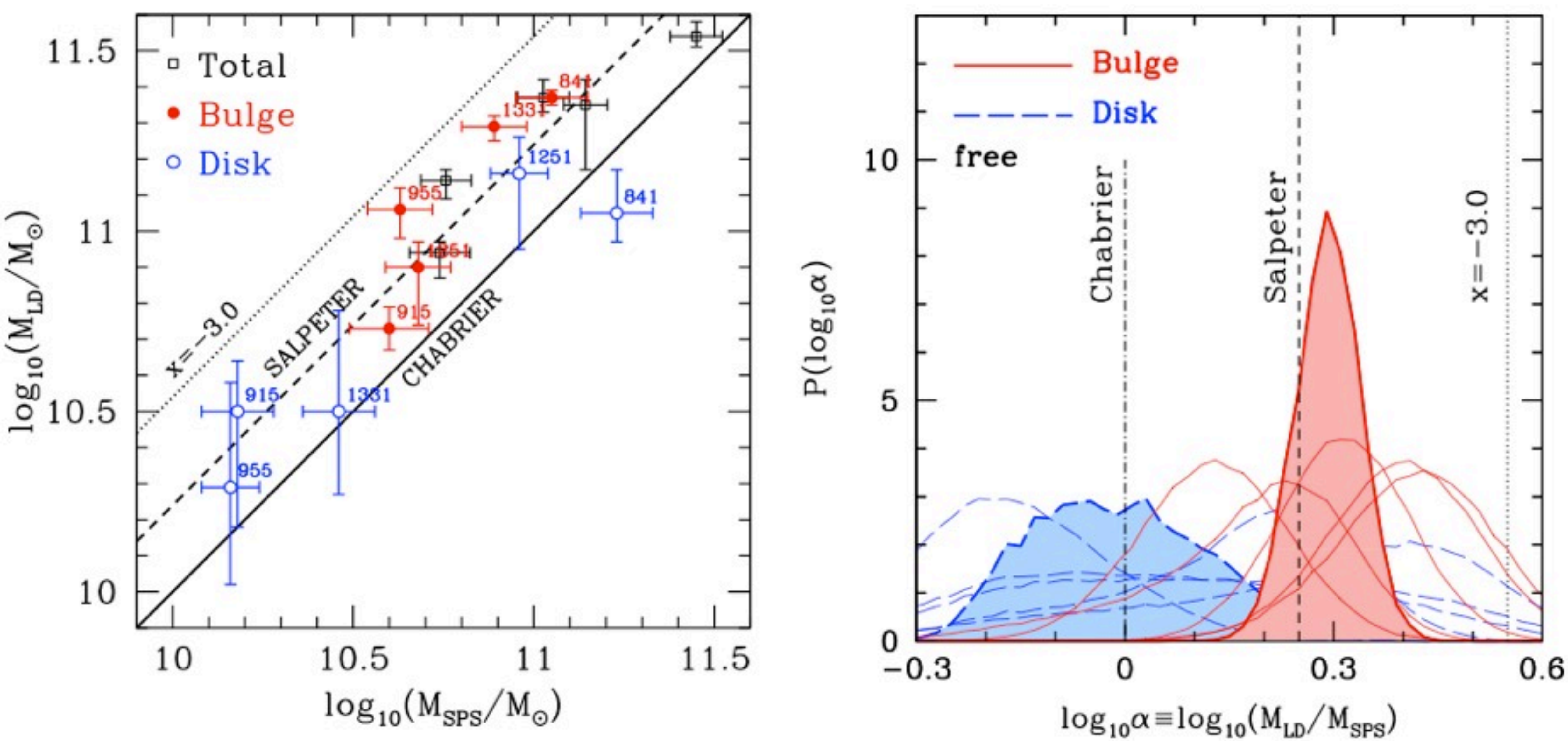

Dutton et al. 2012

Constraint on Stellar & Dark Matter from Microlensing in Strong lenses

Strong-lensing+Microlensing evidence for dark-matter in galaxies

At the lensed image position, the magnification PDF due to stellar ML depends strongly on the fraction of DM in the line-of-sight for FIXED total surface density (from SL).

Caustic networks with increasing microlensing optical depth but fixed surface density (DM+stars)

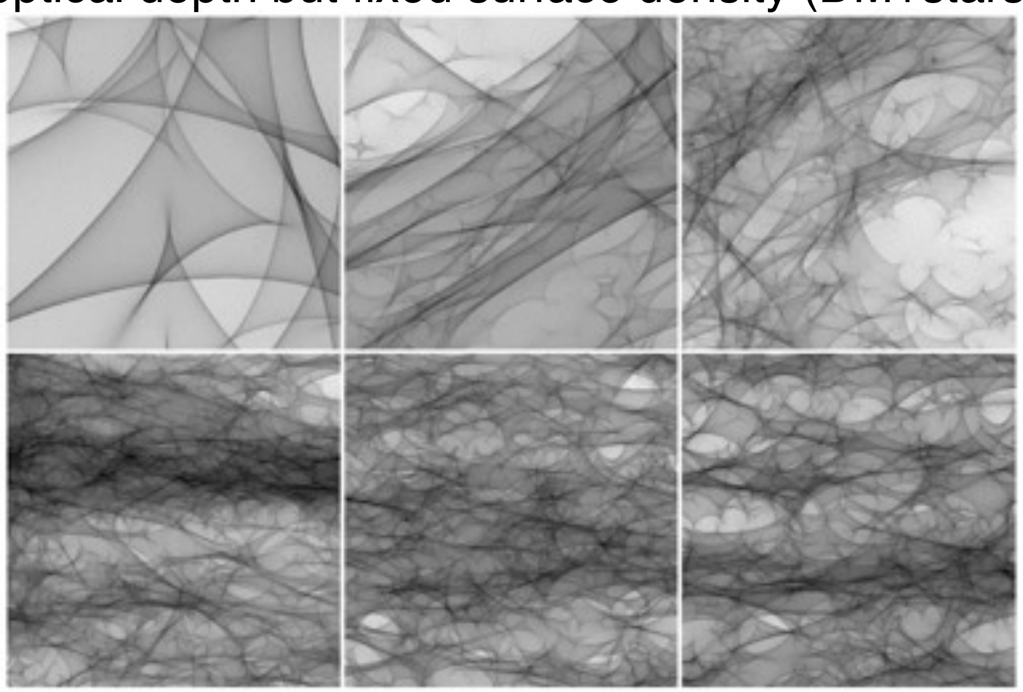

High ML optical depth

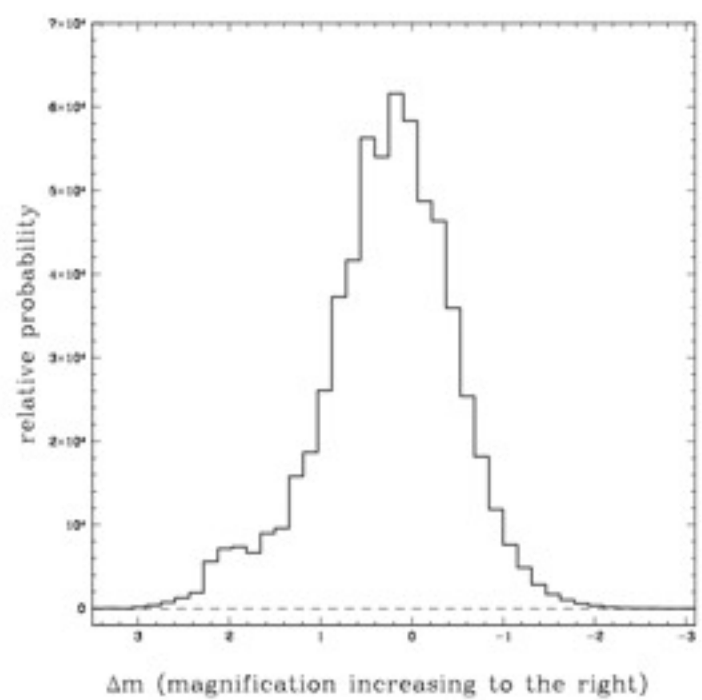

FIG. 2a

Low ML optical depth

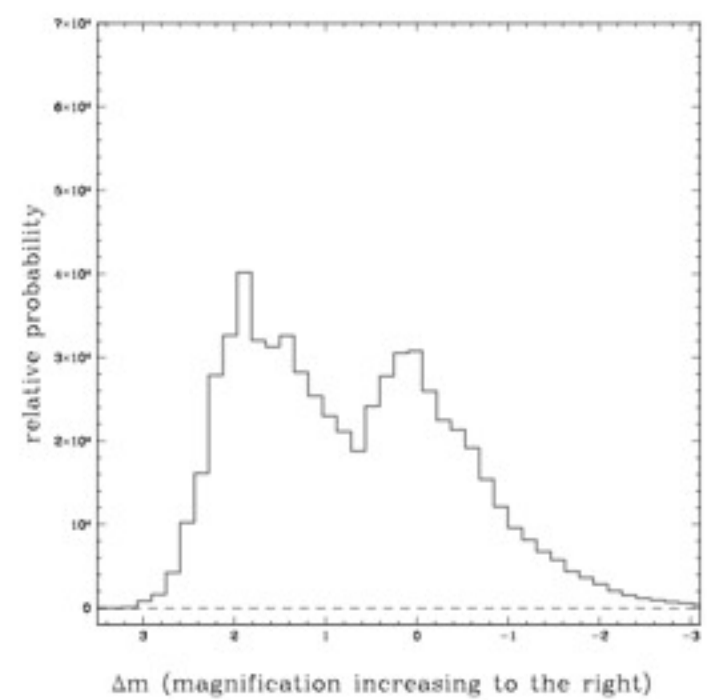

FIG. 2b

Schechter & Wambsganss 2004

Strong-lensing+Microlensing evidence for dark-matter in galaxies

This technique can be applied to either ML light curves of single systems or to an ensemble of single-epoch observations of a sample of lenses.

PG1115+080

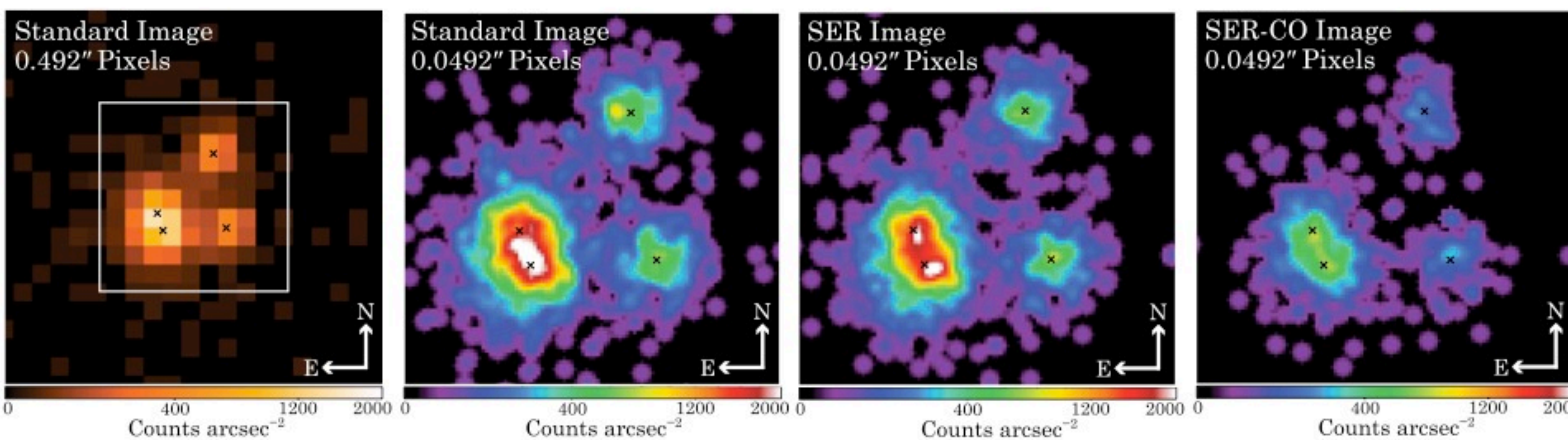

Pooley et al. 2012

Strong-lensing+Microlensing evidence for dark-matter in galaxies

Caustic patterns for all 4 lensed images in PG1115+080 for two different stellar surface densities (the total density is obtained from the SL model).

PG1115+080

10% stars

100% stars

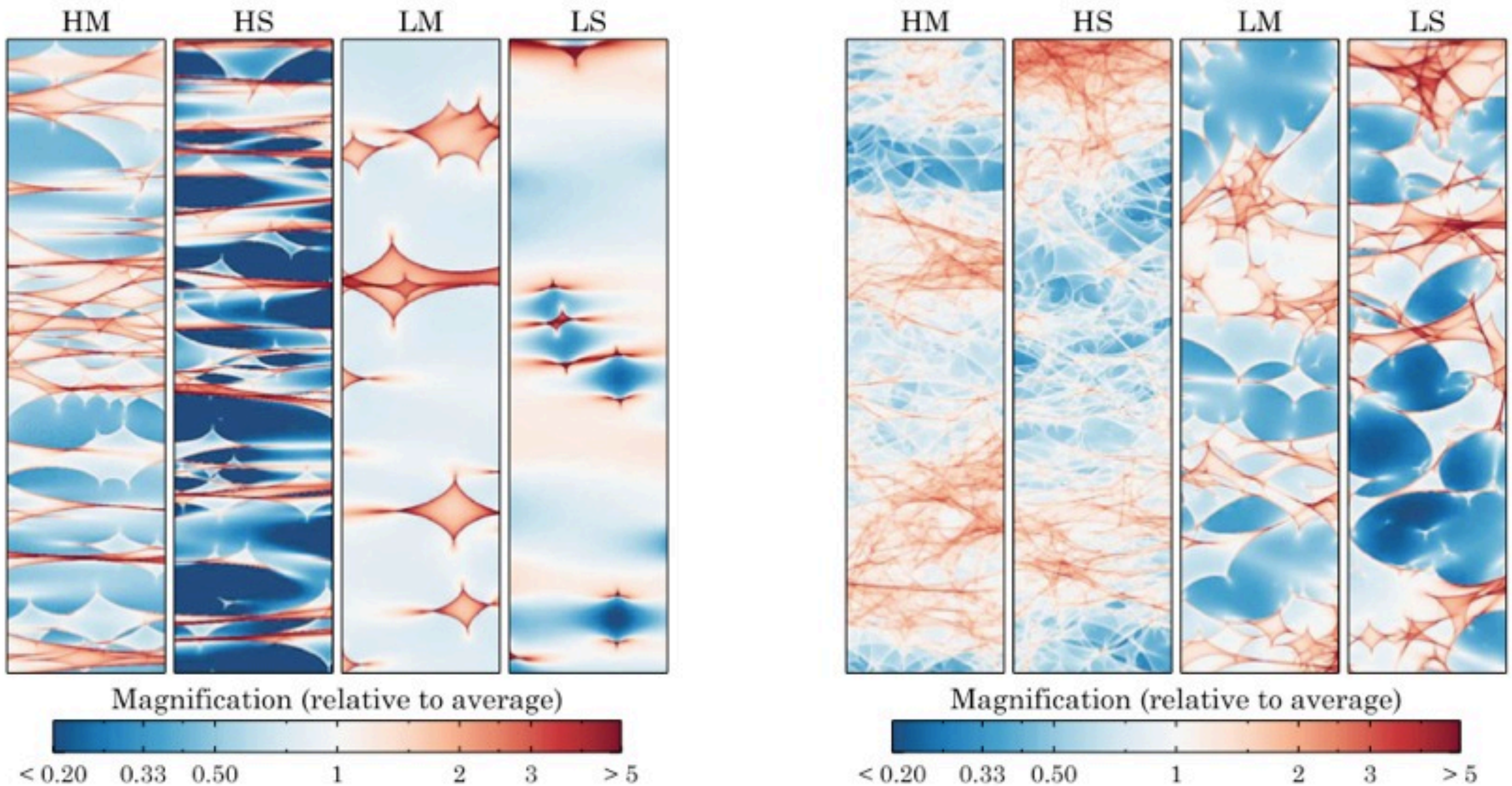

Pooley et al. 2012

Strong-lensing+Micro-lensing evidence for dark-matter in galaxies

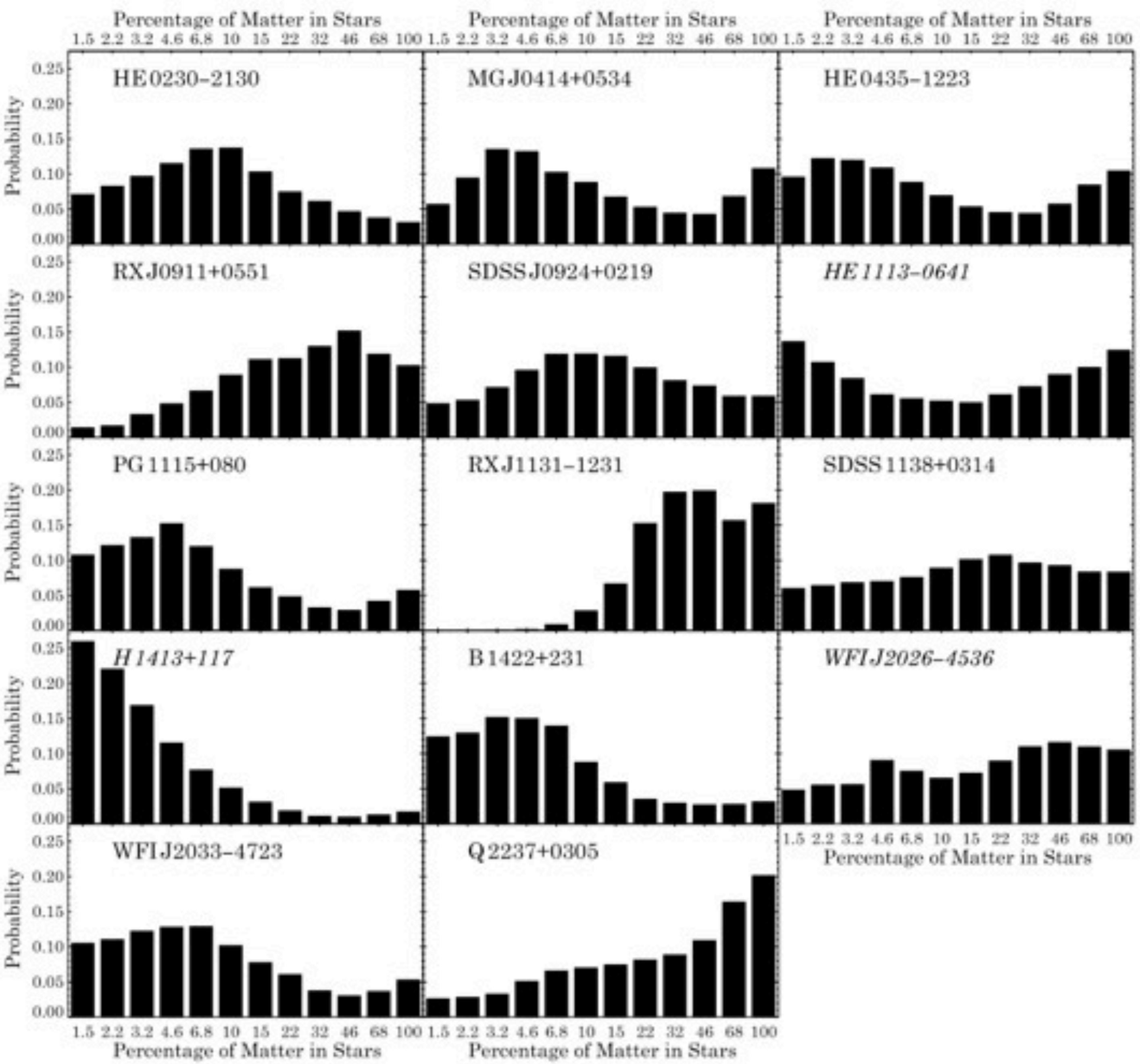

Percentage of matter in stars

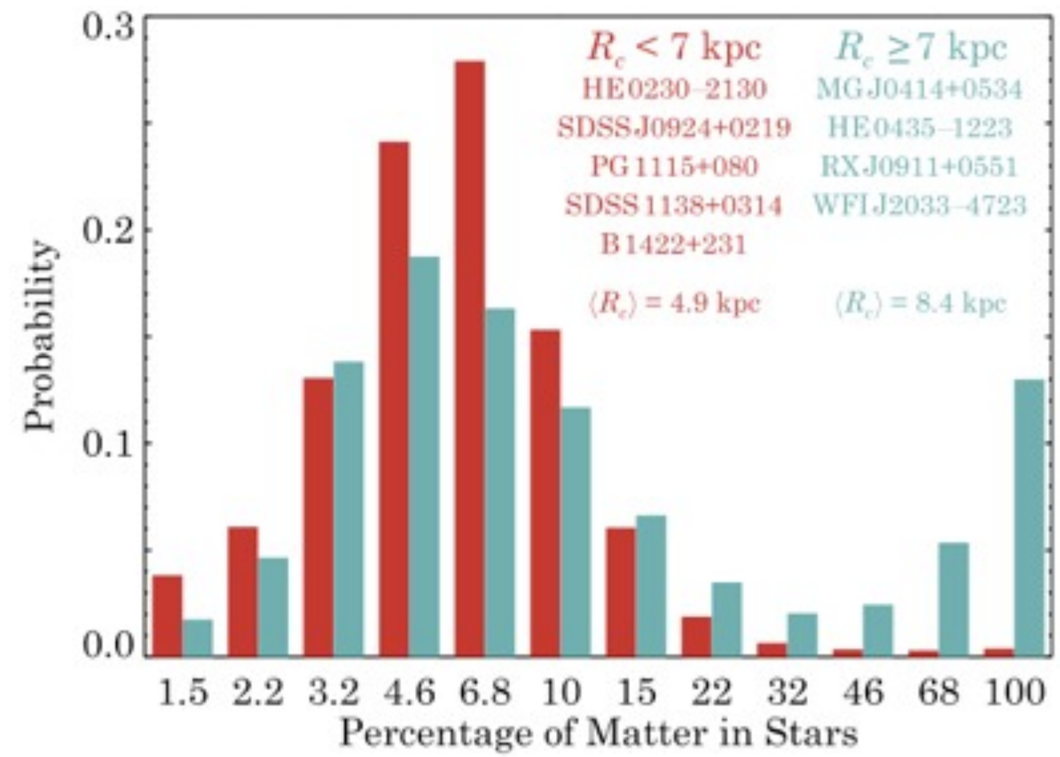

Based on 14 systems and 61 epochs, a Bayesian analysis give that 93% of the surface density is in DM at <R>=6.6 kpc.

Pooley et al. 2012

Strong-lensing+Micro-lensing evidence for dark-matter in galaxies

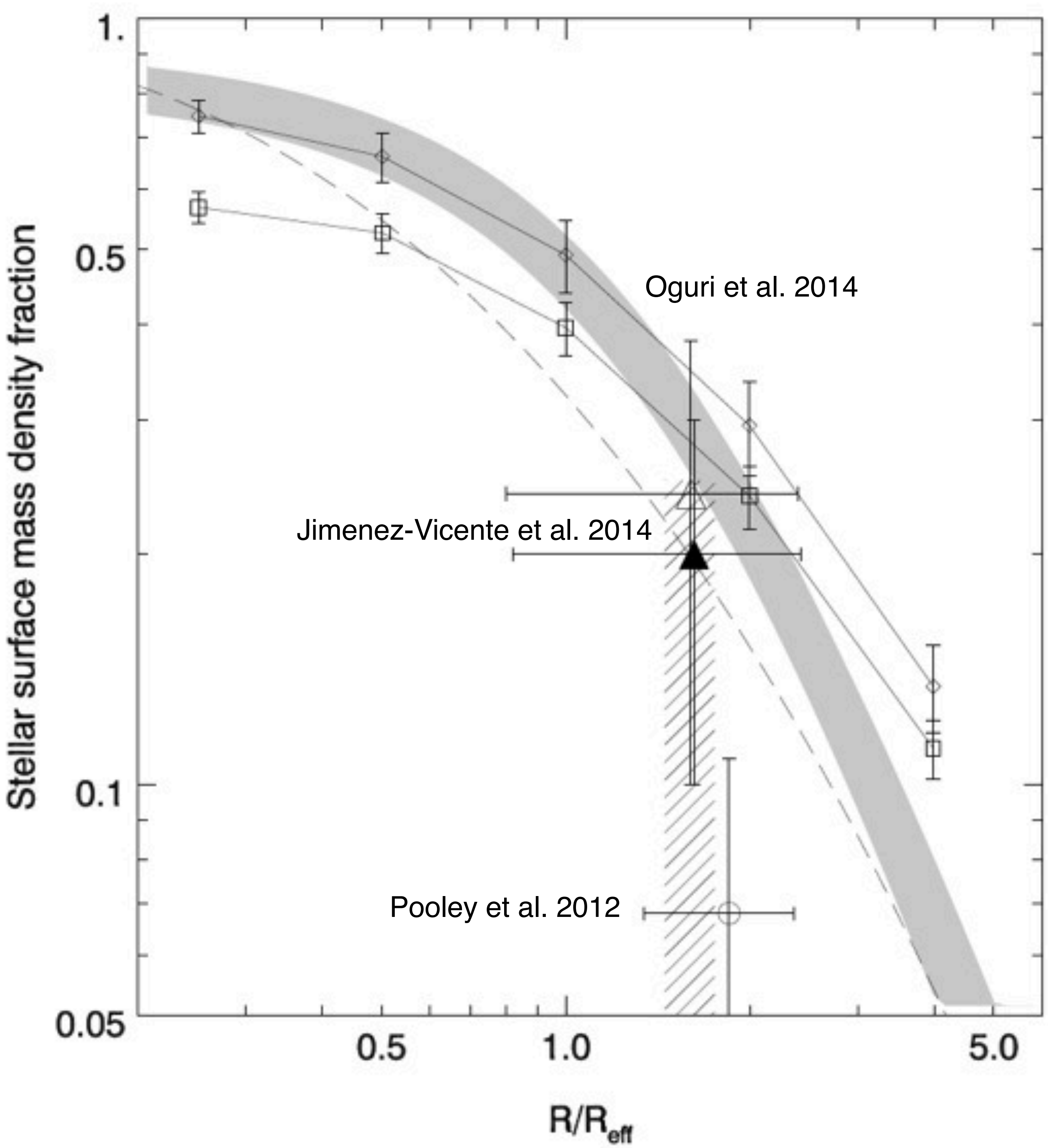

Accretion disk size degeneracy

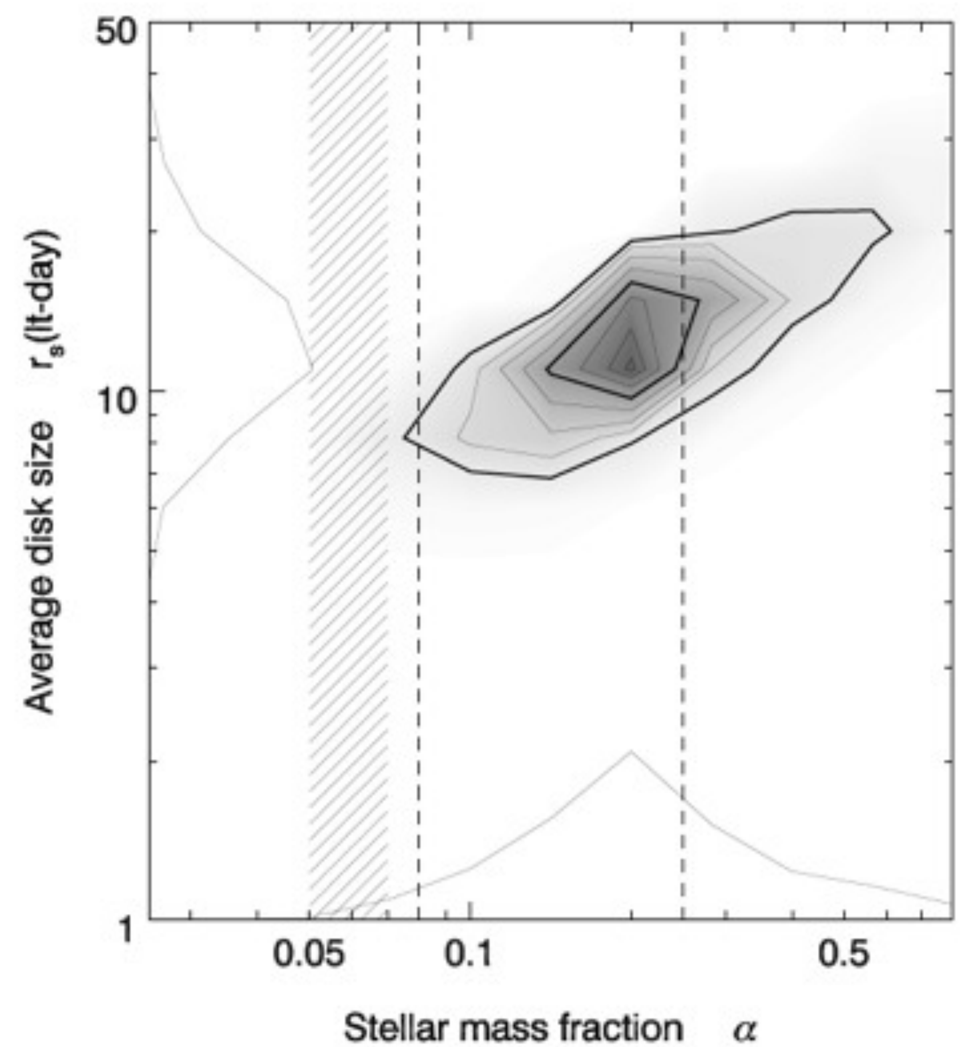

Projected DM fraction at R_{eff} ~ 80%

Jimenez-Vicente et al. 2014

Conclusions

- There is conclusive evidence for DM from strong lenses in both early and late-type galaxies from lensing alone, even more so in combination with dynamics, stellar population studies and micro-lensing.

- In ETG the fraction of DM inside R_{eff} seems to increase with galaxy mass and ranges between 40-80% inside $R_{eff}/2$ in projection for a fixed/universal IMF.

- Evidence is strong that the IMF varies over the σ_*=150-350 km/s range for ETGs which has implications for lensing DM studies and scaling relations.

- Evidence for a varying IMF with galaxy mass flattens the f_{DM} trend to a fraction of f_{DM}=40+-10% inside $R_{eff}/2$ from σ_*=150-350 km/s

- The DM density slope inside $R_{Einst/eff}$ is around 1.3-1.7, steeper than NFW.

- The overall stellar+DM profile is consistent with an adiabatically contracted NFW for Salpeter-like IMFs.

- SL+WL suggest an approximate deV+NFW = $\rho \sim r^{-2}$ total density profile over 1-100R_{eff}

The future of SL studies of galaxies is bright <u>but</u> it (i) requires much larger sample for continual progress and (ii) must possibly re-focus on more unique or complementary science cases.

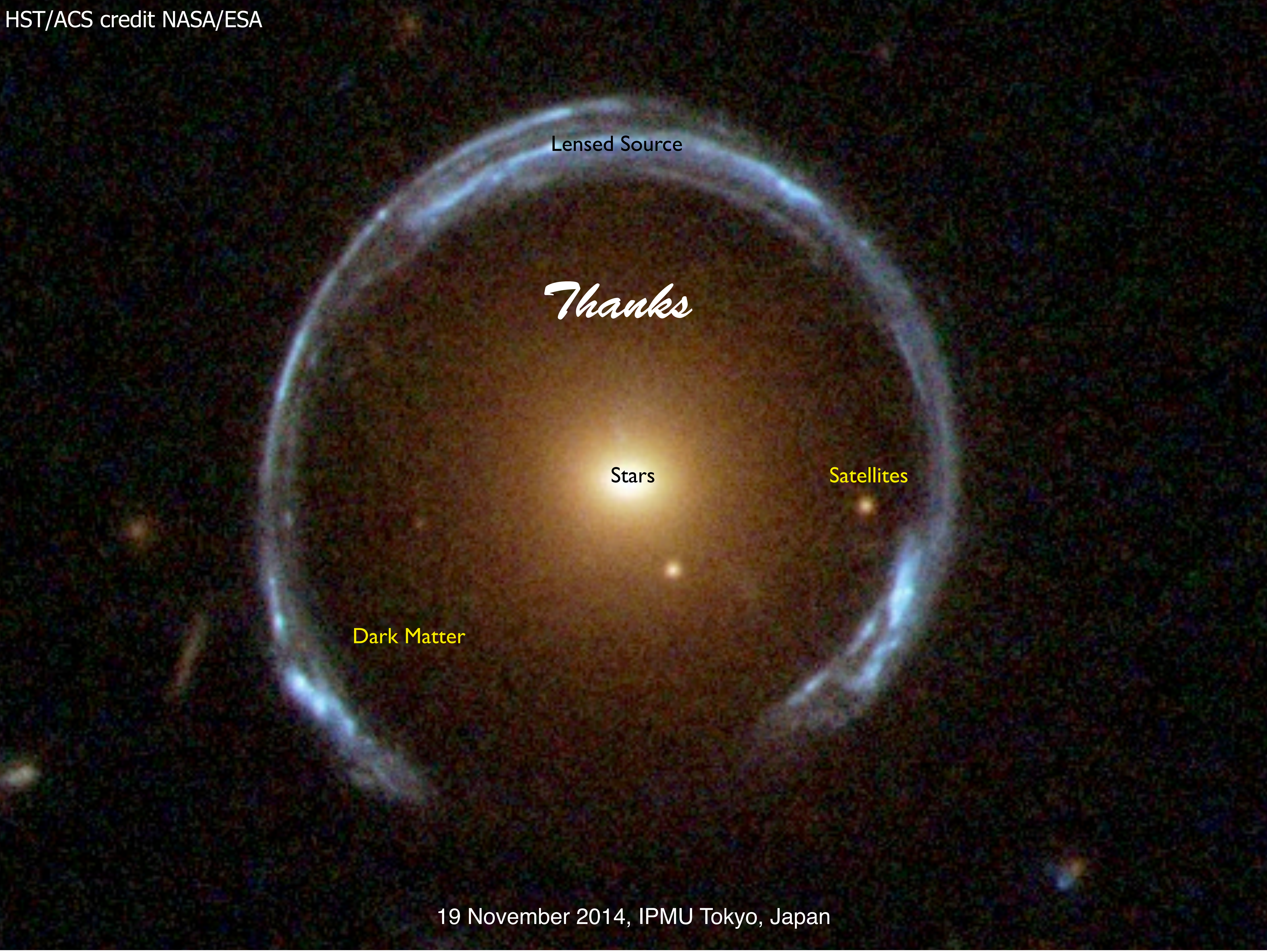
HST/ACS credit NASA/ESA
Lensed Source
Thanks
Stars
Satellites
Dark Matter
19 November 2014, IPMU Tokyo, Japan